AD-A187 504 RESEARCH AND DEVELOPMENT OF SURFACE SKIMMING BULK WAVE DEVICES FOR SENSOR (U) UNITED TECHNOLOGIES RESEARCH CENTER EAST HARTFORD CT D E CULLEN AUG 87 1/1

UNCLASSIFIED UTRC/R87-927145 AFOSR-RR-87-1445 F/G 17/7 NL

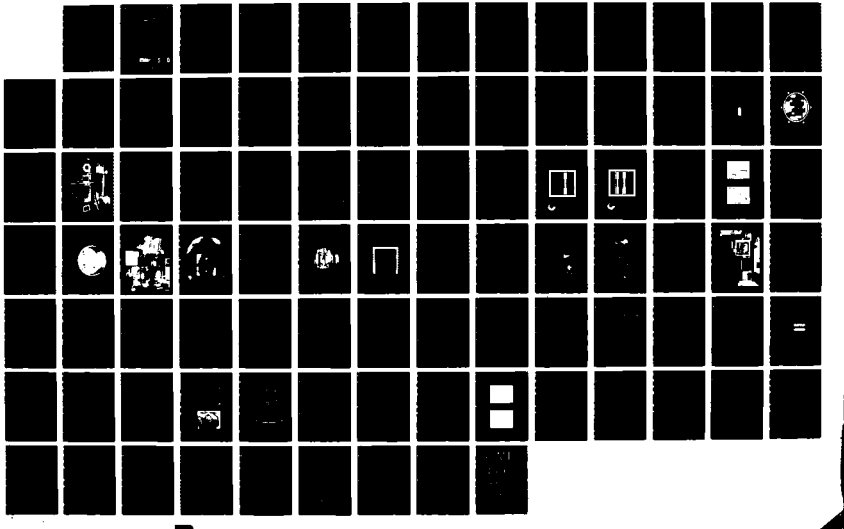

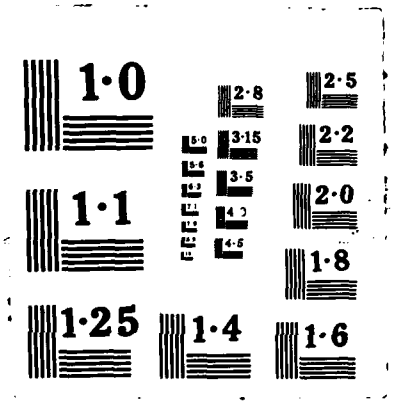
1·0
1·1
1·25
1·4
1·6
1·8
2·0
2·2
2·5
2·8
3·15
3·5

RESEARCH AND DEVELOPMENT OF SURFACE SKIMMING BULK WAVE DEVICES FOR SENSOR APPLICATIONS

D.E. Cullen

Report No. 87-927145

Final Report Period Covered:
April 1, 1985 — June 30, 1987

Air Force Office of Scientific Research
Bolling AFB, D.C. 20332
Contract No. F49620-85-C-0061

UNITED TECHNOLOGIES RESEARCH CENTER

UNCLASSIFIED
SECURITY CLASSIFICATION OF THIS PAGE

REPORT DOCUMENTATION PAGE AD-A187 504

1a. REPORT SECURITY CLASSIFICATION Unclassified	1b. RESTRICTIVE MARKINGS
2a. SECURITY CLASSIFICATION AUTHORITY	3. DISTRIBUTION / AVAILABILITY OF REPORT Unlimited
2b. DECLASSIFICATION / DOWNGRADING SCHEDULE	
4. PERFORMING ORGANIZATION REPORT NUMBER(S) R87-927145	5. MONITORING ORGANIZATION REPORT NUMBER(S) AFOSR-TR- 87-1445
6a. NAME OF PERFORMING ORGANIZATION United Technologies Research Center 6b. OFFICE SYMBOL (If applicable)	7a. NAME OF MONITORING ORGANIZATION Air Force Office of Scientific Research
6c. ADDRESS (City, State, and ZIP Code) East Hartford, CT 06108	7b. ADDRESS (City, State, and ZIP Code) Bld 410 Bolling Air Force Base, Washington, D.C. 20332
8a. NAME OF FUNDING / SPONSORING ORGANIZATION Air Force Office of Scientific Research 8b. OFFICE SYMBOL (If applicable) NP	9. PROCUREMENT INSTRUMENT IDENTIFICATION NUMBER F49620-85-C-0061
8c. ADDRESS (City, State, and ZIP Code) Bolling Air Force Base Washington, D.C. 20332 -6448 Bld 410	10. SOURCE OF FUNDING NUMBERS PROGRAM ELEMENT NO. 61102F PROJECT NO. 2301 TASK NO. A1 WORK UNIT ACCESSION NO.

11. TITLE (Include Security Classification)
Research and Development of Surface Skimming Bulk Wave Devices for Sensor Applications

12. PERSONAL AUTHOR(S)
Donald E. Cullen

13a. TYPE OF REPORT	13b. TIME COVERED	14. DATE OF REPORT (Year, Month, Day)	15. PAGE COUNT
Final Technical Report	FROM 85/4/1 TO 87/6/30	1987 August	85

16. SUPPLEMENTARY NOTATION

17 COSATI CODES			18. SUBJECT TERMS (Continue on reverse if necessary and identify by block number)
FIELD	GROUP	SUB-GROUP	SSBW, Accelerometer, Milli-G

19. ABSTRACT (Continue on reverse if necessary and identify by block number)

The application of surface skimming bulk wave (SSBW) technology to sensors, and to an accelerometer in particular, was investigated through further studies of the properties of the SSBW mode, and through the design, fabrication, and evaluation of a laboratory SSBW cantilever beam accelerometer. The long-term stability of the SSBW mode for devices immersed in a damping fluid was shown to be equal to the stability of vacuum sealed devices (~5ppm/year). The relevant properties of the dual delay line configuration (SSBW devices on both sides of a single substrate) were investigated. The damping of mechanical vibrations in a cantilever quartz beam was studied, establishing the fact that critical damping of the beam can be achieved without difficulty. Evaluation of SSBW accelerometer models showed that the acceleration sensitivity of these devices can be accurately predicted from theory, and that fluid damping can reduce the vibration sensitivity of the SSBW oscillator to less than 5x10-8/G. The results of this study indicate that a practical milli-G range SSBW accelerometer can be developed.

20. DISTRIBUTION / AVAILABILITY OF ABSTRACT ☒ UNCLASSIFIED/UNLIMITED ☑ SAME AS RPT ☐ OTIC USERS	21. ABSTRACT SECURITY CLASSIFICATION Unclassified
22a. NAME OF RESPONSIBLE INDIVIDUAL DR. HOWARD R. SCHLOSSBERG	22b. TELEPHONE (Include Area Code) (202) 767-4906 22c. OFFICE SYMBOL NP

DD FORM 1473, 84 MAR 83 APR edition may be used until exhausted. All other editions are obsolete.

SECURITY CLASSIFICATION OF THIS PAGE
Unclassified

ABSTRACT

The application of surface skimming bulk wave (SSBW) technology to sensors, and to an accelerometer in particular, was investigated through further studies of the properties of the SSBW mode, and through the design, fabrication, and evaluation of a laboratory SSBW cantilever beam accelerometer. The long-term stability of the SSBW mode for devices immersed in a damping fluid was shown to be equal to the stability of vacuum sealed devices (~ 5 ppm/year). The relevant properties of the dual delay line configuration (SSBW devices on both sides of a single substrate) were investigated. The damping of mechanical vibrations in a cantilever quartz beam was studied, establishing the fact that critical damping of the beam can be achieved without difficulty. Evaluation of SSBW accelerometer models showed that the acceleration sensitivity of these devices can be accurately predicted from theory, and that fluid damping can reduce the vibration sensitivity of the SSBW oscillator to less than 5×10^{-8}/G. The results of this study indicate that a practical milli-G range SSBW accelerometer can be developed.

ACKNOWLEDGEMENTS

The author is pleased to acknowledge the individuals who made important contributions during the course of this program. T. W. Grudkowski provided program management. R. Basilica fabricated all of the experimental devices, including the very difficult double-sided SSBW devices; did the packaging and vacuum sealing of the ageing devices, and the assembly of the prototype accelerometers. S. Sheades set up the ageing experiment virtually without assistance, including writing all of the associated computer software. He also packaged the oil-sealed ageing devices, assembled and trimmed all of the oscillator circuits, monitored the ageing experiment, and provided invaluable assistance in the damping experiments and general measurement of device characteristics.

Research and Development of Surface Skimming
Bulk Wave Devices for Sensor Applications

TABLE OF CONTENTS

TABLE OF CONTENTS (Cont'd)

1.0 INTRODUCTION

1.1 Program Scope and Objectives

This research and development program conducted by the United Technologies Research Center (UTRC) was directed toward the continued investigation of surface skimming bulk wave (SSBW) device technology for sensor applications. The program was a logical continuation of the work performed by UTRC under AFOSR Contracts F49620-82-C-0074 and F49620-84-C-0006 in which the properties of several acoustic modes were examined in an effort to find one suitable for sensor applications. This prior work resulted in the identification of a very promising candidate, namely the SSBW mode in BT-cut quartz. With both high strain sensitivity and low temperature sensitivity, this acoustic mode has the basic properties necessary for acoustic sensor development. The principal objectives in this program were: (1) to determine the long term stability of SSBW devices in a sensor environment, (2) to examine the dual oscillator configuration and the mechanical characteristics of cantilever beam SSBW devices, and (3) to demonstrate that a low cost SSBW accelerometer could be developed using acoustic wave technology.

1.2 Background

Surface acoustic wave (SAW) devices, and devices based upon similar surface-oriented acoustic wave modes such as the SSBW mode, are finding ever increasing applications as delay lines, filters, oscillator frequency control elements, and as signal processing elements. The surface nature of these waves allows the control of propagation characteristics, as well as the excitation and detection of the waves through metallic electrode patterns on the surface of the substrate. The small size and weight, and the design precision of these devices has led to their preferred use in numerous systems applications.

These waves are also sensitive to external perturbations of the propagation media through the effect of stresses or surface ambient conditions upon the acoustic wave velocity. This effect can be used to develop devices which are sensitive to temperature and stress or to other external conditions which induce stress or temperature changes in the substrate. In the present program, acceleration induced stresses in the acoustic substrate are exploited in the design of an acoustic accelerometer.

The initial contract in this series, Contract No. F49620-82-C-0074, was designed to explore the properties of known surface-like acoustic modes and to find and study new modes in an effort to identify those with properties suitable for acoustic sensor development. Acoustic modes with high strain sensitivity, low temperature sensitivity, and low sensitivity to surface contamination were sought. The results of this work were reported in technical presentations at the

1982 and 1983 IEEE Ultrasonics Symposiums (Refs. 1 and 2), in a paper titled "Surface and Interface Waves in SiO_2/YX-$LiNbO_3$" (Ref. 3), and in the contract final report (Ref. 4). The principal result of that program was that the SSBW mode in quartz was identified as having outstanding potential for acoustic sensor development.

In a follow-on progam, Contract No. F49620-84-C-0006, the properties of SSBW's in quartz were examined and a simple cantilever beam SSBW accelerometer was built and tested. The sensitivity of SSBW's to substrate strain was measured for the 2 orientations of quartz with zero first order temperature coefficients (BT-cut and AT-cut quartz). The results showed that, despite the higher acoustic losses in the BT-cut, it was the preferred orientation because of: 1) a significantly higher strain sensitivity, and 2) a lower second order temperature sensitivity. Testing of the laboratory accelerometer model indicated that a milli-G SSBW accelerometer was a very realistic objective for further development. The results of this program were presented at the 1984 IEEE Ultrasonics Symposium (Ref. 5) and in the program final report (Ref. 6).

1.3 Description of Program Tasks

This continuation of UTRC's acoustic sensor program was directed toward the further understanding of SSBW devices and the properties of SSBW's that are essential to the development of acoustic sensors. The program was divided into four tasks as follows.

Task I - Investigation of the Dual SSBW Oscillator Configuration

The proposed SSBW accelerometer will employ a dual oscillator configuration which, for SAW devices on a circular diaphragm, has been shown to double the strain sensitivity while reducing the temperature sensitivity by at least two orders of magnitude. To be resolved for SSBW devices were such issues as how closely the SSBW delay lines can be positioned without frequency locking and whether they can be placed on opposite sides of the cantilever beam substrate without deleterious effects. Techniques were developed for fabricating SSBW delay lines on opposite sides of the same substrate, and experiments were conducted to establish an optimum sensoconfiguration.

Task II - SSBW Oscillator Ageing Study

The long term stability, or ageing, of SSBW oscillators is a very important consideration in the development of sensors based upon SSBW technology. Therefore, in order to determine the ageing characteristics of SSBW devices, a statistically meaningful number (>10) of SSBW delay lines were fabricated, packaged, mounted into stable oscillator circuits, and monitored under carefully controlled

conditions for a period of one year. These devices were fabricated using procedures known to yield the lowest ageing SAW devices and packaged using ultra-clean, high vacuum cold-weld packaging techniques. Since the proposed SSBW sensor is to be fluid damped, the ageing of devices immersed in silicone oil was examined by monitoring the variation with time of a second group of SSBW oscillators prepared in the same way as the vacuum sealed devices but packaged so that they can be immersed in oil for the duration of the one year ageing study.

Task III - Investigation of the Mechanical Characteristics of Damped Cantilever Quartz Beams

A cantilever beam SSBW accelerometer must be fluid damped in order to achieve high acceleration sensitivity. The degree of damping that can be achieved with nonconducting fluids suitable for the intended application was examined. The influence of a fluid flow restriction in the cavity on the vibration response spectrum was also examined. The goal of Task III was to determine the fluid and package design combination that provides the best vibration response spectrum consistent with high acceleration sensitivity.

Task IV - Laboratory Prototype SSBW Accelerometer

Laboratory prototypes of dual SSBW oscillator accelerometers were designed, fabricated and evaluated. In order to evaluate the potential of such sensors for further development, the results of the above three tasks were used to design and build fluid damped, cantilever beam, dual SSBW oscillator accelerometer prototypes. These devices were expected to have a high degree of built-in temperature compensation, so that milli-G range acceleration sensitivity could be achieved without precise temperature control. Acceleration sensitivity, temperature sensitivity, and the vibration response spectrum were measured on four prototype devices.

1.4 Summary of Report

The remainder of this report is organized as follows. Section 2 will describe the investigation of the dual delay line configuration, including the very important topic of temperature compensation and the potential for increasing the level of temperature compensation beyond that of the BT-cut quartz substrate alone. Section 3 presents the results of the fluid damping experiments wherein it was learned that critical damping can be achieved in a relatively straightforward manner, thus making it possible to design a SSBW accelerometer with higher acceleration sensitivity. The results of the one year long ageing study are presented in Section 4. This study showed that fluid encapsulated SSBW devices age at a rate of less than 10 ppm/year which is at least as good as the ageing of vacuum sealed devices. Finally, in Section 5, the design, fabrication, and evaluation of a group of four laboratory prototype SSBW accelerometers is described. Section 6 concludes with recommendations for further development.

2.0 DUAL SSBW OSCILLATOR STUDY

2.1 Introduction

The use of two acoustic delay lines on the same substrate to provide increased sensitivity to the parameter being measured while, at the same time, providing added temperature compensation was demonstrated at UTRC in earlier work on SAW pressure sensors (Ref. 7). In that case, a decrease in temperature sensitivity by a factor of 10^3 over that of the Y-cut quartz substrate was obtained. The temperature sensitivity of SSBW's on BT-cut quartz is much less than that of SAW's on Y-cut quartz, so that a similar decrease in sensitivity through the use of the dual delay line configuration was not to be expected with the SSBW accelerometer. The analysis in Section 2.3 will show that a decrease in sensitivity by two orders of magnitude is not an unreasonable expectation, and it was anticipated that a decrease by a factor of at least 10 would be realized in the laboratory prototype SSBW accelerometers.

Two aspects of the dual delay line configuration, as it was to be applied to the SSBW accelerometer, were unknown and were to be examined in this program. First was with regard to the placement of the two delay lines on the substrate, and the second was the degree of precision that would be required in the fabrication of the delay lines in order to achieve the desired temperature compensation. The first concern was related to such questions as: how close could the two delay lines be positioned without deleterious effects, i.e., could they be located directly opposite one another, and what problems would arise in the fabrication of transducers on opposite sides of a single substrate? Section 2.2 will discuss the experiments conducted to answer these questions.

The second concern turned out to be very difficult to evaluate. Achieving a high degree of repeatability in the thermal characteristics of devices on opposite sides of a substrate turned out to be far more difficult than anticipated. While a reduction in temperature sensitivity by only a factor of 10 from that of the BT-cut substrate would be sufficient for the realization of a practical sensor, even that level of compensation requires a very high degree of precision in the fabrication of devices. The experimental work on dual SSBW oscillator temperature compensation will be discussed in Section 2.3.

2.2 Dual SSBW Delay Line Designs

Figure 2-1 shows the general SSBW accelerometer geometry. Delay lines are fabricated on opposite sides of the cantilevered quartz substrate with a relative separation of Xr = Xb - Xt between them. Since the stresses in the beam increase as one moves away from the mass end of the beam, maximum acceleration sensitivity is realized by placing both delay lines as close to the fixed end of the beam as

FIG. 2-1

SSBW ACCELEROMETER GEOMETRY

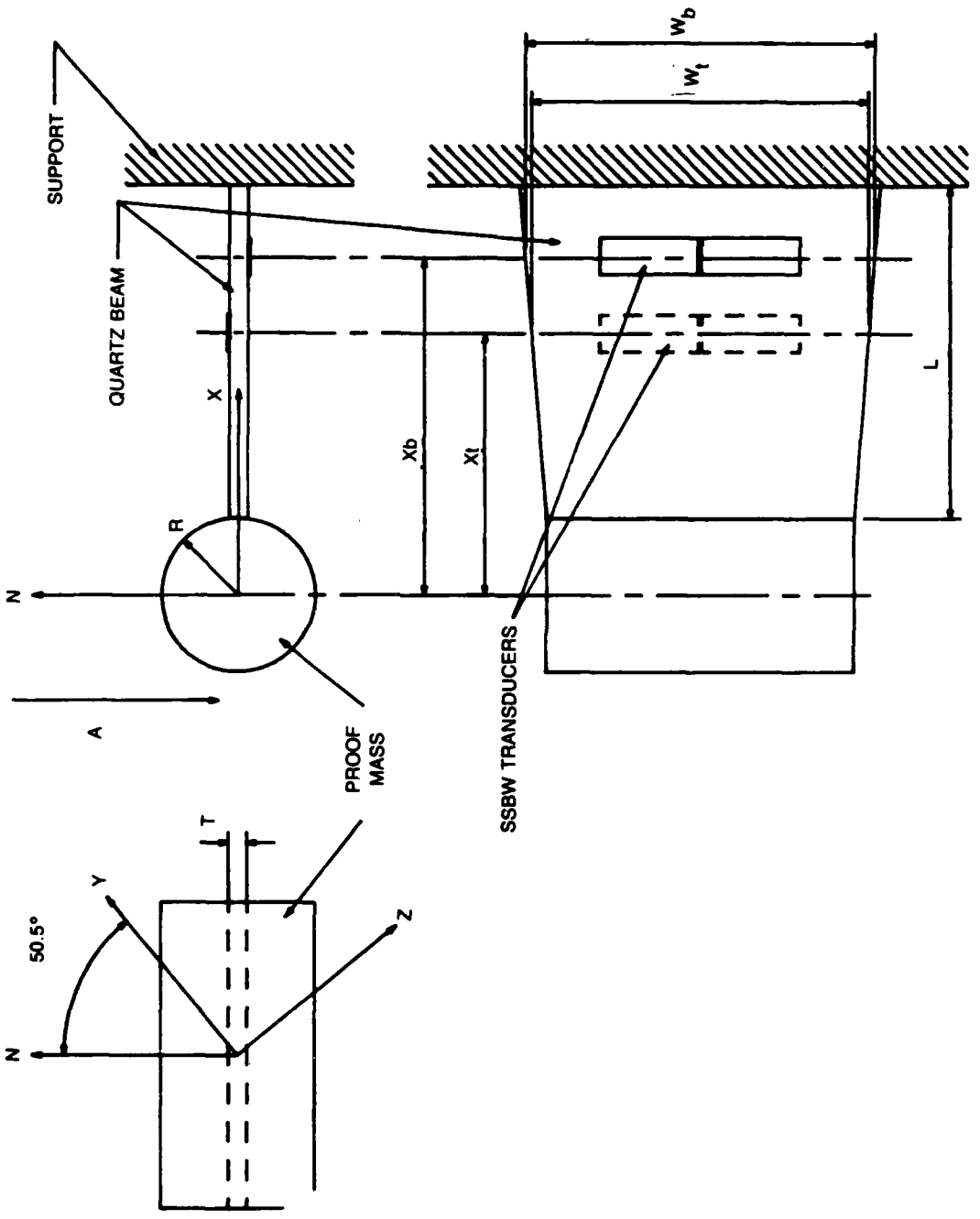

87-8-17-1

possible. However, because the stress field is likely to be distorted near the fixed end due to a lack of precision in the geometry of the epoxy bond, it was decided to keep the centerline of the nearest delay line 3 mm from the bond line. Within this guideline, maximum acceleration sensitivity is obtained when both delay lines on opposite sides of the beam are at this 3 mm position, that is, Xr = 0.

While it was expected that there would be some coupling between the two delay lines, the coupling was not expected to be a limiting factor because the accelerometer design incorporated a frequency separation between the two SSBW devices. The frequency separation was approximately 3 MHz and was determined by photomask limitations. That is, the smallest increment that could be obtained in a 1X photomask for split-finger transducers is 0.4 microns, so that one delay line had a wavelength of 20.0 microns and a SSBW frequency on BT-cut quartz of 166.4 MHz, with the second having a wavelength of 20.4 microns and a frequency of 163.1 MHz. Since a Xr = 0 design would provide the highest acceleration sensitivity, and it was anticipated the that coupling between delay lines would not be a problem, initial plans were to proceed with a Xr = 0 design for the laboratory prototype accelerometers.

In order to determine the extent of the coupling, identical delay lines with varying relative separation, Xr, were fabricated on both sides of 0.035 in. BT-cut quartz substrates. Measurements showed that, for Xr = 0, the insertion loss (IL) for a delay line composed of an input transducer on one side of the substrate and an output transducer on the opposite side was 8 to 10 dB below the IL for a normal delay line with both transducers on the same surface. When similar substrates were prepared with delay lines with the 3 MHz frequency separation, the coupling was >20 dB down from the normal delay line due to the frequency selection characteristics of the interdigital transducers. The coupling fell off rapidly with increasing Xr until it was negligible when Xr > acoustic aperture. Figure 2-2 illustrates the dual oscillator circuit. Frequency locking between SSBW oscillators employing delay lines on the same substrate was not observed when frequency of the two oscillators were separated by 3 MHz. As a result, it is concluded that the coupling between delay lines on opposite sides of a substrate does not prevent a Xr = 0 design when a sufficient frequency separation between the two delay lines is provided.

Problems did arise in the fabrication of the interdigital transducers in the Xr = 0 design however. The photomask pattern definition for the second side delay line was found to be more difficult in all cases where there was overlap, or even close proximity, of the two delay line patterns. This difficulty was due to reflections from the first delay line pattern. A photoresist designed to alleviate the reflection problem became avaliable during the course of this work and was used in processing of all of the usable double-sided devices. While the difficulty of processing of devices with overlap was reduced, it was not eliminated. As a result, and because the processing of the double-sided devices was

FIG. 2-2

DUAL SSBW OSCILLATOR ACCELEROMETER CIRCUIT

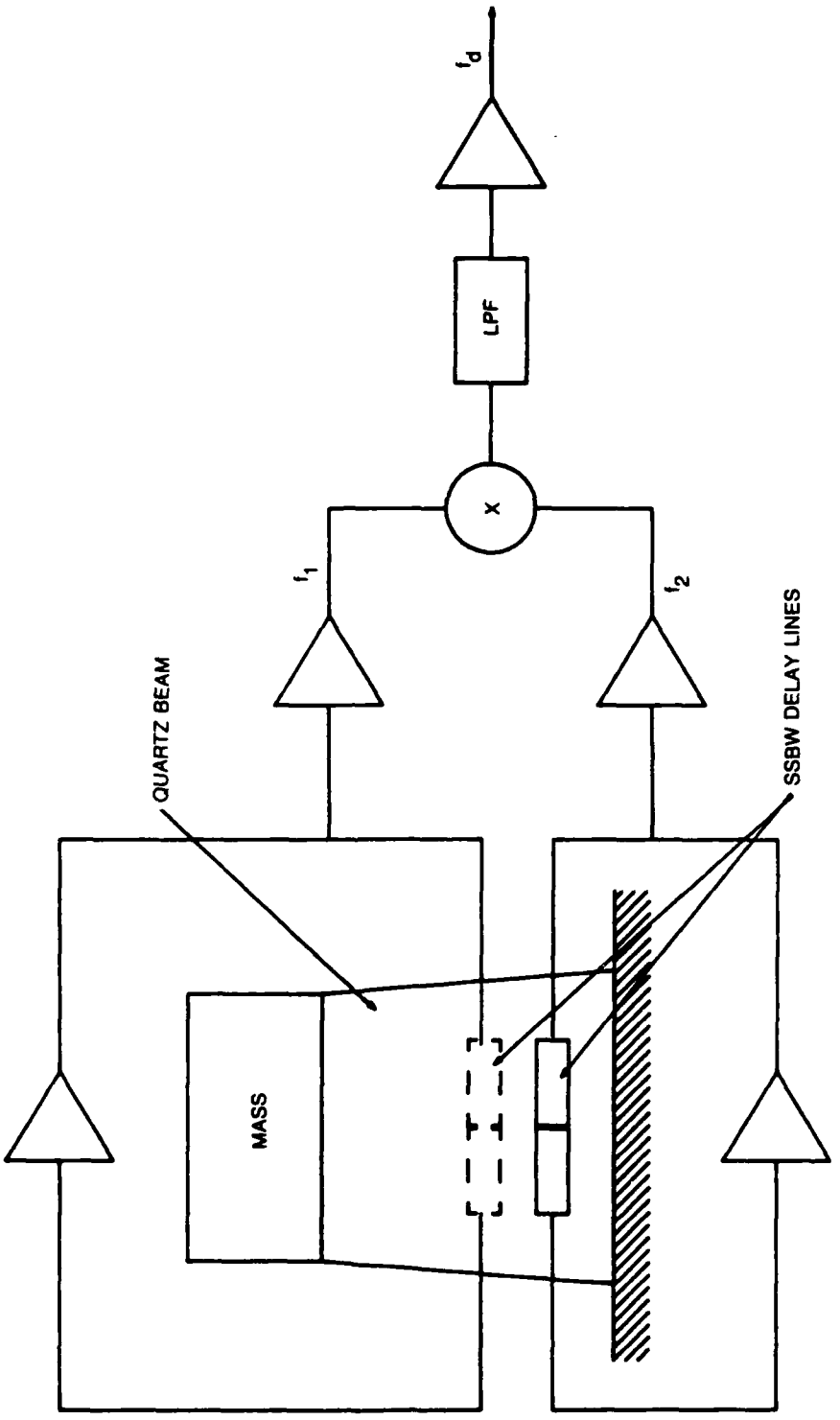

87-8-17-2

difficult for other reasons and did not have a good yield, the decision was made to avoid delay line pattern overlap in the laboratory prototype devices. Some acceleration sensitivity would be sacrificed, but the reduction in sensitivity could be calculated and would be known.

2.3 Temperature Sensitivity

The temperature sensitivity of a SSBW delay line on BT-cut quartz is described by the relation

$$(f - fo)/fo = Tbt*(T-To)^2 \qquad (2-1)$$

where f is the frequency at temperature T, Tbt is the second order temperature coefficient, and fo is the frequency at the turnover temperature To. For +50.5 degree rotated Y-cut quartz (referred to as BT-cut quartz although the BT-cut angle is not exactly +50.5 degrees, having been defined for bulk shear waves in quartz), Tbt has a value of approximately - 0.03 ppm/°C^2, and To is approximately 40°C. Both Tbt and To are strong functions of the orientation of the substrate and have not yet been precisely defined in the literature. Figure 2-3 shows the SSBW temperature sensitivities for substrate orientations between +50 and +51 degrees. In the figure, To is seen to be a very strong function of substrate orientation, varying nearly 1°C for every 0.01 degree of rotation of the crystal. This extreme sensitivity of the turnover temperature makes it difficult to reproduce the turnover temperature with devices on different substrates. Even though X-ray orientation may indicate that the substrates are within 0.01 degrees, minor differences in device fabrication can shift the turnover temperature. Fortunately, reproducing the turnover temperature from substrate to substrate is not critical to the development of a SSBW sensor. Achieving a high degree of temperature compensation within a given device is critical however. With the acceleration sensitivity limited to approximately 100 ppm/G maximum, variations in output with temperature have to be held to less than 0.1 ppm if 1 milli-G accuracy is to be achieved.

The low temperature sensitivity of SSBW's on BT-cut quartz provides an excellent starting point in the quest for a high degree of temperature compensation. With Tbt = - 0.03 ppm/°C^2, a 1°C temperature change results in only a 0.03 ppm change in output frequency. For some applications, particularly those where tight temperature control is readily achieved, this level of temperature sensitivity is sufficiently low.

For more critical applications, or those where temperature control is not desired or not possible, a dual delay line configuration, such as that proposed for the SSBW accelerometer, offers the potential for significant reductions in temperature sensitivity. Because the 2 delay lines of the SSBW accelerometer are in close proximity on the same substrate (albeit on opposite sides of the

FIG. 2-3

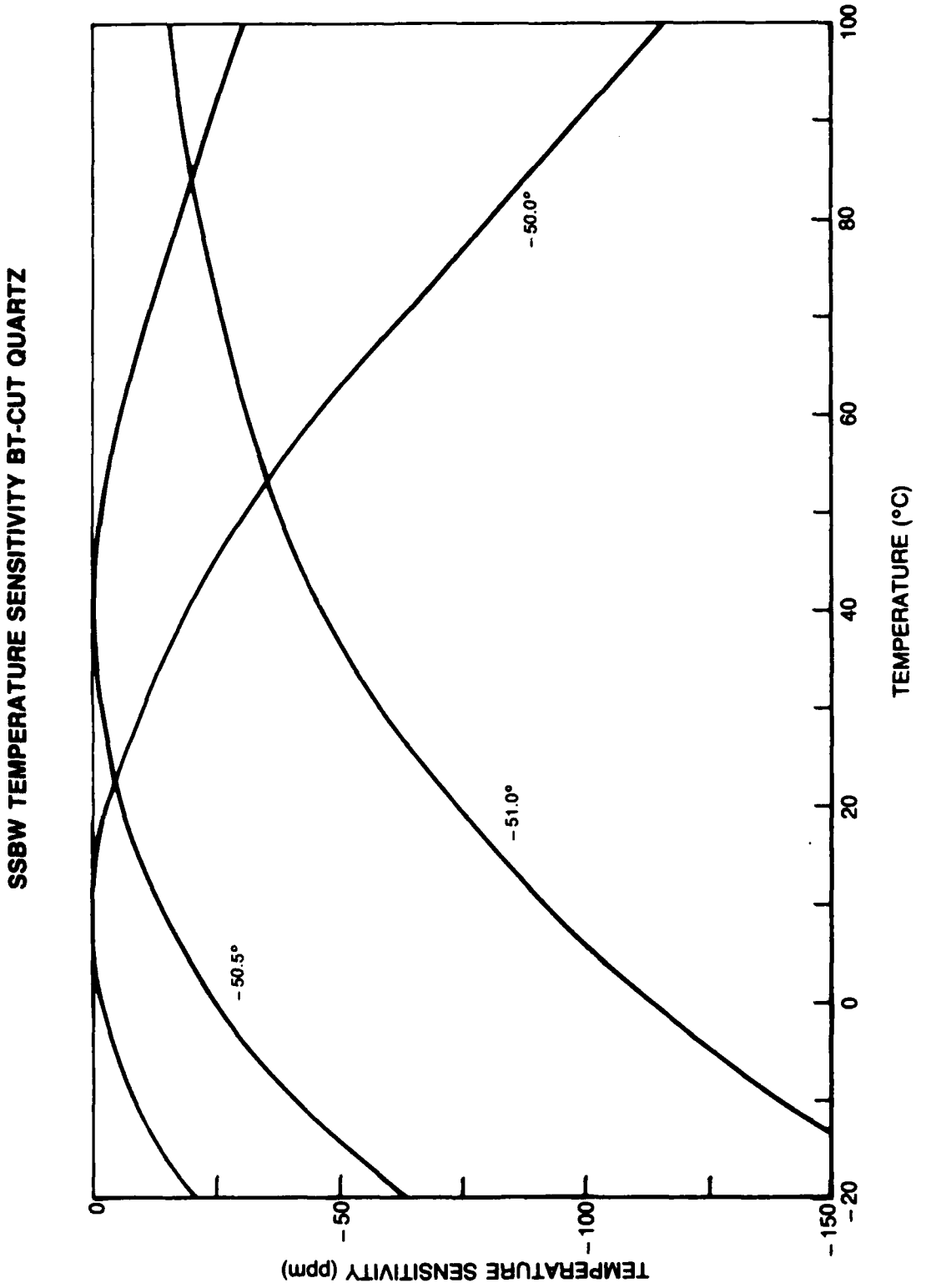

87-8-17-3

FIG. 2-4

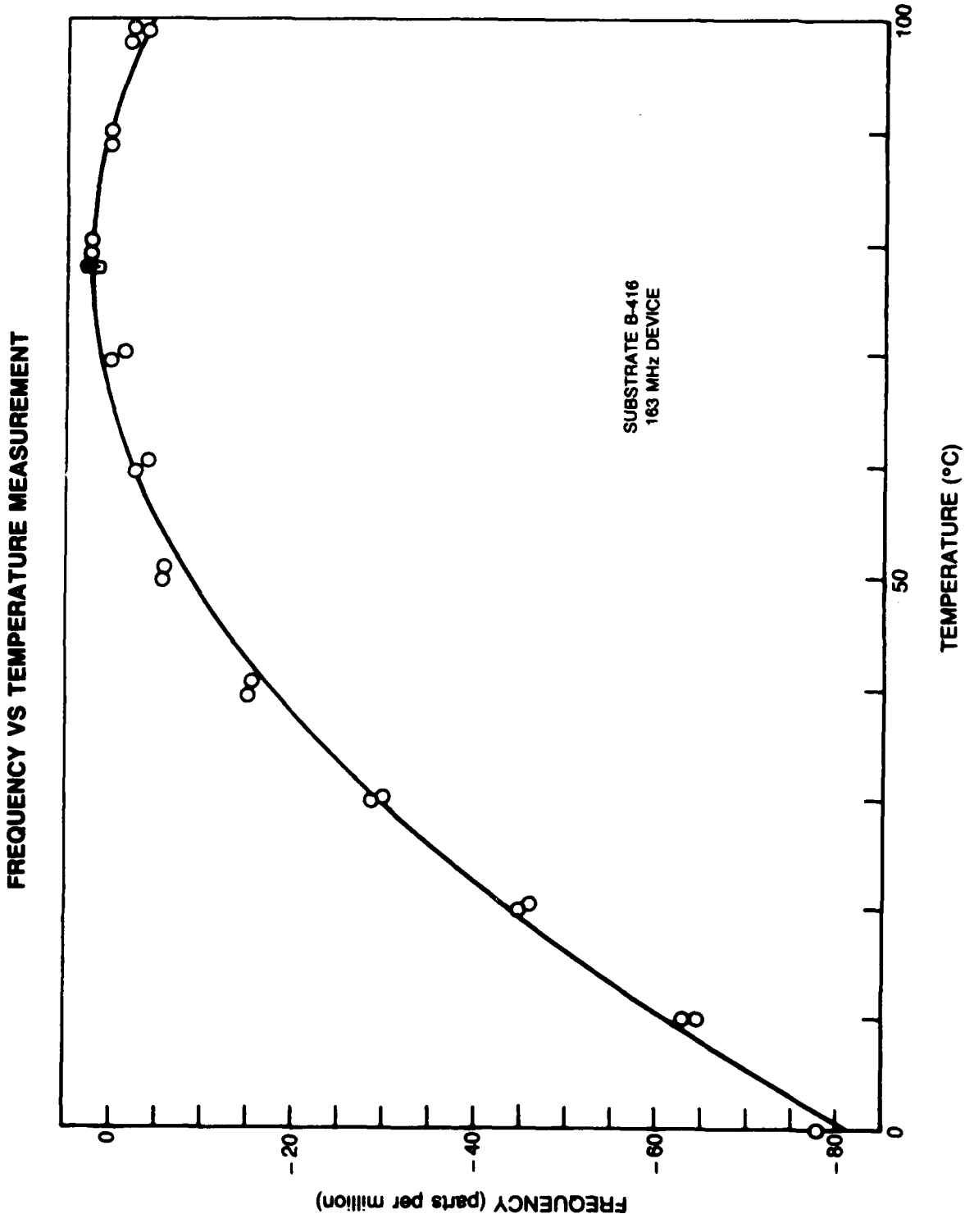

87-8-17-4

FIG. 2-5

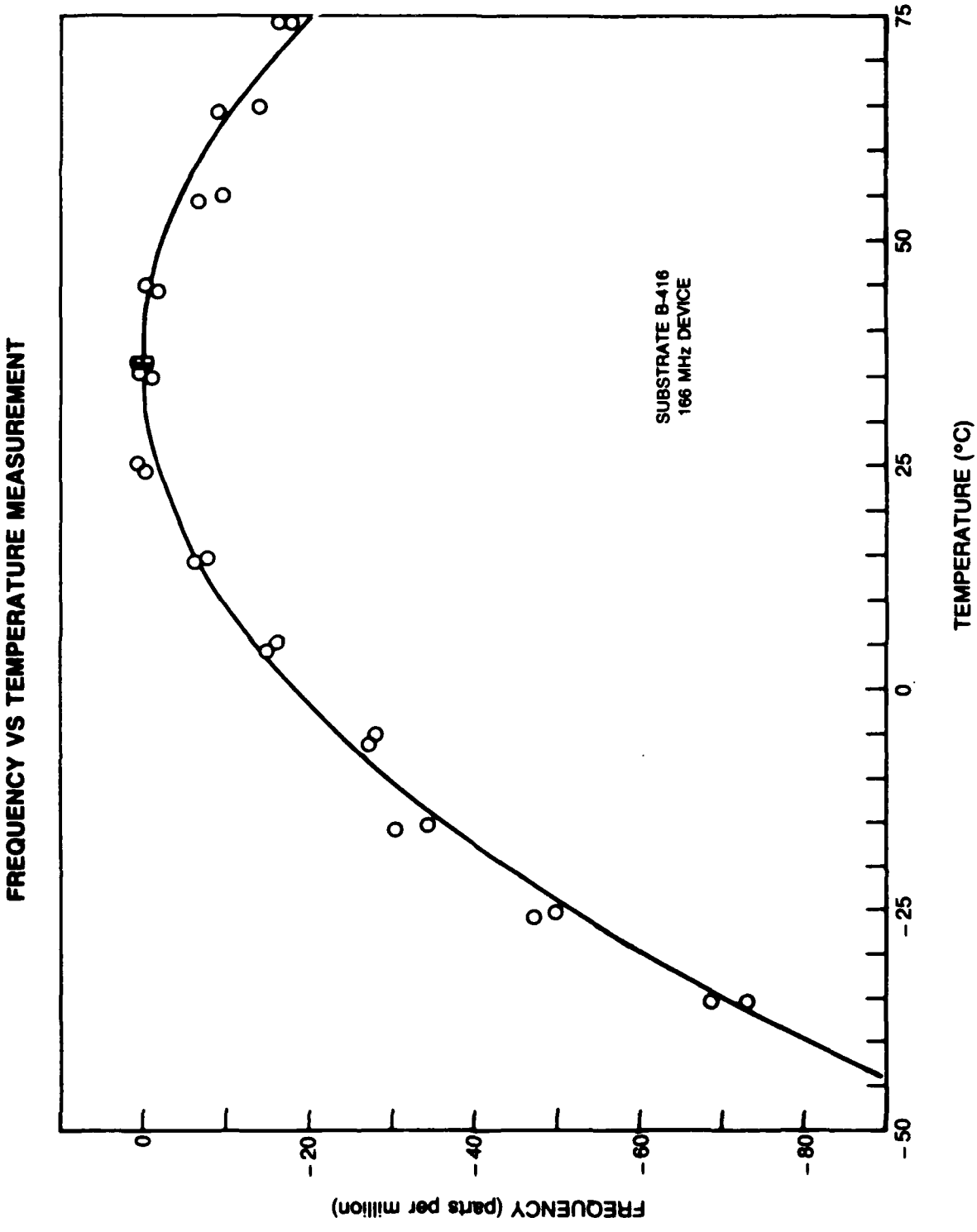

87-8-17-5

substrate), they would be expected to have identical, or nearly identical, thermal properties. Therefore, if the outputs from the 2 SSBW oscillators were combined in a mixer and the difference frequency extracted as the sensor signal output, the temperature effects would nearly cancel, and the overall sensor would exhibit greatly reduced temperature sensitivity. This dual delay line temperature compensation scheme was successfully demonstrated in earlier work at UTRC on a SAW pressure sensor. In that case, the temperature sensitivity was reduced by a factor of 10^3 over the sensitivity of the Y-cut quartz substrates.

In the present case, where the temperature sensitivity of SSBW's on BT-cut quartz is already approximately 10^3 below that of SAW's on Y-cut quartz, a further reduction by such a large factor should not be expected from the dual oscillator configuration. The degree of compensation that can be anticipated can be estimated from the following analysis.

If each of the 2 SSBW delay lines has a temperature sensitivity of the form of Eqn. 2-1, i.e.,

$$(f1 - fo)/fo = Tbt*(T-To)^2,$$
$$(f2 - f2o)/fo2 = Tbt2*(T-To2)^2,$$

where f1 and f2 are functions of T, and fo and fo2 are the frequencies at To and To2, and

$$fo2 = fo + \Delta fo,$$
$$Tbt2 = Tbt + \Delta Tbt,$$
$$To2 = To + \Delta To,$$

then the overall temperature sensitivity is given to first order by

$$\Delta f/fo = \text{constant} + 2*Tbt*To*(\Delta fo/fo - \Delta Tbt/Tbt - \Delta To/To)*T - Tbt*(\Delta Tbt/Tbt + \Delta fo/fo)*T^2. \quad (2-2)$$

where $\Delta f = f2 - f1$. In the ideal case, ΔTbt and ΔTo are zero, and $\Delta fo/fo$ can be made < 0.01 by design, so that

$$\Delta f/fo = \text{constant} - Tbt*(\Delta fo/fo)*(T-To)^2$$

and the temperature sensitivity in the dual oscillator configuration is reduced by $\Delta fo/fo$, or by a factor of 100 or more over that of the individual devices.

Unfortunately, this degree of temperature compensation has yet to be demonstrated in the laboratory for SSBW devices. Measurements of the temperature characteristics of SSBW devices fabricated on opposite sides of the same substrate show substantial differences in both Tbt and To. Figures 2-4 and 2-5 show temperature versus frequency data from the 2 SSBW delay lines on opposite sides of substrate B-416. The values of Tbt and To for these 2 delay lines are -0.028 ppm/°C^2 and 78.0°C for the 163 MHz device and -0.014 ppm/°C^2 and 36.6°C for the 166 MHz device. The discrepancy between the Tbt values and the large difference between the turnover temperatures are not understood. The temperature characteristics of 4 such double sided substrates were measured and the Tbt and To values obtained are given in Table 2-1.

If the paramaters from the best of these pairs is used in Eqn. 2-2, the net frequency sensitivity of substrate B-417 is given by

$$\Delta f/fo = \text{constant} - 0.72*T + 0.0042*T^2$$

and the large linear term results in nearly a 1 ppm/°C temperature sensitivity. This is far too large a temperature effect for a practical device. The second order coefficient of temperature is reduced by an order of magnitude over that of the BT-cut substrate, however, combining the temperature dependencies results in a large linear term due to the differences in Tbt and To.

These differences in thermal properties between devices on opposite sides of the same substrate have two possible causes. One is that the two surfaces of the quartz substrate may actually have different thermal properties. The lapping and polishing of the substrates is not done by UTRC but by a vendor with many years experience in preparing acoustic substrates. Conversations with the vendor indicate that there were no differences in the way that the two sides of the substrates were processed, and it therefore does not seem likely that substrate preparation is the source of the problem. Also, the tolerances on thickness uniformity rule out any significant orientation differences between the two sides of the substrates.

The second and more likely cause of the problem is differences in the processing of the substrates. Three of the most obvious potential sources of difficulty are: 1) differences in transducer metallization thickness, 2) differences in transducer finger-to-gap ratio, 3) alignment errors between the delay line patterns on the two sides of the substrate. A strong effort was made to control all of the parameters of the delay line processing, however, small differences remained. For example, the metal films forming the SSBW transducers

TABLE 2-1

MEASURED TEMPERATURE CHARACTERISTICS OF BACK-TO-BACK SSBW DELAY LINE DEVICES

Substrate	Cut-Angle	Frequency(MHz)	Tbt(ppm/°C^2)	To(°C)
B-416	50°31'	163.2	-0.028	78.0
		166.4	-0.014	36.6
B-417	50°26'	163.2	-0.011	55.6
		166.6	-0.015	69.2
B-418	50°30'	163.1	-0.012	66.5
		166.3	-0.025	80.8
B-422	50°27'	163.1	-0.010	58.0
		166.3	-0.019	86.7

are only 1000 angstroms thick and can only be controlled to within 50 angstroms or so without a post-processing trimming technique.

Trimming techniques have been devised at UTRC to adjust the frequency of SAW resonators and delay lines, and similar methods could be devised to adjust the temperature characteristics. In the case of frequency trimming, the feedback information necessary to control the trimming operation (the frequency) is readily measured. A similar trimming technique could be used to vary the temperature characteristics, however the feedback information is far more difficult to obtain in that case, and the process could become prohibitively time consuming.

If ΔTbt and ΔTo can be reduced to acceptable levels, the dual delay line design will no doubt be able to provide added temperature compensation beyond that of the substrate alone. The large differences observed experimentally between the thermal properties of devices on opposite sides of the same substrate were not anticipated, and there was not sufficient time within the present program for an in-depth investigation of the problem. As a result, the goal of demonstrating dual delay line temperature compensation could not be reached. The potential for a significant reduction in temperature sensitivity using this method exists, but further work is required to develop that potential.

3.0 DAMPING OF MECHANICAL VIBRATIONS

3.1 Introduction

In the design of any accelerometer, both high acceleration sensitivity and a high mechanical resonance frequency are sought. High sensitivity to accelerations is essential if the device is to be a useful accelerometer. A high mechanical resonance frequency is necessary because the lowest mechanical resonance is above about 1 kHz, the device will be unduly influenced by low frequency vibrations that are unrelated to the acceleration to be measured. In a cantilevered beam type of accelerometer, these two properties are mutually exclusive. Acceleration sensitivity is given by (Ref. 9)

$$As = Const*M*L/(W*T^2), \qquad (3\text{-}1)$$

where

M = proof mass,
W = width of beam,
L = length of beam, and
T = thickness of beam,

and the lowest mechanical resonance frequency f is given by

$$f = Const*(T/L)*\sqrt{[W*T/(M*L)]}. \qquad (3\text{-}2)$$

Increasing the sensitivity by adjusting one of the parameters results in a decrease of the resonant frequency and vice versa. Both quantities cannot be simultaneously adjusted for optimum performance.

To illustrate this graphically, Fig. 3-1 shows plots of acceleration sensitivity versus resonant frequency with mass, beam length, and beam thickness as variable parameters. Clearly there is a design trade-off between sensitivity and resonant frequency. With a SSBW strain sensitivity of 1.95 ppm/microstrain, there is no practical beam design that will yield a SSBW accelerometer with both sufficiently high acceleration sensitivity and a mechanical resonance frequency above 1 kHz.

However, because the SSBW acoustic mode can propagate in a fluid environment without excessive losses, it is possible to use fluid damping to alleviate the problem of mechanical vibrations. If the dampening can be made high enough that critical damping is achieved, the effects of mechanical vibrations would essentially be eliminated. The remainder of this section describes the study

FIG. 3-1

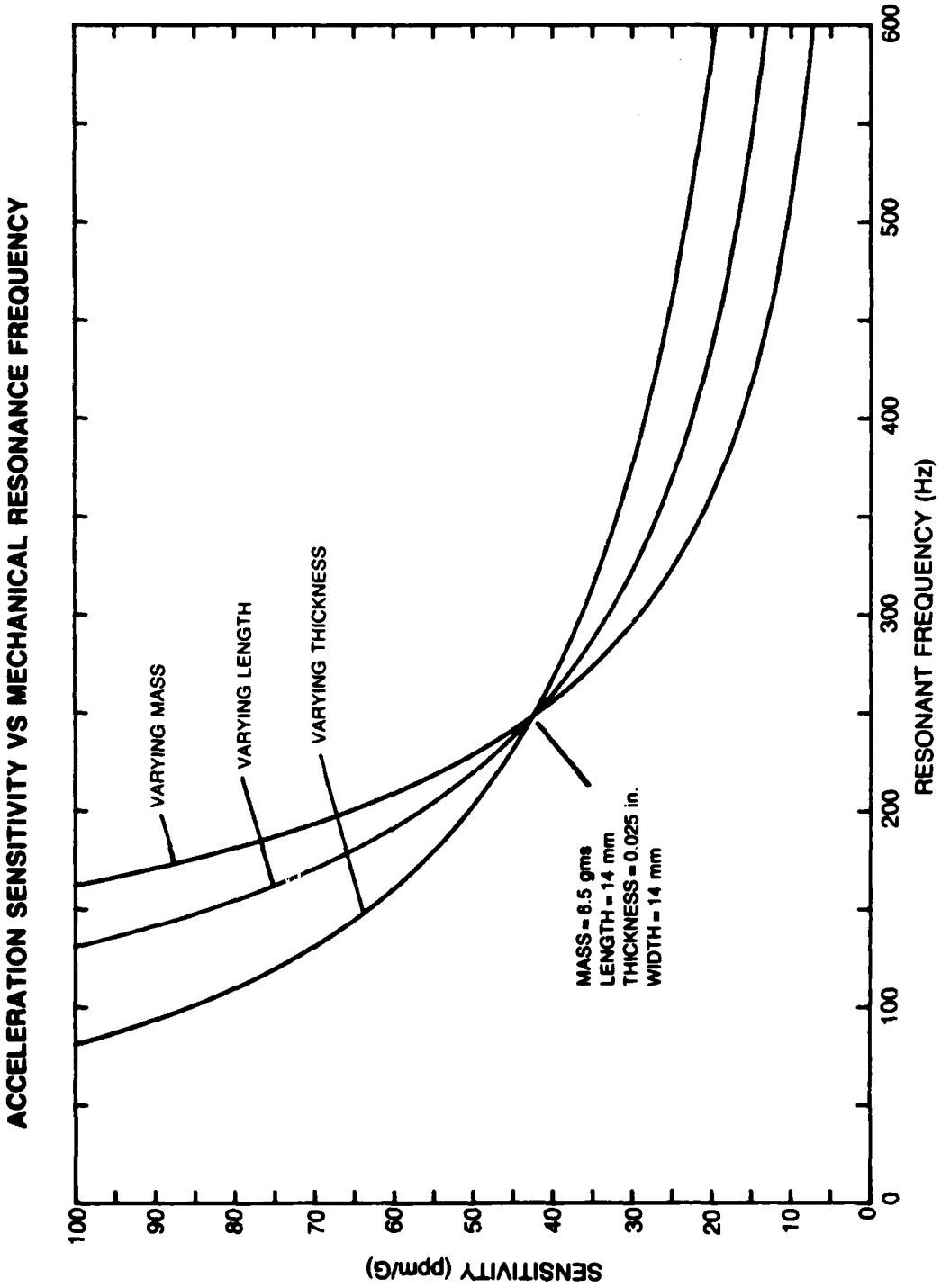

87-6-17-6

conducted to determine the fluid damping characteristics of cantilevered quartz beams for an SSBW accelerometer.

3.2 Fluid Damping Experiments

Vibration damping experiments were conducted to determine the effects of damping fluids on the amplitude of vibration of the quartz beam. The use of fluid flow restrictions were investigated with the goal of increasing the effectiveness of the damping and possibly reaching the critical damping point. The basic experiment consisted of mounting a quartz beam so that it could be excited by an electrodynamic shaker and recording the amplitude of the mechanical vibrations of the beam as a function of shaker frequency and acceleration level.

The quartz beams employed in the vibration testing were the same thickness and were cut into the same trapazoidal shape as those used in the laboratory prototype SSBW accelerometers. A photograph of one of the quartz beams with attached strain gage is shown in Fig. 3-2. A Micro-Measurements No. EA-06-031DE-120 strain gage was bonded to the beam in the orientation shown to measure the longitudinal strain at the surface of the beam. A cylindrical tungsten mass was epoxy bonded to the narrow end of the beam and the opposite end epoxy bonded into a machined support piece. This assembly was then mounted into a circular chamber as shown in Fig. 3-3. The chamber was, in turn, mounted onto an electrodynamic shaker for vibration testing. The chamber was fitted with O-rings so that it could be filled with a damping fluid.

Figure 3-4 is a schematic of the vibration test setup and Fig. 3-5 is a photograph of the apparatus. The electrodynamic shaker provides a sinusoidal excitation with an amplitude and frequency controlled by a servo system. The maximum acceleration level can be held constant while sweeping over the desired frequency range. That is, if the displacement and acceleration are given by

$$x = A * \sin(\omega t), \qquad d^2x/dt^2 = -A\omega^2 * \sin(\omega t),$$

the quantity $A\omega^2$ is held constant as the frequency is varied. The vibration servo provides a signal proportional to the frequency which was used to drive the X-axis of the X-Y recorder. The output of the Wheatstone bridge circuit containing the strain gage is a measure of the strain in the quartz beam and hence the amplitude of the deflection of the beam. This AC output at frequency $f = 2\omega$ was monitored with an oscilloscope. A DC signal proportional to the AC bridge circuit output was provided by a RMS voltmeter, and this DC voltage was used to drive the Y-axis of the recorder. In operation, the acceleration level was set to the desired level and the frequency swept over a range known to include the

FIG. 3-2

QUARTZ BEAM WITH ATTACHED STRAIN GAGE

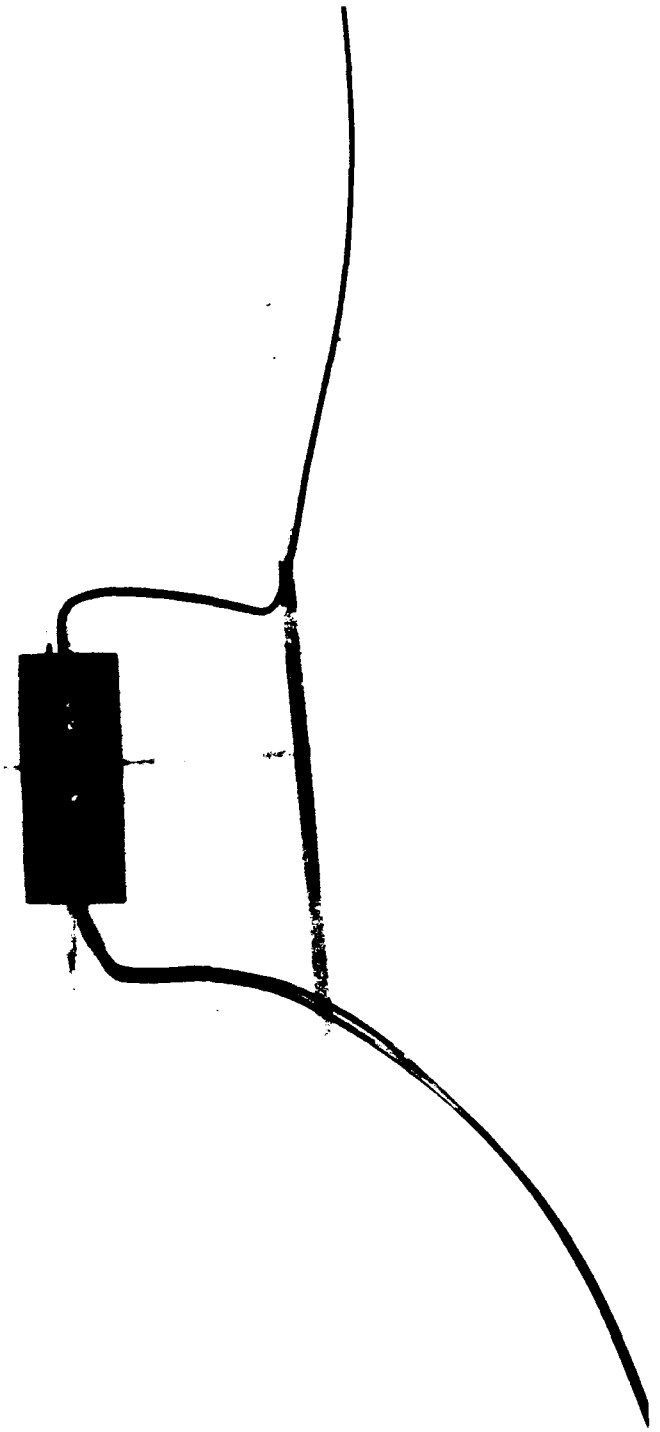

85 - 262

87 - 7 - 34 - 3

FIG. 3-3

VIBRATION EXPERIMENT SAMPLE CHAMBER

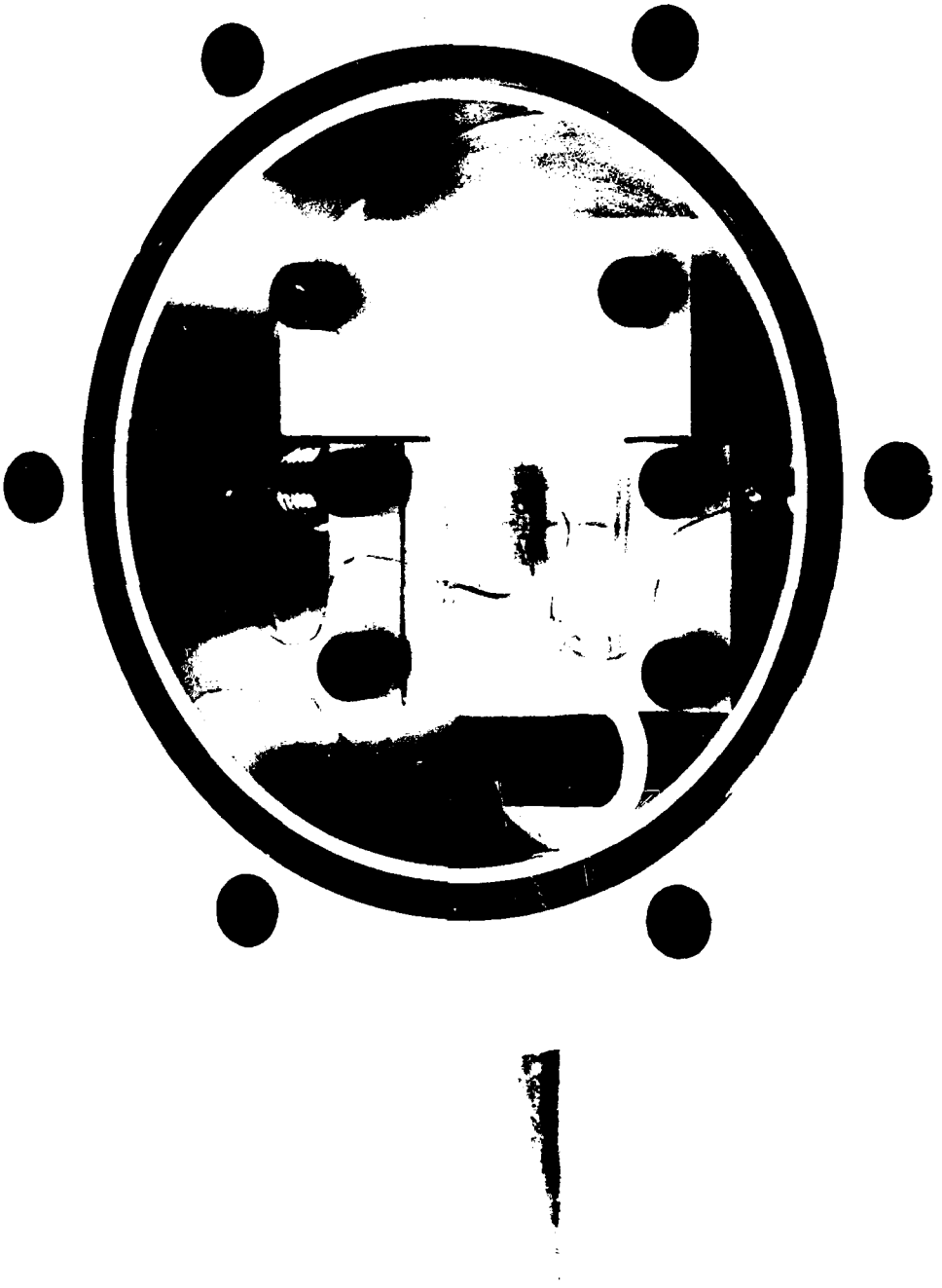

86 - 9A

87 - 7 - 34 - 4

FIG. 3-4

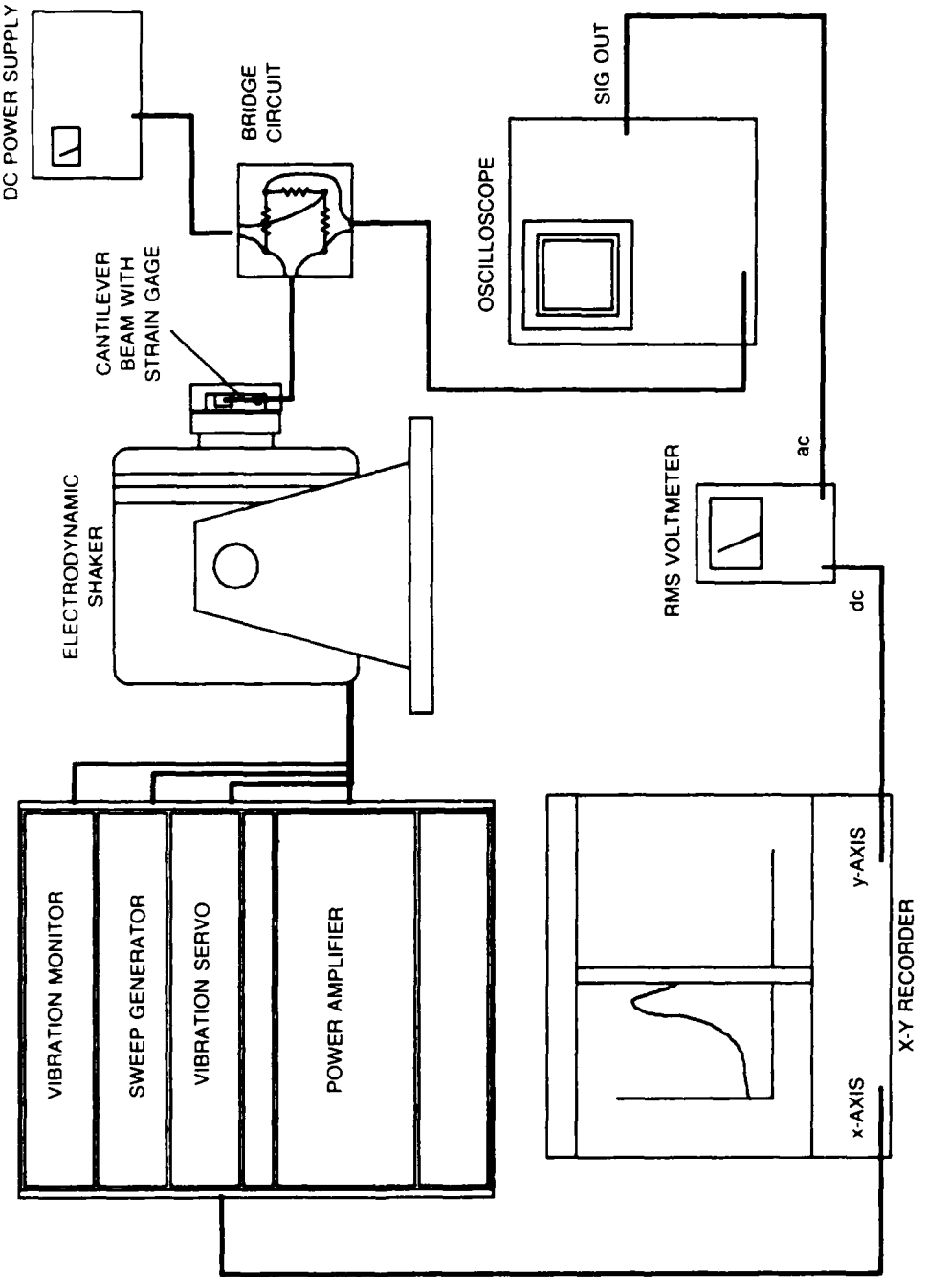

87-8-17-9

VIBRATION TEST APPARATUS

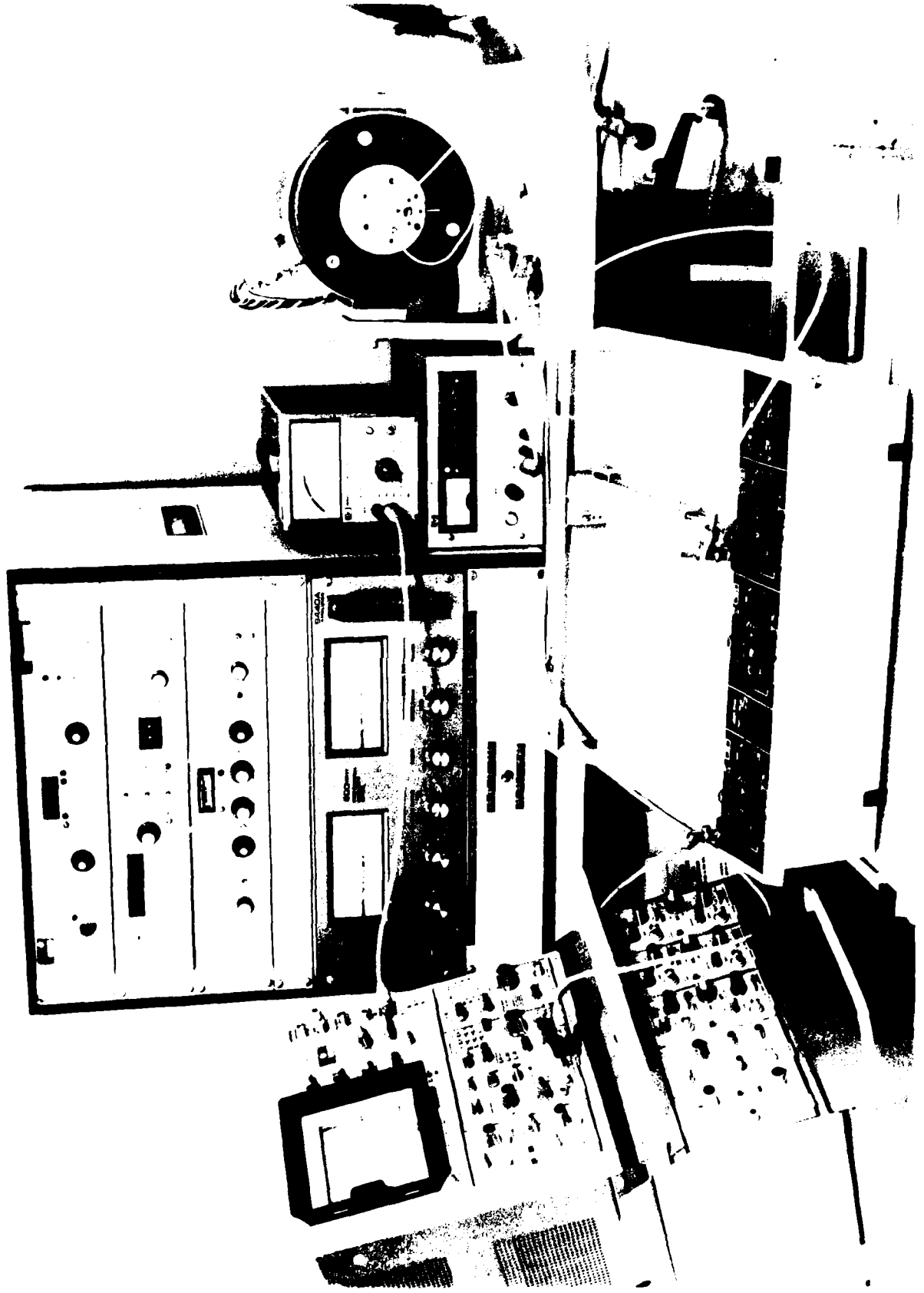

86 - 93 - 6

87 - 7 - 34 - 5

lowest mechanical resonance of the quartz beam and mass. The signal proportional to the amplitude of vibration was recorded as a function of frequency.

Figure 3-6 is a plot of relative amplitude versus frequency for device SGB3 showing the relative amplitude both with and without an oil damping fluid. The addition of the damping fluid produces a large reduction in amplitude and a shift of the resonance toward lower frequency. Several different kinds of oil with different viscosities were examined and all produced approximately the same level of damping. None provided enough damping to critically damp the beam. Most of the testing was done with Sargent-Welch No. 1407K-11 silicone vacuum pump oil.

Additional damping was sought with the addition of a fluid flow restriction in the form of a surface positioned close to the beam. The metal piece under the quartz beam in Fig. 3-3 provides a flat surface within 0.016" and extending over 95% of the area of the beam. As the beam vibrates, the motion of the beam forces the damping fluid to flow into and out of the thin cavity between the beam and the flow restricting surface. If the surface is positioned closer to the beam, the damping is increased. At some point, the energy required to pump the fluid back and forth equals or exceeds the energy of the mechanical oscillation and the vibrations cease. The beam is then critically damped. If that point can be reached with a "reasonable" beam-to-surface spacing, then critical damping can be achieved relatively easily. If the critical damping spacing is less than a few thousandths of an inch, implementation of the flow restriction would be considerably more difficult.

Figure 3-7 shows the increase in vibration damping obtained by positioning a surface 0.016" from one side of the quartz beam. The larger amplitude curve in Fig. 3-7 is the same as the smaller amplitude curve in Fig. 3-6 replotted at a magnified scale. Clearly the 0.016" flow restriction provides a substantial increase in damping, but the critical damping point still has not been reached. In Fig. 3-8 the effects of reducing the spacing to 0.011", 0.009", 0.008", and finally 0.006" is shown. Critical damping is achieved at approximately 0.009" spacing.

This experimental study of vibration damping of cantilevered quartz beams has shown that by implementing a flow restriction to impede the free flow of the damping fluid, critical damping can be achieved, and that the spacing at which critical damping is obtained is large enough (0.008" to 0.010" over 95% of one side of the beam) to be readily implemented in a device design. Because of the severe trade-off between acceleration sensitivity and the mechanical resonance frequency, it is absolutely necessary that vibration damping be employed in the SSBW accelerometer. The fact that critical damping can be achieved in a straightforward manner provides the device designer with added flexibility.

AMPLITUDE OF FORCED VIBRATIONS VERSUS FREQUENCY

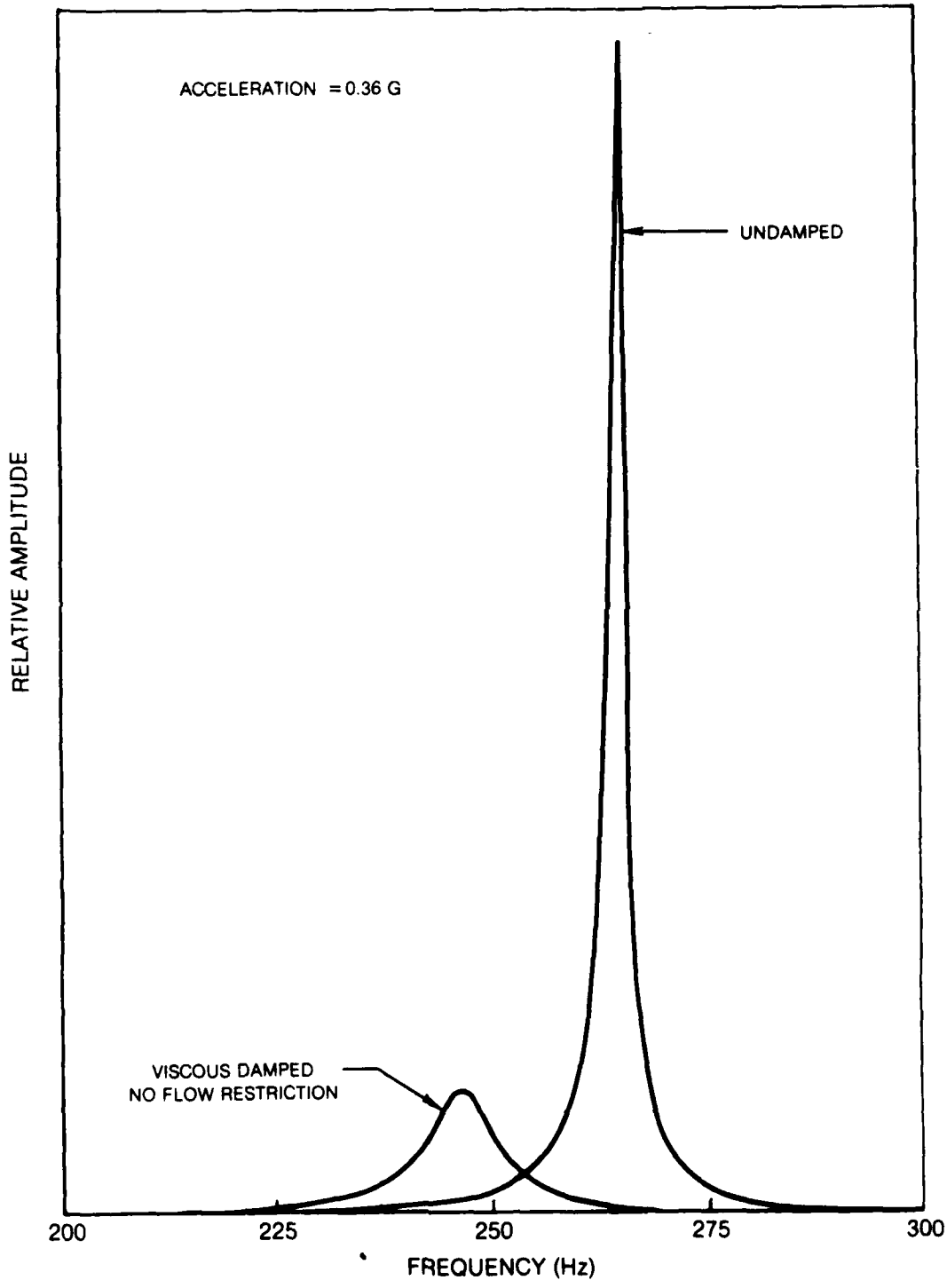

86-1-83-1

AMPLITUDE OF FORCED VIBRATIONS VERSUS FREQUENCY

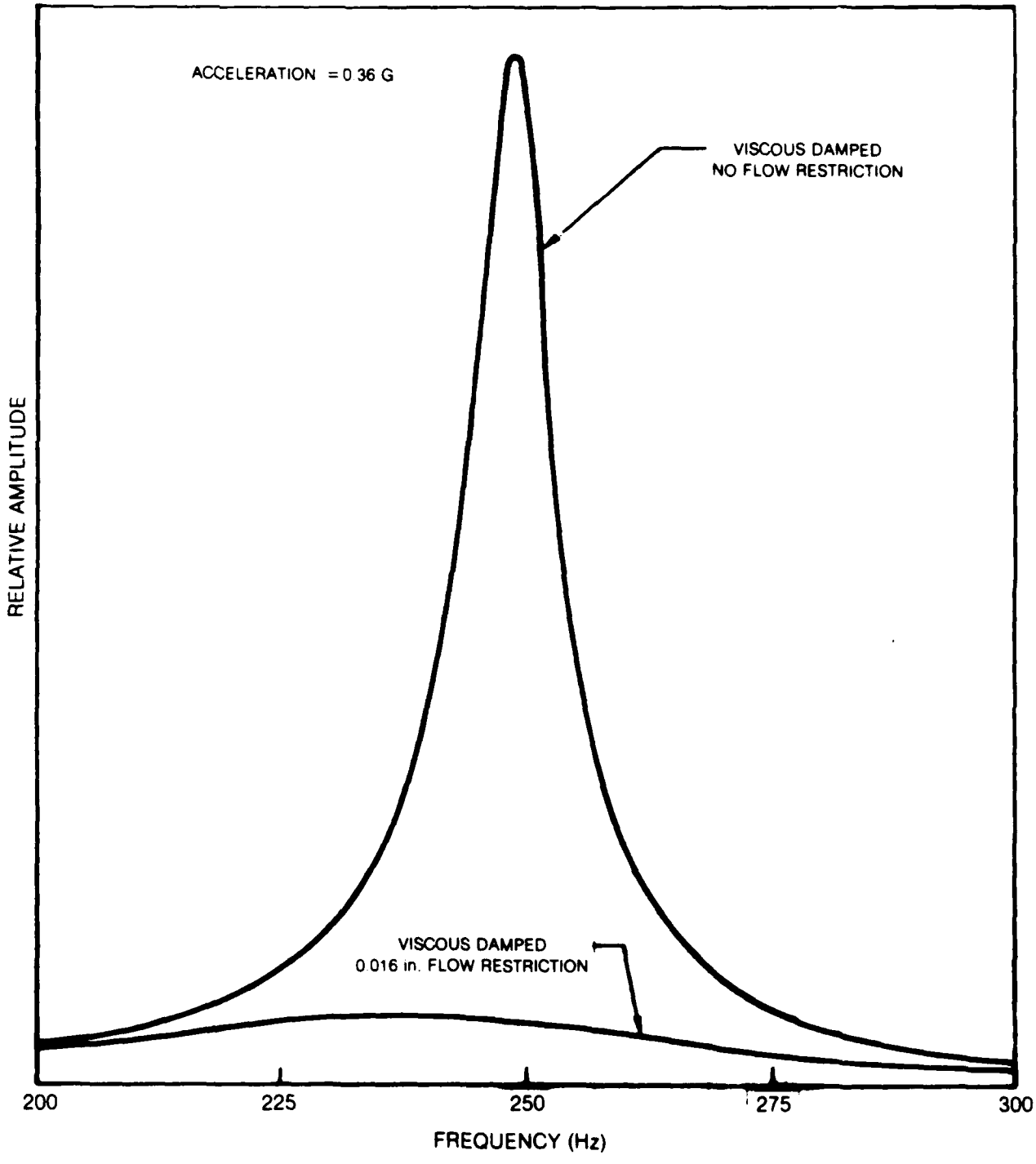

86-1-83-2

AMPLITUDE OF FORCED VIBRATIONS VERSUS FREQUENCY

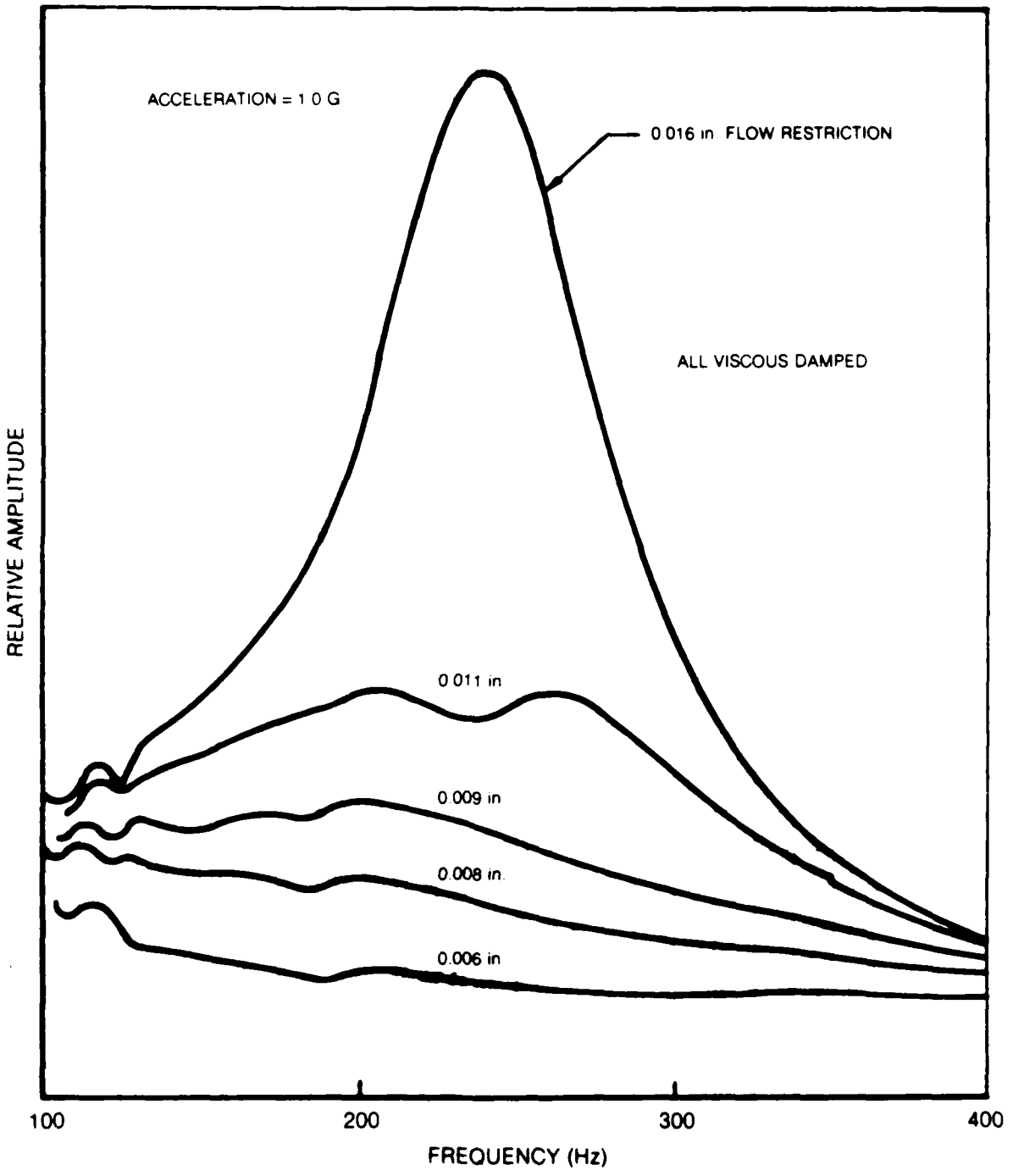

86-1-83-3

4.0 SSBW AGEING STUDY

4.1 Introduction

Devices which are intended to be incorporated into precision sensors must be stable over long periods of time. Thus the long term stability, or ageing, of SSBW delay lines on BT-cut quartz is of critical importance to the successful development of the SSBW accelerometer. The state-of-the-art of SAW device ageing is about 1.0 ppm/year (Refs. 10 to 14). It has been conjectured that SSBW devices should exhibit better ageing characteristics than SAW devices because the SSBW mode is less sensitive to the conditions on the surface of the substrate (Ref. 15). To date, however, there has been little reported work in the area of SSBW ageing, and no definitive studies. The purpose of the present ageing study was: 1) to establish the ageing rate of vacuum sealed SSBW delay lines, 2) to investigate the ageing of pairs of delay lines on the same substrate, and 3) to determine the ageing of SSBW delay lines immersed in a damping fluid.

A reference group of 12 SSBW delay line devices was prepared using state-of-the-art processing and packaging techniques. These devices were mounted into stable oscillator circuits, assembled together in the ageing test apparatus, and monitored for a period of one year. The performance of these twelve devices would set a baseline to which comparisons could be made.

Because the SSBW accelerometer, as it is presently envisioned, requires SSBW delay lines on both sides of the beam, the ageing of pairs of devices on opposite sides of a substrate is also of great interest. If the sources of ageing affect both devices in a like manner, it is possible that the two devices will age in such a way that they "track" one another. If that is the case, then the difference frequency extracted from the pair of SSBW oscillators using delay lines fabricated on opposite sides of the same substrate will have better ageing characteristics than either of the individual oscillators. Therefore, in addition to the primary group of single-sided devices, a second group of 6 double-sided devices (12 SSBW oscillators) was fabricated and included in the ageing study. Any sensor employing acoustic wave devices would naturally be designed to use pairs of devices to provide temperature compensation, so that the ageing of pairs is very important for acoustic sensor development.

The third group of 6 SSBW delay line devices included in the ageing study were sealed in silicone oil rather than being vacuum sealed. The design of the SSBW accelerometer is based upon the use of fluid damping to minimize the effects of mechanical vibrations, and it was therefore essential to determine the effects of the damping fluid on the ageing characteristics of the SSBW devices.

The remainder of Section 4 is divided into four parts. Section 4.2 describes the design, fabrication, and packaging of devices, Section 4.3

describes the oscillator circuits and the overall ageing test facilities, Section 4.4 presents the results of the study, and Section 4.5 lists the conclusions to be drawn from the ageing study.

4.2 Device Design, Fabrication and Packaging

4.2.1 SSBW Delay Line Design

Because the losses in SSBW delay lines on BT-cut quartz are rather high compared to SAW delay lines or even SSBW delay lines on AT-cut quartz, the delay line designs employed in this study were optimized for minimum loss, using the work performed under AFOSR Contract No. F49620-84-C-0006 as a guide (see Ref. 6). The wavelength, and hence the frequency of the SSBW delay line, was determined by: 1) the need to keep the overall size of the delay line small enough that it would fit onto a cold-weld header, and 2) the desire to have the photomasks made at 1X, directly from the pattern generator. The finger width for the split-finger transducers that are necessary for SSBW devices is one-eighth wavelength. Therefore, with a pattern generator with a 2.5 micron lower limit on exposure width, the minimum wavelength transducer that can be generated is 20.0 microns. The SSBW velocity on BT-cut quartz is 3330 m/sec, thus the transducer center frequency is 166.5 MHz. In order to provide a frequency offset for the back-to-back devices, a second delay line pattern with a wavelength of 20.4 microns was also generated. This wavelength produces a frequency of 163.2 MHz giving a frequency separation of 3.3 MHz.

Figure 4-1 shows a printout of a computer analysis of the SSBW delay line design employed. The transducer length was first chosen to minimize losses and the acoustic aperture was then chosen to provide a 50 ohm match to the external circuit. The width of the fingers in these transducers is ideally 2.5 microns. The actual width of the fingers on the quartz substrate after processing is somewhat greater, varying from about 2.8 microns to 3.0 microns. If the finger to gap (f/g) ratio is adjusted to account for the increased finger width, the acoustic aperture must also be adjusted to provide the same transducer capacitance. As a result, rather than the computed 66.2 wavelength aperture, the actual aperture used was 60 wavelengths for the 20.0 micron wavelength design and 62 wavelengths for the 20.4 micron wavelength design. (The finger width enlargement was less with the 20.4 micron design because the pattern generator tape called for the same 2.5 micron fingers rather than 2.55 microns = wavelength/8). Figures 4-2 and 4-3 are photographs of two of the photomasks used in this study. The same SSBW delay line designs that were used in the ageing study were also used in the laboratory prototype accelerometers to be described in Section 5.

The transducer metallization was 100 angstroms of chrome and 1000 angstroms of aluminum, and surface electrodes rather than recessed electrodes were used. Unlike the case of SAW devices where recessed electrodes reduce scattering,

SAW DELAY LINE ANALYSIS

a)

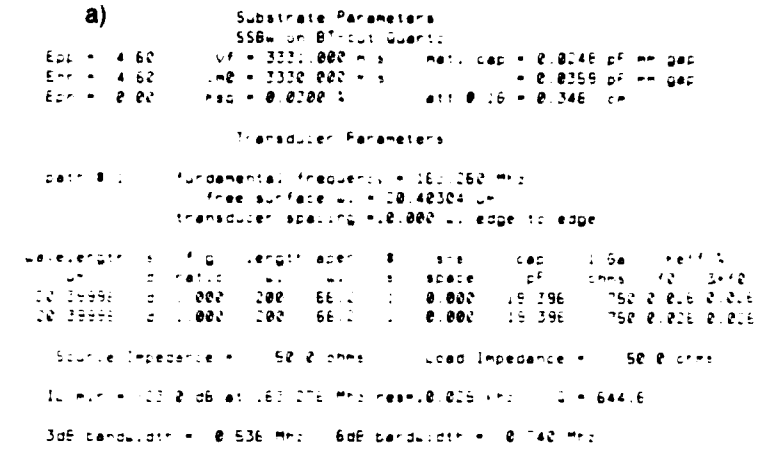

b) INSERTION LOSS VS FREQUENCY

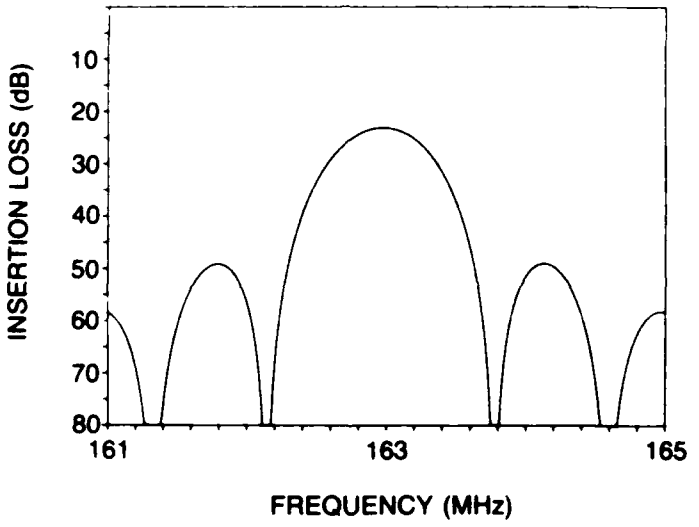

c) INPUT IMPEDANCE VS FREQUENCY

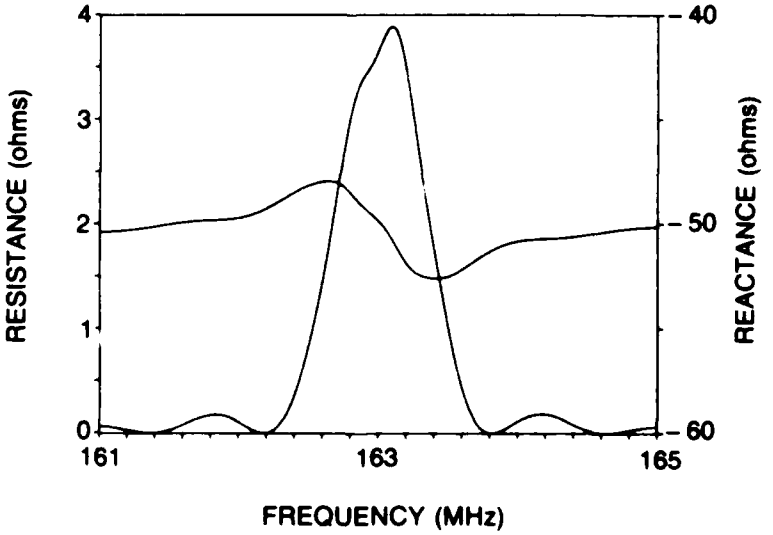

87-8-17-11

FIG. 4-2

SSBW 14

WL20P4 200X62 TRUD

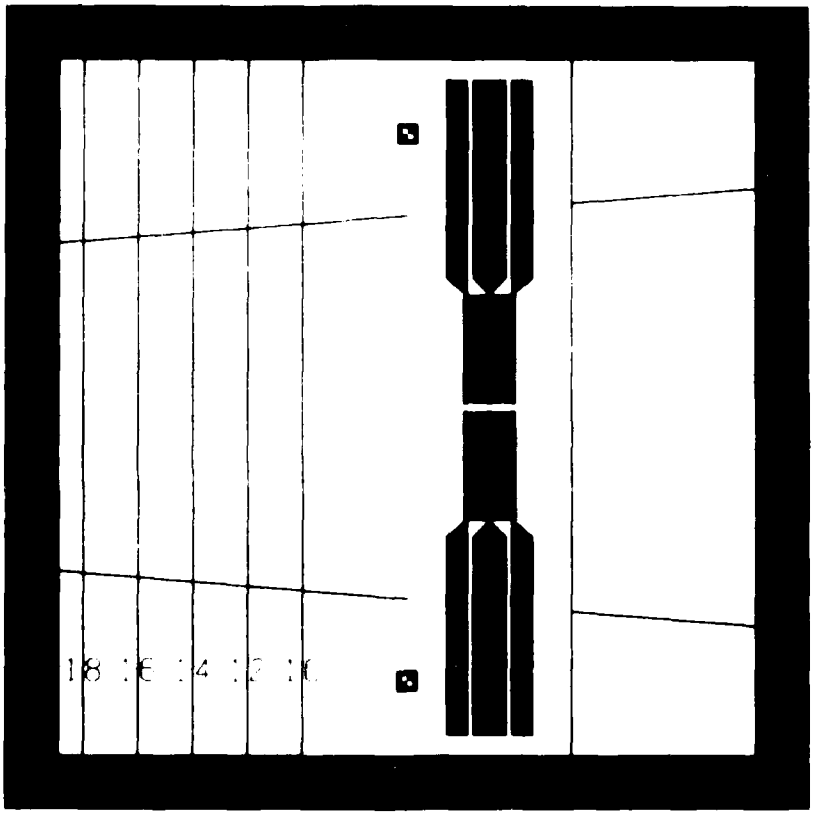

UNITED
TECHNOLOGIES
RESEARCH
CENTER

SSBW 15

WL20P4 200X62 TRUD

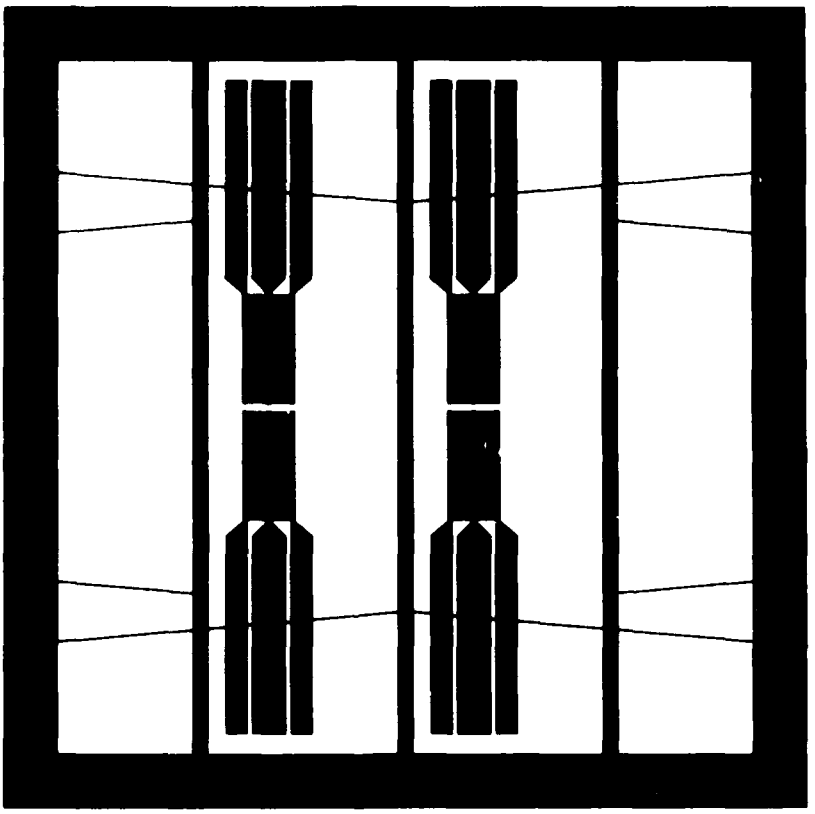

UNITED
TECHNOLOGIES
RESEARCH
CENTER

recessed electrodes on SSBW devices were found experimentally to increase scattering and to lead to higher losses. Figure 4-4 shows IL versus frequency plots for a typical SSBW delay line in a 50 ohm circuit. The characteristic is seen to be very clean, and the 29.7 dB loss at the minimum is on the high side of the 28.5 to 30.0 dB range observed with these devices. These IL values are optimum for SSBW's on BT-cut quartz.

4.2.2 Quartz Substrates

The +50.5 degree rotated Y-cut quartz substrates (BT-cut) were specified to have been made from 0.035 in. thick, premium Q synthetic quartz with an orientation accuracy of ± 15 minutes of arc. Tolerances on the substrate specifications were made as tight as possible without inducing unnecessarily high costs. Additionally, the vendor was required to make X-ray orientation determinations of the plate and edge normals for each substrate and to supply that information with the substrate. Those measurements fix the orientations within 1 minute of arc. Table 4-1 lists the ageing study devices according to group and indicates the plate normal and edge normal orientations. The variation of the orientations about their nominal values is not expected to influence significantly the ageing of the devices. The precise orientation is most critical when attempting to control the temperature characteristics of these devices. In order to obtain a temperature turnover within a few degrees celsius in the 20 to 60 degree Celsius range, the substrate orientation has to be controlled to better than one minute of arc (see Fig. 2-3). Such orientation precision is costly and was not considered necessary for the purposes of the present study. The substrates were etch-polished (Ref. 16) to minimize the surface damage and the resulting stresses caused by polishing alone.

4.2.3 Processing and Packaging of Substrates

Studies of the ageing of bulk wave and SAW crystal oscillators have shown that there are two primary sources of device ageing. The two sources are: 1) stresses and stress relaxation resulting from thermal expansion differences and changes in the metal films due to migration, and 2) the adsorption and desorption of contaminants within the sealed container. Both ageing mechanisms are temperature dependent. While neither thermal stresses nor contamination can be eliminated entirely, in the best oscillators they are minimized through careful attention to the attachment of electrical leads and the mounting of the oscillator crystal, and the use of processing techniques known to minimize contamination of the crystal and the environment within the packaged device. The processing of devices for the SSBW ageing studies was carried out with great care using proven techniques in order to minimize both substrate stress and contamination of the package environment.

The single sided substrates to be vacuum sealed were processed according to the following schedule:

FIG. 4-4

INSERTION LOSS VS FREQUENCY FOR SSBW ON BT-CUT QUARTZ

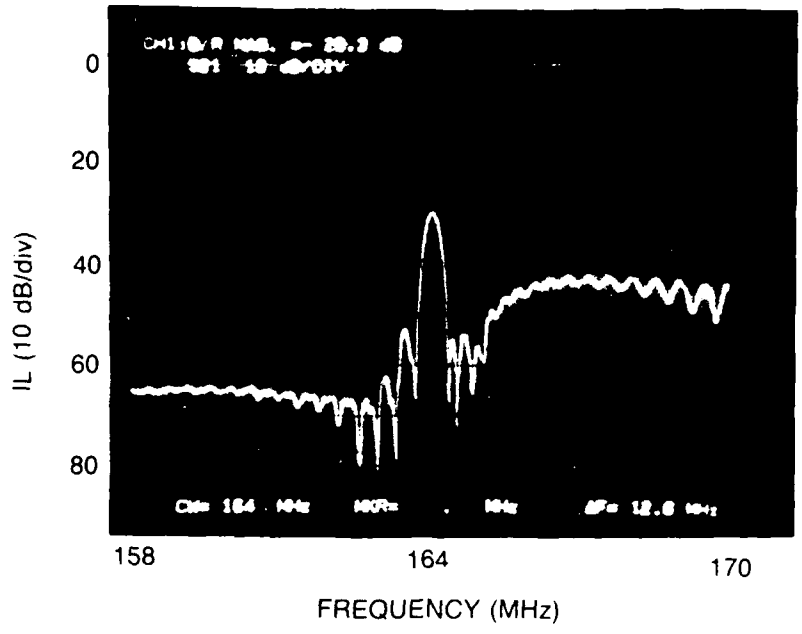

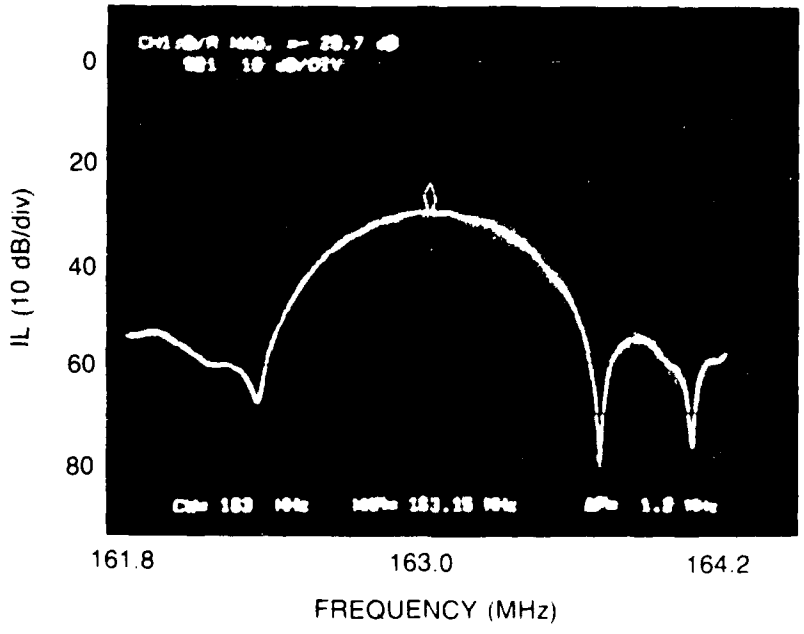

87 7 34 8

TABLE 4-1

LISTING OF SSBW AGEING TEST DEVICES AND SUBSTRATE ORIENTATIONS

Device No.	Type	Substrate Normal Angle	X-axis Face Angle
B366	.	50°41'(+11)	X + 4'
B368	double	50°28'(-2)	X + 9'
B369	sided	50°26'(-4)	X - 5'
B371	vacuum	50°35'(+5)	X + 0'
B372	sealed	50°27'(-3)	X - 6'
B374	.	50°29'(-1)	X - 2'
B397a	.	50°24'(-6)	X - 3'
B399a	.	50°27'(-3)	X - 10'
B399b	.	50°27'(-3)	X - 10'
B402a	single	50°31'(+1)	X + 11'
B402b	sided	50°31'(+1)	X + 11'
B403a	vacuum	50°27'(-3)	X - 8'
B403b	sealed	50°27'(-3)	X - 8'
B404a	.	50°39'(+9)	X - 5'
B404b	.	50°39'(+9)	X - 5'
B405a	.	50°34'(+4)	X + 3'
B414	.	50°26'(-4)	X - 7'
B415	.	50°33'(+3)	X - 3'
B394a	.	50°35'(+5)	X + 6'
B394b	.	50°35'(+5)	X + 6'
B396a	oil	50°25'(-5)	X - 2'
B396b	sealed	50°25'(-5)	X - 2'
B401a	.	50°22'(-8)	X - 9'
B401b	.	50°22'(-8)	X - 9'

1) Through cleaning of the substrate with high purity solvents -

2) Baking in air at 200 degrees celsius for 18 hours - this baking step removes low volitility contaminants and adsorbed water vapor from the quartz crystal

3) Application of photoresist and exposure of SSBW pattern -

4) Development of exposed photoresist -

5) Thermal evaporation of 100 Å of chrome and 1000 Å of aluminum -

6) Lift-off of metal and photoresist in alcohol - a high purity alcohol is used

7) Recoating with photoresist - to protect surface during subsequent substrate cutting operation

8) Cutting of substrate to final size -

9) Removal of photoresist and cleaning in high purity alcohol -

10) Mounting of substrate onto cold-weld header - the substrate is held in place on the header by the same 1 mill wires used to make the electrical connections to the device - (see Fig. 4-5)

11) Ultra-violet/ozone cleaning step - exposure to intense UV light for a short period of time is a highly effective means of removing a variety of organic contaminants - (see Ref. 17) - the device is then immediately mounted into the cold weld sealing system for vacuum baking and sealing -

12) Vacuum bake at 200 C and 10^{-6} torr for 18 hours in cold weld sealing system - this system is oil free - the chamber is roughed and pumped by cryogenic pumps - (see Figs. 4-6 and 4-7)

13) Cold weld sealing of package at 100°C and 10^{-7} torr -

The processing schedule was designed to produce a substrate and an environment that is as free of contaminants as possible, and to provide a stress free mounting for the substrate. The header mounted substrate and the package lid were both UV/ozone cleaned immediately prior to mounting in the vacuum chamber of the cold-weld sealing system. Cold-weld sealing is a very positive method of vacuum encapsulation that produces a reliable vacuum tight seal. Mounting of the substrate to the header using only the bond wires insures that thermal expansion differences between the quartz substrate and the kovar header will not stress the substrate when temperatures are varied. The processing and packaging of these

FIG. 4-5

SINGLE SIDED SSBW SUBSTRATE BONDED TO COLD WELD HEADER

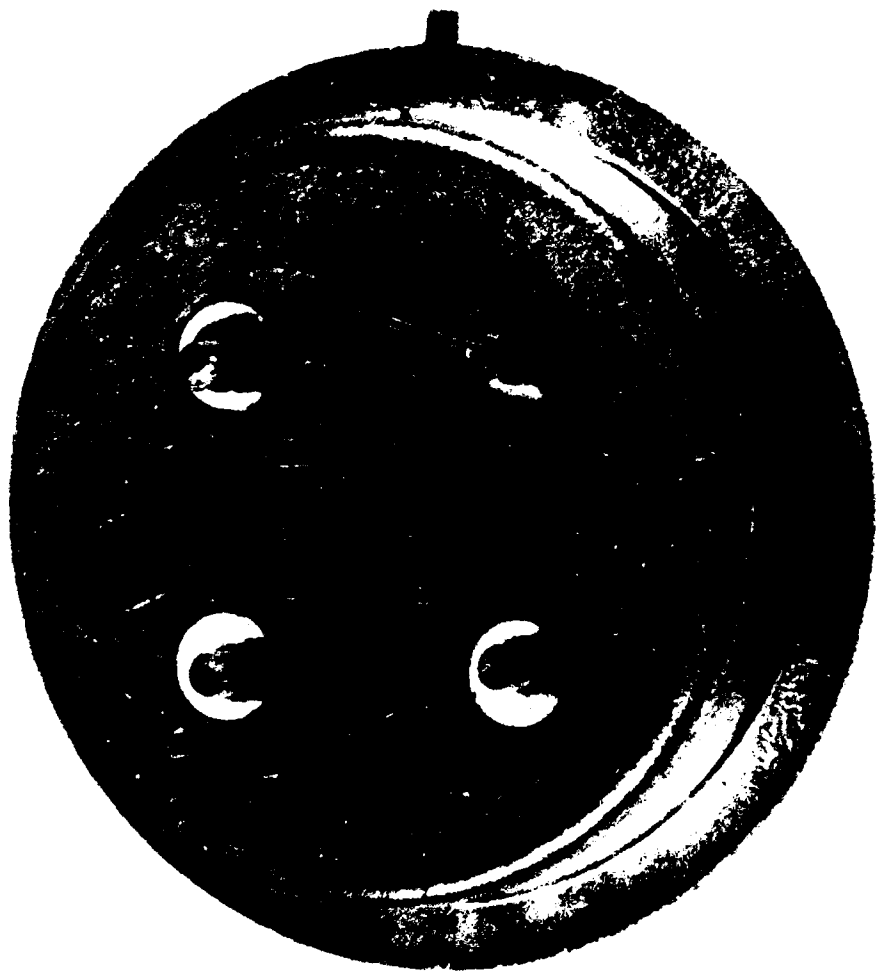

87 - 205C

87 - 7 - 34 - 9

FIG. 4-6

UTRC'S HIGH VACUUM COLD WELD PACKAGE SEALING SYSTEM

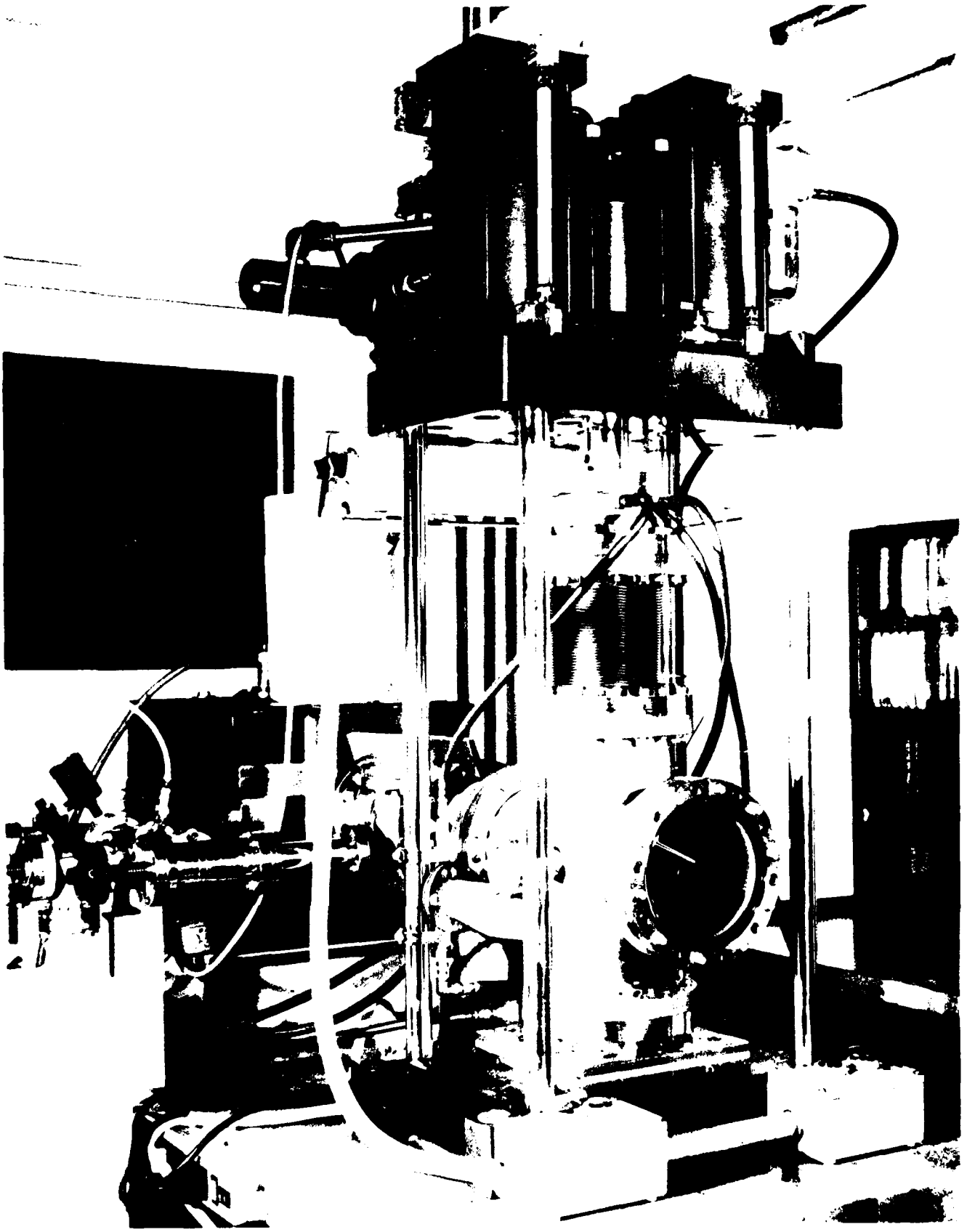

CLOSE-UP VIEW OF COLD WELD PACKAGE SEALING CHAMBER

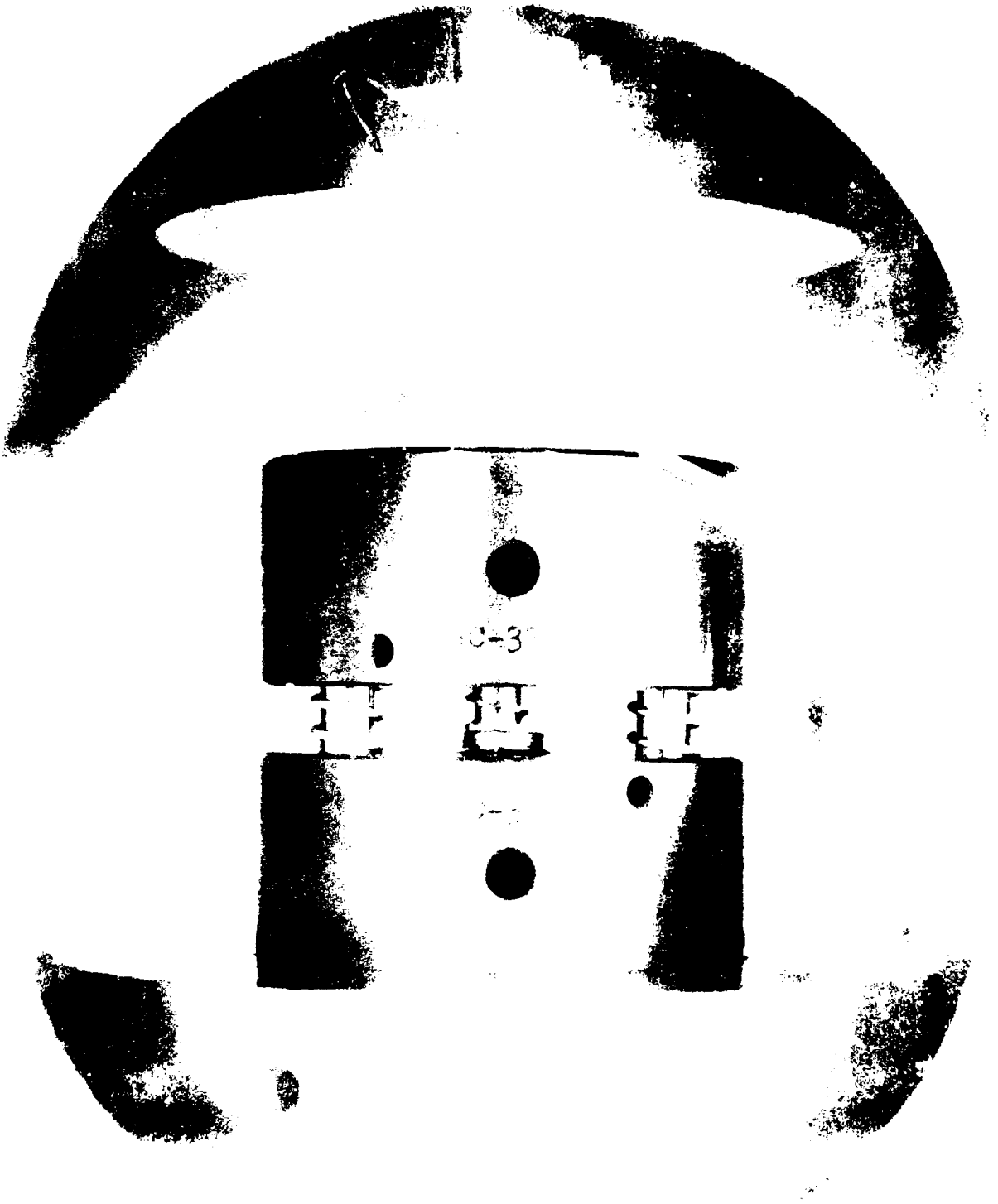

devices was carried out with a great amount of care in anticipation of achieving state-of-the-art ageing results for SSBW delay lines.

The processing of the double sided devices basically followed a similar processing schedule except that steps #3 thru #6 were repeated in order to produce the second delay line pattern on the back side of the substrate. These double sided devices turned out to be much more difficult to produce than anticipated. In addition to the obvious problem of having to protect one surface while the other was being patterned, other problems arose to greatly complicate the processing of the double sided devices.

For example, reflections from the first metallization made achieving a good defect free transducer pattern on the reverse side almost impossible. Fortunately, during the time this work was in progress, a new type of photoresist, specifically designed to alleviate this back side reflection problem, became available (Ref. 8).

A second major problem was the attachment of the electrical leads to the substrate. Unlike the case with the single sided devices, the double sided devices could not be wire bonded. Instead, the transducer pads were built up with a layer of copper followed with a layer of nickel, and gold ribbon measuring 0.002 in. by 0.010 in. was then soldered to the pads. After mounting of the substrate to the header, the gold ribbons were soldered to the header pins (hot leads) and body (ground leads).

The double sided substrates were mounted to the header on edge as shown in Fig. 4-8 using polyimide cement. This cement is suitable for an ageing study from a contamination standpoint since it does not outgas after the vacuum bake, step #12. Bonding of the substrate to the header with polyimide does raise the possibility of introducing thermal stresses. In order to minimize such stresses, the bond area was localized to one end of the substrate and kept as small as possible. The principal purpose of the double sided devices was to assess the ageing of the two devices with respect to one another, and the possible introduction of thermal stresses due to the polyimide bond was not expected to interfere with the interpretation of the ageing data.

The devices to be aged in oil presented a special packaging problem. Because the IL of these devices in oil was from 4 to 6 dB greater than the IL in air or vacuum, it was necessary to find a package with better feedthru characteristics than that of the cold weld headers. The feedthru of the headers was only 40 to 45 dB down, and the IL of the devices in oil was between 33 and 36 dB. A small IC flatpack with a feedthru level of -55 dB was selected.

The processing of these substrates followed the same schedule as the single sided devices to be vacuum sealed up to step #10. The devices to be aged in oil were mounted into the flatpack using only bond wires as shown in Fig. 4-9.

DOUBLE-SIDED SSBW SUBSTRATE MOUNTED ON COLD-WELD HEADER

SINGLE-SIDED SSBW SUBSTRATE BONDED INTO IC FLATPACK

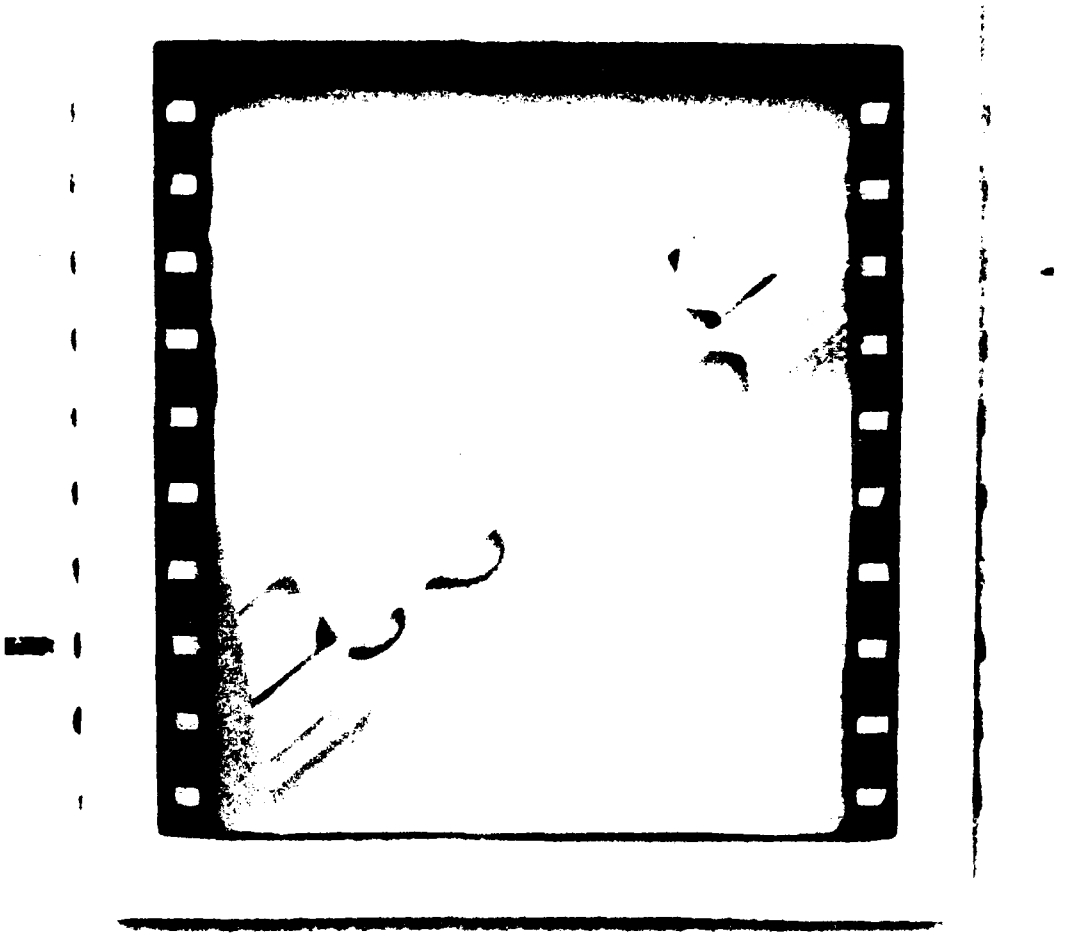

Again, this mounting technique insures that thermal expansion differences between the quartz substrate and the package will not lead to stresses in the substrate with changes in temperature. After bonding the device into place, the flatpack was sealed by epoxying on an aluminum cover with a small hole. A silicone oil was injected into the cavity of the flatpack with a hypodermic needle and the hole then sealed with epoxy.

4.3 Ageing Test Apparatus

4.3.1 SSBW Oscillator Circuits

Schematics of the two RF oscillator circuits used in the ageing study are shown in Fig. 4-10. The SSBW devices that were aged in oil required more gain in the circuit because of their higher loss, hence two 20 dB amplifiers were used rather than the 20 dB and 14 dB combination used for the vacuum sealed devices. The amplifiers were high quality Avantek 502's and 512's. A series inductor was employed to trim each circuit to provide the correct loop phase delay so that the frequency of oscillation corresponded to the IL minimum for the SSBW device. The 15 pF capacitor served to shunt the 3rd harmonic to ground to prevent the circuit from oscillating at the 3rd harmonic frequency.

Figure 4-11 is a photograph showing both sides of the printed circuit board (PCB) and the aluminum chassis that contained the PCB. The PCB was designed for the double sided devices, that is, it contained two separate oscillator circuits. The same board was used for the single sided devices, using just half of the board.

4.3.2 Ageing Test Facilities

Figure 4-12 is a photograph of the stack of 24 chassis as they were assembled together for the ageing test. Threaded rod and the aluminum plates at the top, bottom, and middle of the stack were used to hold the stack together. The three plates also contained the six Analog Devices AD590 semiconductor IC temperature transducers from which the average temperature of the stack was obtained. Figure 4-13 is a sketch of the layout of the devices within the stack showing the relative position of the temperature probes.

Figure 4-14 is a photograph of the complete ageing test facility. The oscillator stack was placed in a Tenny Jr. environmental control chamber. This unit is capable of holding any temperature in the -80°C to +200°C range within ± 0.15°C. For the SSBW ageing test the temperature was set to +60°C. The output from each oscillator was connected via coaxial cable to a computer controlled RF switch complex. All frequency measurements were taken with a Hewlett-Packard 5345A electronic counter. A Hewlett-Packard 9816 desktop computer was dedicated to the SSBW ageing study.

SSBW AGING STUDY OSCILLATOR CIRCUITS

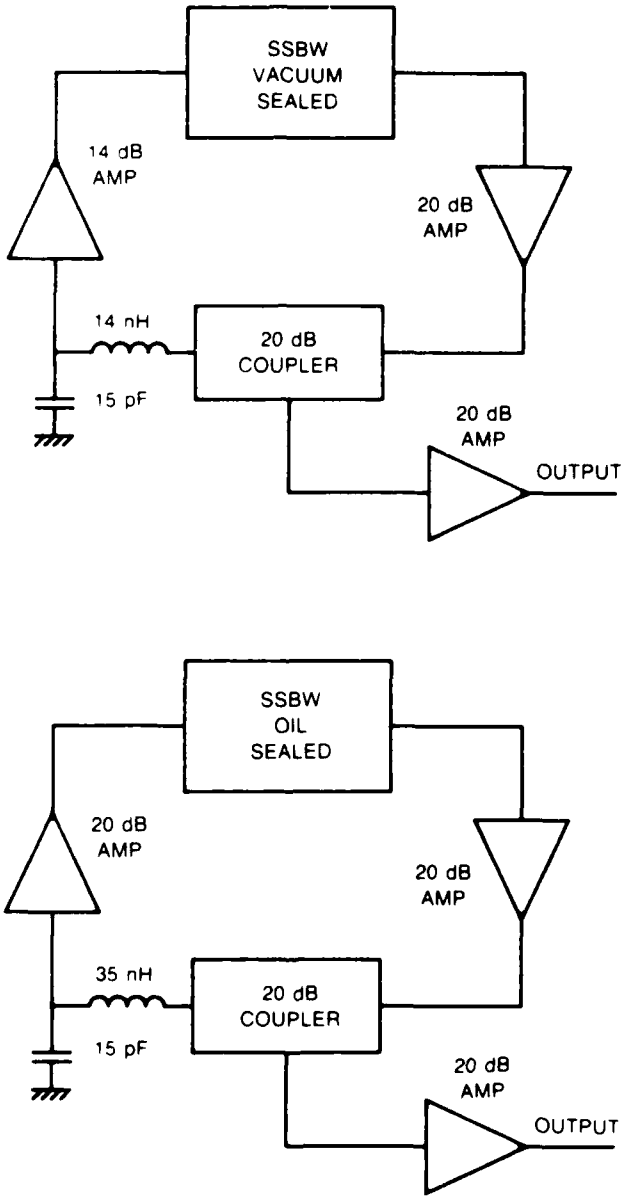

87-8-17-18

FIG. 4-11

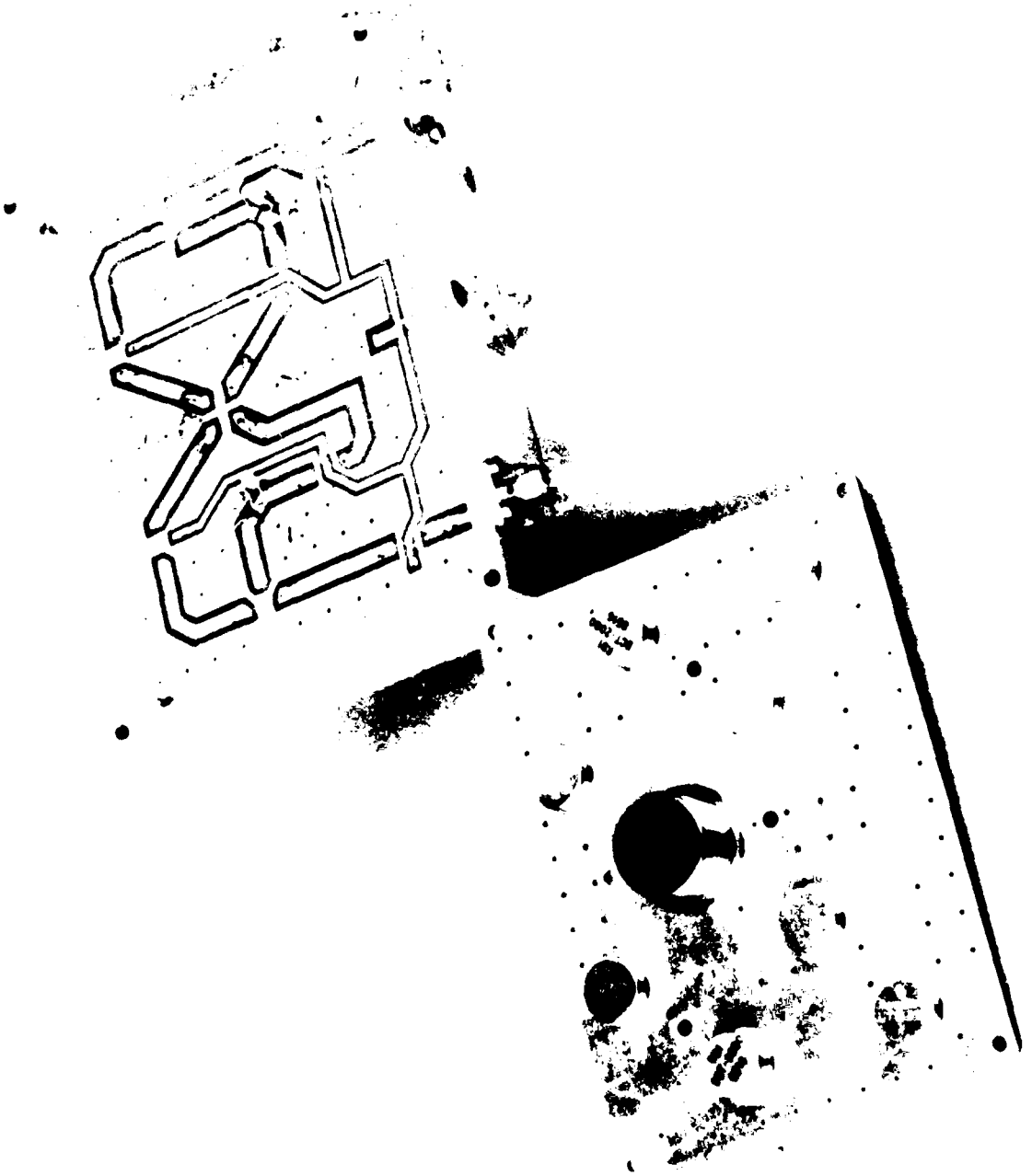

DUAL RF OSCILLATOR CIRCUIT BOARD AND CHASSIS

ASSEMBLY OF SSBW OSCILLATOR CHASSIS FOR AGING TEST

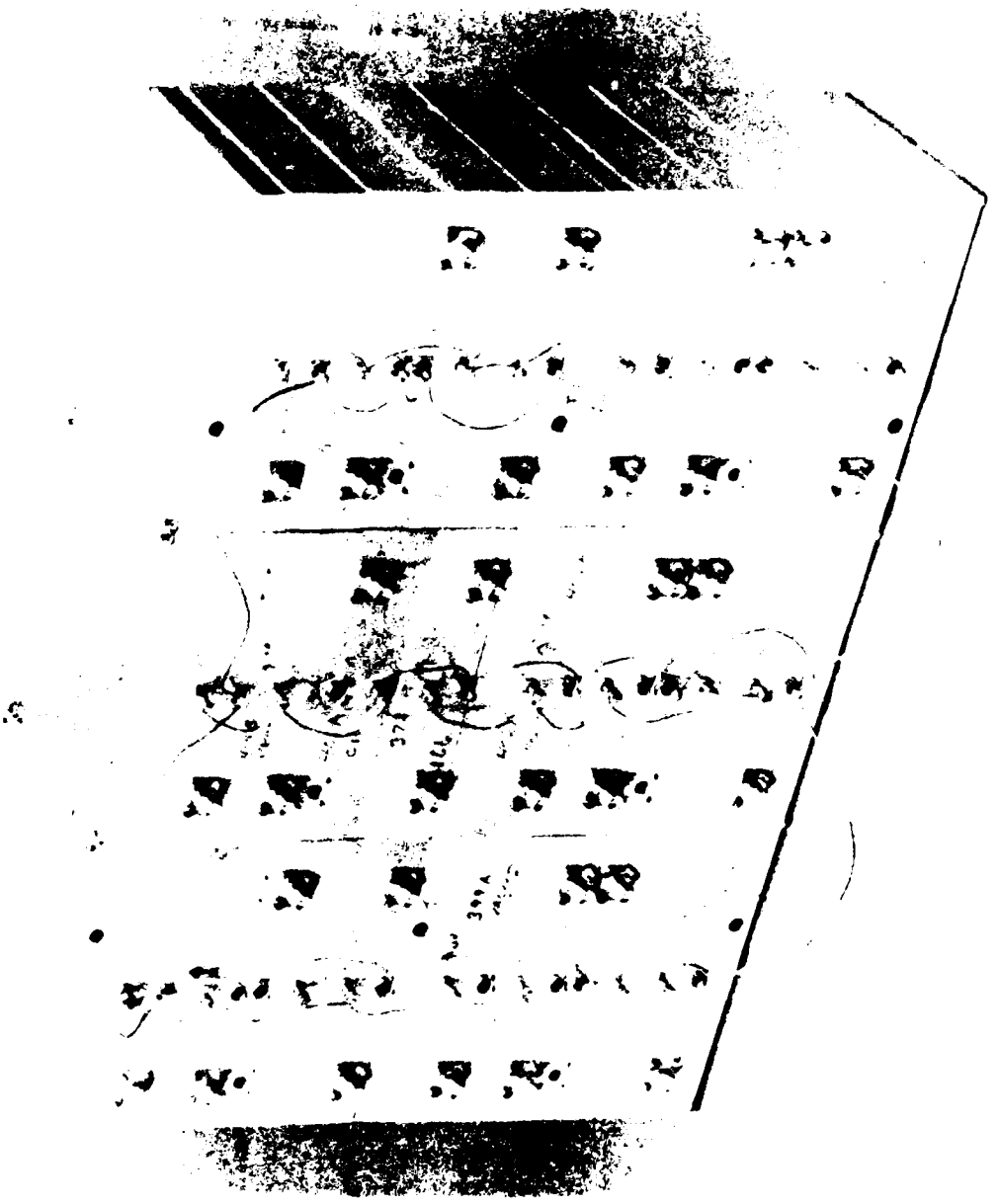

ARRANGEMENT OF SSBW OSCILLATOR CHASSIS & THERMOCOUPLES WITHIN AGING STACK

T5 O		O T6
415 VACUUM	414 VACUUM	404a VACUUM
403a VACUUM	404b VACUUM	402b VACUUM
394 OIL	401a OIL	401b OIL
371 DOUBLE	372 DOUBLE	374 DOUBLE
T3 O		O T4
399a VACUUM	402a VACUUM	405a VACUUM
336 DOUBLE	368 DOUBLE	369 DOUBLE
394a OIL	396a OIL	398a OIL
397a VACUUM	403b VACUUM	399b VACUUM
T1 O		O T2

87-8-17-21

FIG 4-14

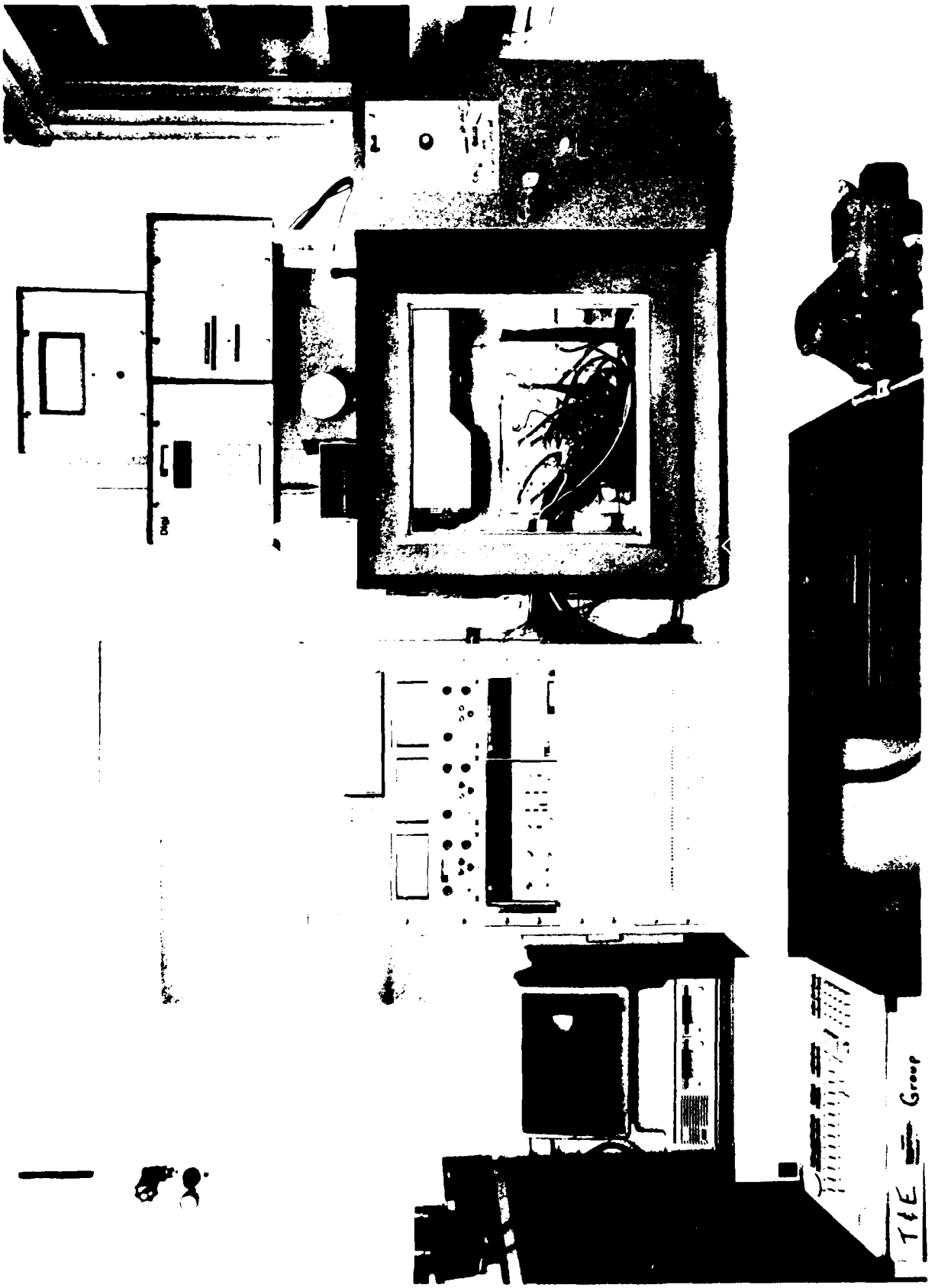

SSBW AGING TEST FACILITY

4.3.3 Ageing Data Acquisition

The computer was programmed to interrogate the 30 oscillators and the 6 thermocouples twice each day, starting at 1 AM and 1 PM, and to store the data on a floppy disc. During each of the two sampling periods, the frequency of each of the oscillators was sampled 300 times with a one second gate time (one hertz accuracy) and the average value computed and stored. Sampling of all 30 oscillators required 2.5 hours. Temperature data was taken 4 times during this period, once prior to sampling of the oscillators, and then after groups of 10 oscillators had been sampled. Each of the 4 temperature measurements was an average of the readings from the 6 temperature probes.

4.4 Results of SSBW Ageing Study

The 30 SSBW devices in this ageing experiment were not "pre-aged" in any way. Researchers studying the ageing of SAW devices have noted that devices initially age at faster rates before settling down to a lower rate as the test continues (Ref. 10). They therefore "pre-age" their devices at an elevated temperature for several weeks before beginning the actual ageing test. Except for the fact that the first of the SSBW devices fabricated for this test were ready several months before the last device was finished, there was no deliberate "pre-ageing" of any devices. While the ageing of 4 SSBW devices (1 of the double sided vacuum sealed devices and 2 of the oil packaged devices) was severe, no devices were "lost" during the course of the 1 year ageing experiment due to faulty bonding, circuit failures, or other causes.

Several events occurred during the course of the year long ageing test period that caused perturbations in the data. At the 4 week point, power was lost over a weekend. Data taking was resumed the following Monday after the temperature was stabilized in the Tenny Jr. chamber. A frequency counter malfunctioned during the 33rd week requiring replacement of the counter and this again resulted in the loss of several days data. During the 32nd week and again during the 39th week, there were unexplained increases in the temperature of a degree or less. These increases were probably foretelling the more serious problems to arise with the chamber starting during the 41st week. At that point, one stage of the compressor on the chamber's refrigeration system failed. Since the temperature appeared to be holding without the compressor with only a rise of about 1°C, it was decided not to disrupt the chamber to repair the compressor, but to continue the ageing test at the slightly elevated temperature. Unfortunately the temperature did not remain stable at the slightly elevated level but continued to slowly increase over the next 10 weeks. Finally, at the end of the 51st week, the second stage compressor failed and the temperature rose abruptly. These events are clearly evident in Fig. 4-15 where the chamber temperature is plotted as a function of time. Also note in the figure that the temperature

FIG. 4-15

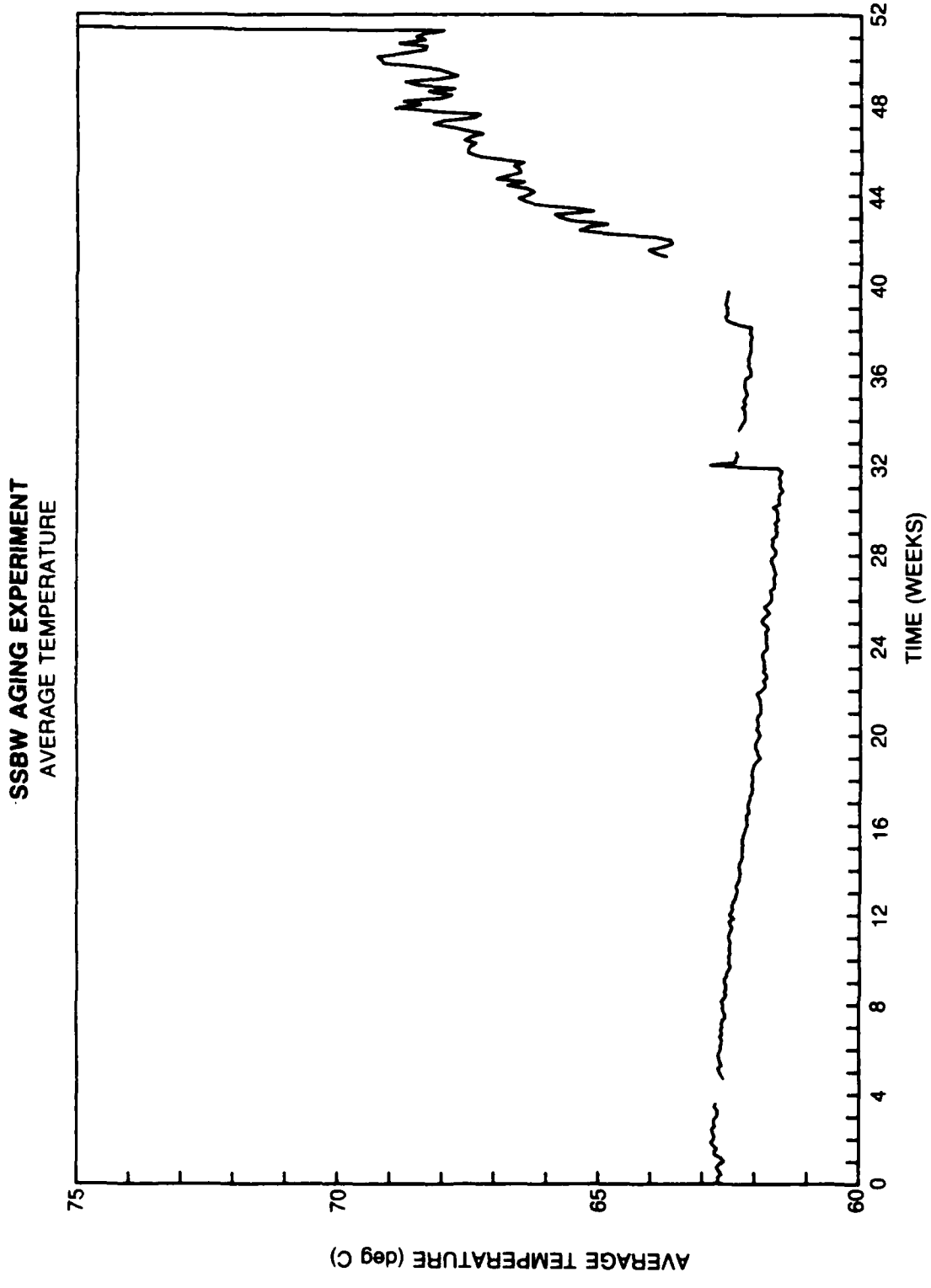

87-8-17-23

decreased steadily during the first 32 weeks of the test period, dropping by 1.2 C during that time (0.038°C/week).

The result of these problems is that the data for the last 20 weeks of the one year test period is of limited usefulness. The data does demonstrate the temperature compensation capabilities of the double sided devices, and plots of the frequency difference between the 2 oscillators from devices on the same substrate illustrate this. The principal conclusions on ageing of SSBW devices will be drawn from the data for the first 222 days of the ageing study. Plots of the data for all 30 oscillators for the entire year long study are presented as Appendix 1.

Ageing is measured by the change in SSBW oscillator frequency as a function of time. The frequency change is given in units of parts per million, i.e.,

$$ppm = [f(t) - f(t=0)]/f(t=0)$$

where f(t=0) is the frequency at the start of the test and f(t) is the frequency at time t.

Table 4-2 summarizes the ageing data for all 30 SSBW oscillators. Included in the table are: (1) the ageing at the 222nd day, (2) the ageing rate for each device, and (3) the projected ageing for the full 1 year period. The ageing at the 222nd day is actually an average of the data for the 10 day period up to and including the 222nd day. This was done to average out daily fluctuations and provide a more accurate estimate of the ageing to that point. The ageing rate was obtained by computing the linear fits to the data for the 100 day period from day 123 to day 222. The linear fits were found to be excellent representations of the ageing data for that 100 day period. The projected value for the ageing at the end of the 1 year test period was then computed from the following expression.

Ageing at 1 year = Ageing at 222nd day + Ageing rate*(365-222)/365

Clearly there is the possibility of error in this method, however, lacking the appropriate data for the full 365 days, some approximate approach was required to arrive at an ageing rate in ppm/year. Another option was to simply project the value at the 222nd day to 1 year, i.e., Ageing at 222nd day*(365/222). This latter approach was rejected because most of the devices exhibited faster ageing at the beginning of the test period before settled down to a lower rate as time progressed.

4.4.1 Ageing of Single Sided Vacuum Sealed Devices

Figure 4-16 presents the data for the 12 vacuum sealed single sided SSBW delay line oscillators for the first 222 days of the ageing test period. All but

FIG. 4-16

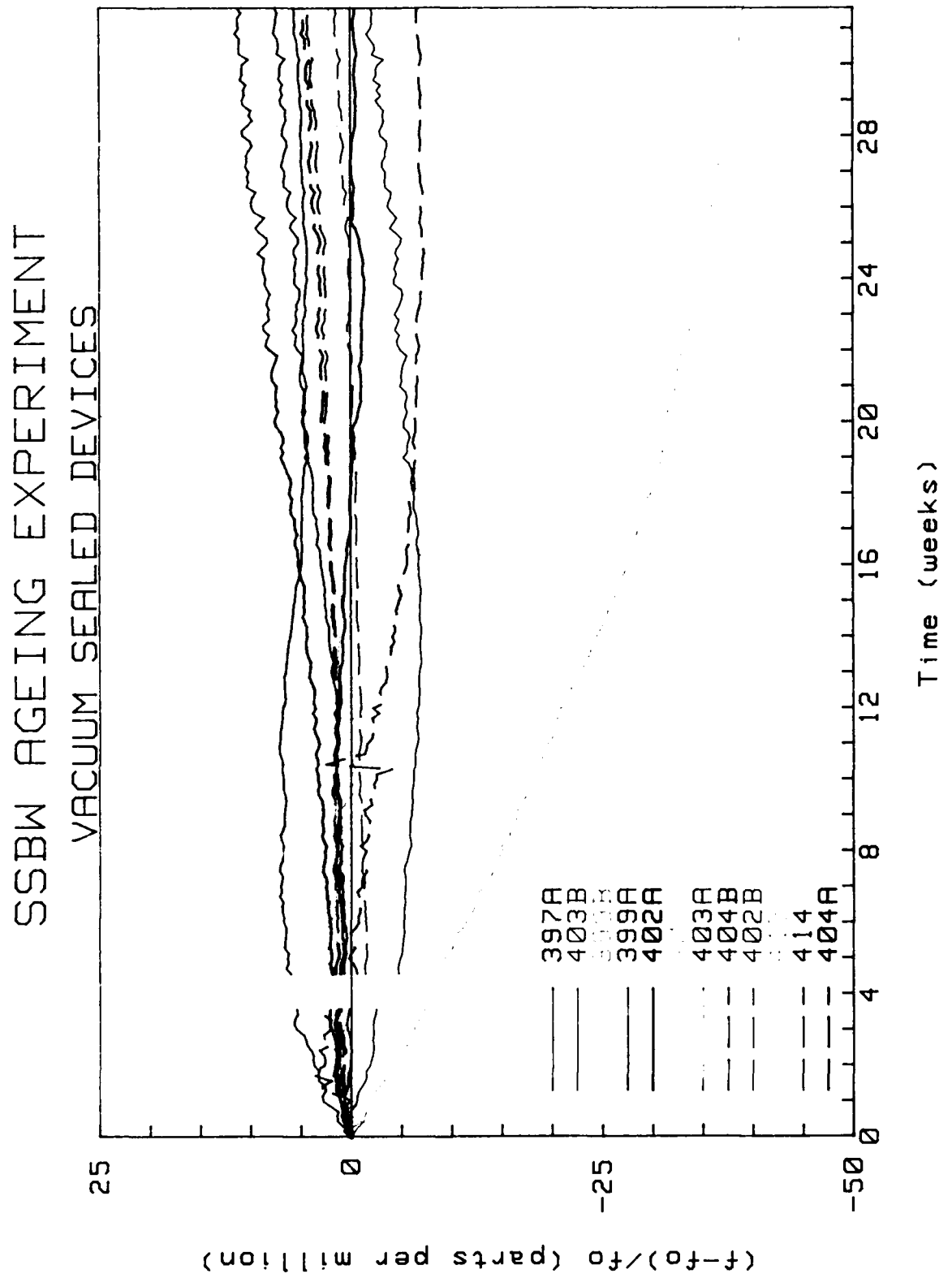
SSBW AGEING EXPERIMENT
VACUUM SEALED DEVICES
(f-fo)/fo (parts per million)
25
0
-25
-50
0
4
8
12
16
20
24
28
Time (weeks)
397A
403B
399A
402A
403A
404B
402B
414
404A

2 of the 12 oscillators are within ± 11.1 ppm of their starting frequency, and 67% of them are within ± 6.1 ppm. The frequency of the best device changed by only -0.41 ppm during that period. Projecting these values to one year gives ± 19.1 ppm for the 10, ± 8.2 ppm for 67% of the oscillators, and -0.22 for the best device. While it is generally accepted that ± 1 ppm is the state-of-the-art of SAW oscillator ageing, typical studies yield values in the range 1 to 10 ppm/year, with only the best devices as low as 1 ppm/year (Ref. 11). The results of the present study therefore show that SSBW devices and SAW devices age at very similar rates.

All of these BT-cut SSBW devices have negative temperature coefficients, so that the 0.038°C/week downward drift of the temperature chamber during the first 222 days of the test would result in an increase in the oscillator frequencies or a positive ageing rate during that period. Examination of the ageing rates (see Table 4-2) of the 12 devices shows that 9 of the 10 best devices have positive rates. Some portion of that is undoubtedly due to the temperature drift. Because of the extreme sensitivity of the temperature coefficient to the orientation angle of the substrate (see Fig. 2-3), the values of the coefficients are not accurately known, so that the data was not corrected for the temperature drift. Even though the temperature characteristics of many of the 30 devices in the ageing test were measured, the data is not precise enough to allow the correction to be made. However, there is no doubt that the temperature drift resulted in an increase in the oscillator frequencies with time and the real ageing of these SSBW devices may actually be less than that represented by the data in Fig. 4-16.

4.4.2 Ageing of Double Sided Vacuum Sealed Devices

Figure 4-17 presents the data for the 6 double sided vacuum sealed devices. The package containing the pair of devices on substrate 374 most likely had a small leak as the frequency of both oscillators dropped rapidly with time. The remaining 5 pairs exhibited good ageing rates over the course of the experiment even though the fluctuations in frequency were greater than those of the single sided devices. This was most likely due to the relaxation of stresses since these double sided devices could not be mounted in the same stress free manner as the single sided devices. The polyimide mounting of the substrate and the solder bonding of the leads are potential sources of stress.

One pair of oscillators, on substrate 368, showed outstanding ageing characteristics with rates of -1.4 and -1.8 ppm/year for the individual oscillators and a differential rate of only 0.40 ppm/year. In 4 of the 5 pairs, the differential rate was less than the greater of the 2 individual oscillators. This shows that pairs of devices on the same substrate and in the same environment do tend to track one another, so that the differential ageing of such pairs is less than that of the individual oscillators. This is important in the application of SSBW oscillators to sensors where it is necessary to extract a difference signal from

TABLE 4-2

SUMMARY OF SSBW OSCILLATOR AGEING STUDY

	Device Number	Ageing at 222nd day (ppm) *	Ageing Rate (ppm/year) **	Projected Ageing at 1 year (ppm) ***
	402A	- 0.41	0.47	- 0.22
	402B	1.42	7.6	4.40
	399B	2.04	3.84	3.54
Single	403B	- 2.12	15.7	4.05
Sided	414	4.14	8.09	7.31
Devices	404A	4.58	9.1	8.15
Sealed	397A	5.49	2.66	6.53
In	404B	- 6.07	- 2.79	- 7.79
Vacuum	399A	7.35	13.7	12.7
	403A	11.1	20.3	19.1
	405A	- 24.5	- 60.2	- 48.1
	415	- 38.9	- 36.8	- 53.3
	368A	- 1.36	- 0.06	- 1.39
	368B	- 1.21 (0.15)	- 1.50 (1.44)	- 1.79 (0.40)
	372A	+ 6.60	18.3	13.8
Double	372B	+ 3.65 (2.95)	13.7 (4.61)	9.0 (4.75)
Sided	371A	+ 3.75	8.21	6.97
Devices	371B	+ 7.25 (3.50)	12.9 (4.70)	12.32 (5.35)
Sealed	369A	- 4.97	- 19.3	- 12.5
In	369B	+ 0.04 (5.01)	- 12.0 (7.25)	- 4.66 (7.85)
Vacuum	366A	- 13.8	- 4.40	- 15.5
	366B	- 1.96 (11.8)	13.4 (17.8)	3.30 (18.8)
	374A	---	---	---
	374B	---	---	---
Single	394A	- 0.40	- 0.65	- 0.65
Sided	401A	+ 0.95	2.92	2.10
Devices	396A	- 2.27	- 3.95	- 10.81
Packaged	398A	- 26.0	- 9.33	- 36.6
In	401B	---	---	---
Oil	394B	---	---	---

* average of day 213 thru day 222

** linear fit to the data for 123rd thru 222nd days

*** Projected Ageing = Ageing at 222nd day + Ageing rate*(365-222)/365

Numbers in brackets ( ) are differential ageing and differential ageing rates

FIG. 4-17

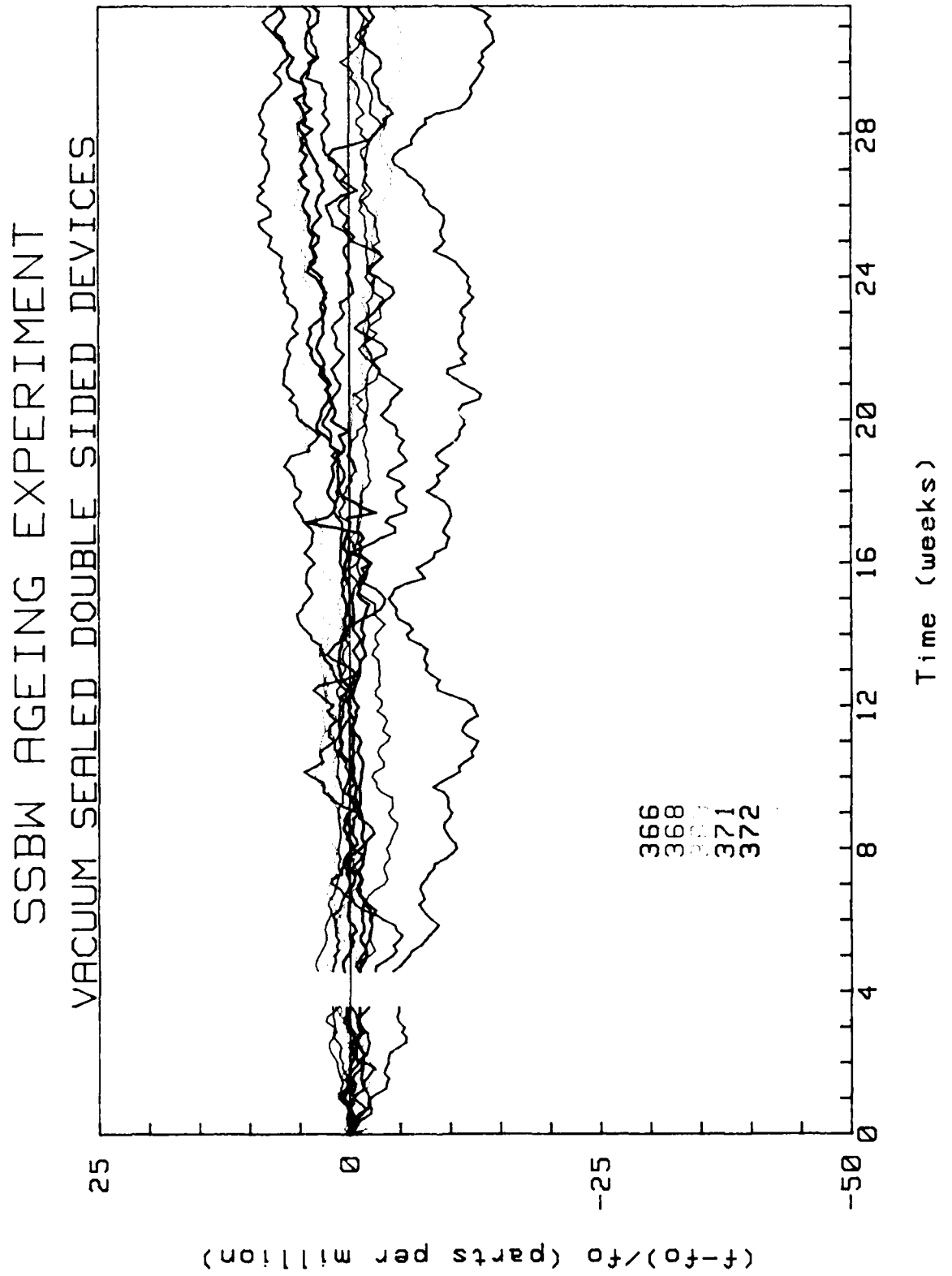
SSBW AGEING EXPERIMENT
VACUUM SEALED DOUBLE SIDED DEVICES
25
0
-25
-50
(f-fo)/fo (parts per million)
0
4
8
12
16
20
24
28
Time (weeks)
366
368
371
372

pairs of oscillators in order to provide the necessary degree of temperature compensation.

4.4.3 Ageing of Devices Packaged In Oil

Figure 4-18 presents the data for the 6 SSBW delay line oscillators that were aged in a silicone oil environment. The 2 worst devices, 398A and 401B, dropped rapidly in frequency during the first 32 weeks of the test before leveling off somewhat at a rate of about -60 ppm/year. A third device, 398A, decreased initially at a rate of about 3 ppm/week and then leveled off to a rate of -0.16ppm/week for an annual rate of -8.2 ppm/year. The remaining 3 oil sealed devices showed excellent ageing characteristics, with +1.56, -0.66, and -3.73 ppm/year ageing rates. The ageing of these 3 oil sealed devices is nearly identical with the 3 best ageing vacuum sealed SSBW devices. This is the most important result of the SSBW ageing study. SSBW devices not only survive quite well in the silicone oil, but the oil environment does not seem to adversely effect the ageing rate.

4.5 Conclusions from the Ageing Study

The results of the ageing test were successful in demonstrating three important points concerning the ageing of SSBW oscillators.

* The ageing of SSBW oscillators can be reduced to the same level as that for SAW oscillators, namely 1 to 10 ppm/year.

* Pairs of devices in the same package tend to track one another so that the difference ageing of pairs is less than that of the individual devices.

* The ageing characteristics of SSBW delay lines in a silicone oil environment are at least as good as the characteristics of vacuum sealed devices.

This last point is critical to the development of a SSBW accelerometer since fluid damping is a necessity if the device is to be a useful sensor. The results of this study bring the SSBW accelerometer one step closer to reality and open the way to the development of other SSBW sensors in which oil encapsulation can be used to provide damping, temperature stability, or other desireable features.

FIG. 4-18

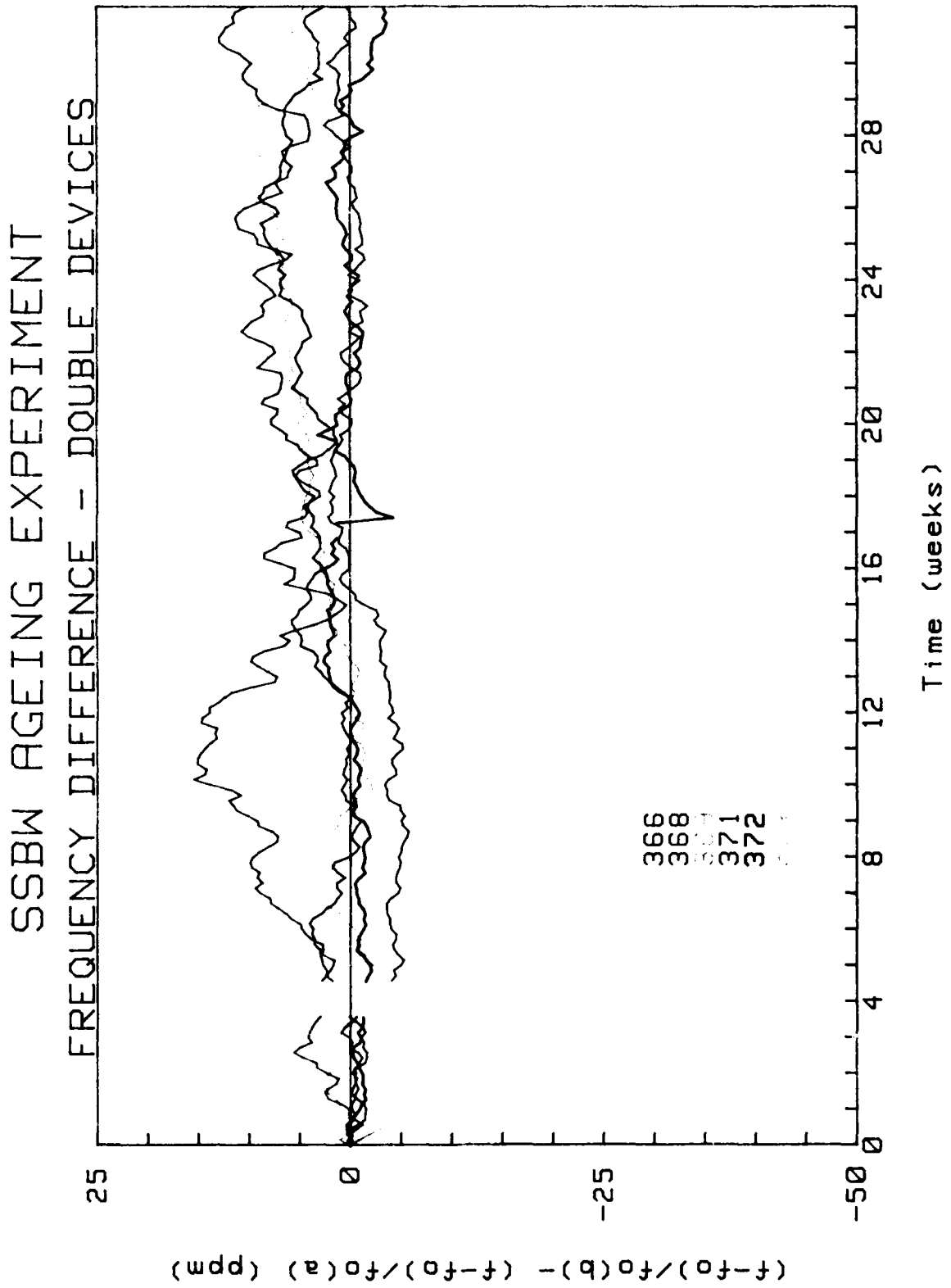
SSBW AGEING EXPERIMENT
FREQUENCY DIFFERENCE - DOUBLE DEVICES
(f-fo)/fo(b)- (f-fo)/fo(a) (ppm)
25
0
-25
-50
0
4
8
12
16
20
24
28
Time (weeks)
366
368
371
372

FIG. 4-19

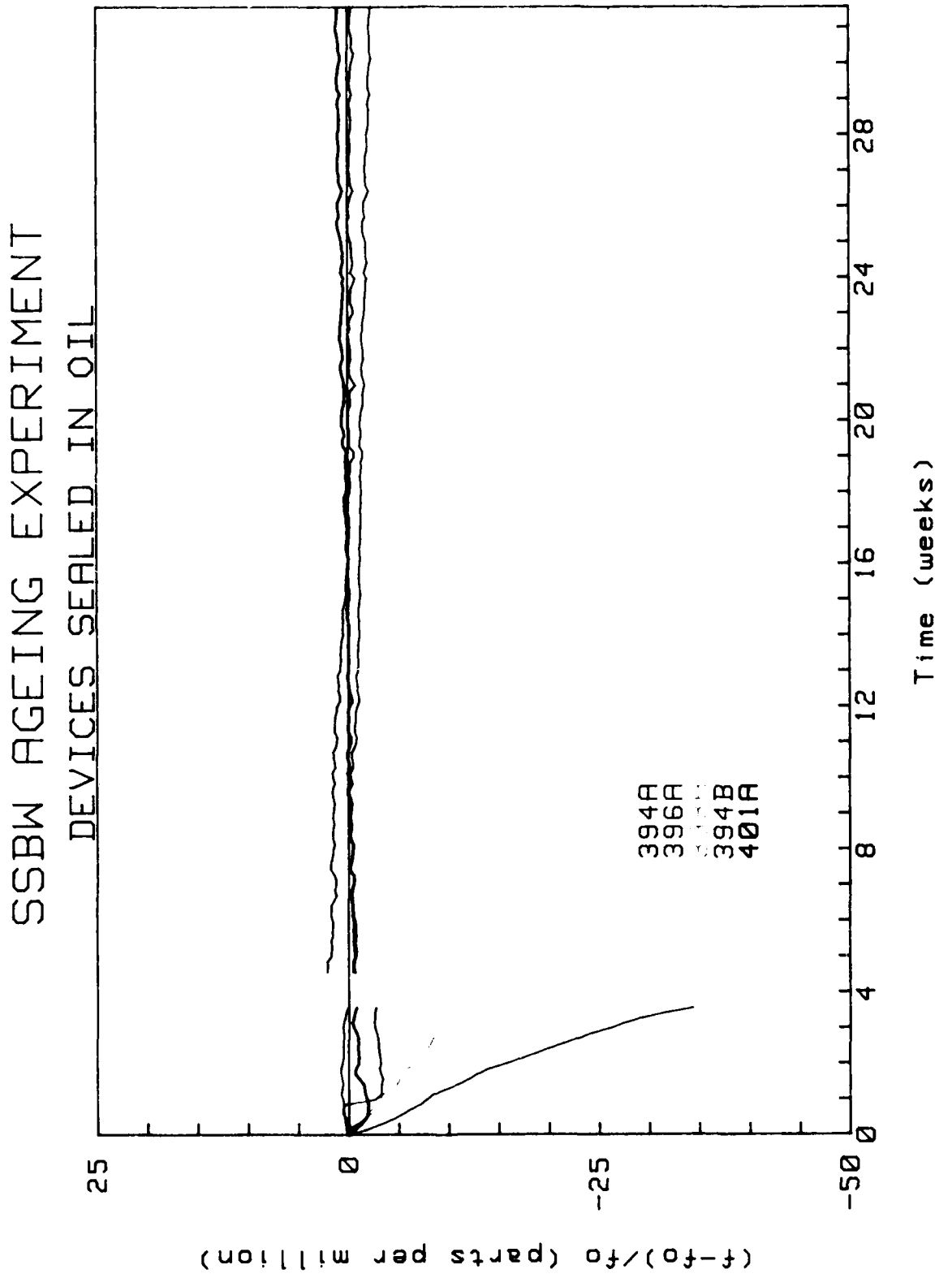
SSBW AGEING EXPERIMENT
DEVICES SEALED IN OIL
394A
396A
394B
401A
25
0
-25
-50
0
4
8
12
16
20
24
28
Time (weeks)
(f-fo)/fo (parts per million)

5.0 LABORATORY SSBW ACCELEROMETERS

5.1 Introduction

A laboratory SSBW accelerometer was designed and 4 prototypes were built and evaluated in order to assess the potential of such sensors for further development. These devices used a BT-cut quartz cantilever beam with SSBW delay lines on either side of the beam. The beam was fluid damped, and a fluid flow restriction was employed to increase the damping beyond that which is obtainable with the viscous damping alone. Special consideration was given to the routing of the RF signals to and from the SSBW transducers so as to minimize feedthru and achieve the best device characteristics in the accelerometer chassis. An effort was also made to keep the overall size of the prototypes as small as possible within the limitations imposed by the size of the SSBW devices, the RF connectors used, etc. Section 5.2 continues with a detailed discussion of the accelerometer design, and Section 5.3 presents the results of the evaluation of the prototype sensors.

5.2 Accelerometer Design and Fabrication

The design of a cantilever beam accelerometer is constrained by trade-offs between acceleration sensitivity, the mechanical resonance frequency, and beam strength requirements. Being able to critically damp the beam relieves the resonance frequency constraint, and so beam strength, or maximum strain considerations, set the limit on acceleration sensitivity.

5.2.1 Acceleration Sensitivity and Strain

A parametric relation for the acceleration sensitivity was given in Section 3.1. A more detailed examination of the relationship between acceleration sensitivity and the strain in the beam can be derived as follows. Referring to Fig. 5-1, a proof mass M, with diameter D, is attached to the end of a BT-cut quartz beam of length L, width W, and thickness T. SSBW delay lines on both sides of the beam are oriented so that the acoustic propagation is in the direction perpendicular to the X-axis at a distance Ls from the root end of the beam. When an acceleration A is applied in the direction shown in Fig. 5-1, the beam experiences a force F = M*A and a bending moment M(X) = F*X and deflects accordingly. The dominant stress at the upper surface of the beam is the normal stress in the X direction and is given by (Ref. 18)

$$Tx(Xt) = 6*M*A*Xt/(Wt*T^2), \qquad (5\text{-}1)$$

where Xt denotes the position of the SSBW delay line on the top surface of the beam and Wt is the width at Xt (Xb and Wb for the lower delay line). The stress

FIG. 5-1

SSBW ACCELEROMETER GEOMETRY

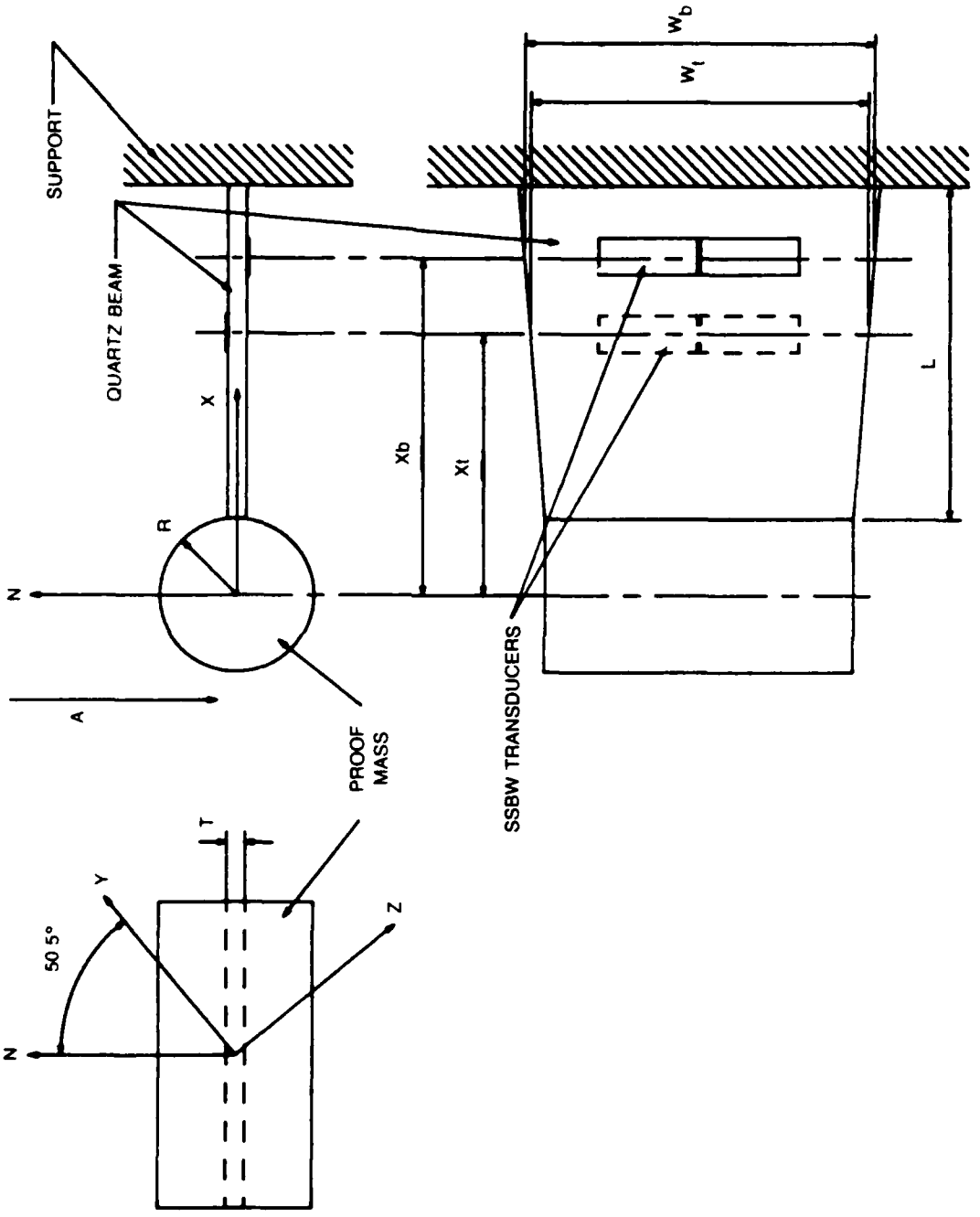

87-8-17-24

on the bottom of the beam has the same magnitude but is a compressive stress and hence negative in sign. The associated strain is

$$Sx = Tx/Cx. \tag{5-2}$$

where Cx is the appropriate element of the C matrix for the BT-cut quartz plate ($Cx = 12.6 \times 10^6$ psi). If the applied acceleration equals the acceleration of gravity G, then the strain is the strain/G and will be denoted by Sxg.

The SSBW delay lines on the top and bottom of the beam experience strains of opposite signs. When the signals from the 2 SSBW oscillators are combined subtractively, the acceleration sensitivities (which are proportional to the strains) add, with the net acceleration sensitivity As given by

$$As = Gx*(Sxg(Xb) - Sxg(Xxt), \tag{5-3}$$

where Gx is the appropriate coefficient from the relationship between SSBW velocity and strain, i.e.,

$$V(S) = Vo*(1 + Gx*Sx + Gy*Sy + Gz*Sz + Gxz*Sxz + Gxy*Sxy + Gyz*Syz). \tag{5-4}$$

In the case of a cantilever beam with a width approximately equal to the length, Sx is large compared to the other components that they can be ignored with little error. The coefficients Gx (-1.95) and Gy (1.80) were measured experimentally as part of the predecessor AFOSR contract.

If an accelerometer were to be designed for an acceleration range of ± 10 G's with a maximum strain of 0.0005 at the SSBW delay line position, then the acceleration sensitivity would be

$$As = (-1.95)*[(-50 \text{ ppm/G}) - (50 \text{ ppm/G})] = 195 \text{ ppm/G}.$$

A strain of 0.0005 is conservative, for with proper chemical polishing, crystalline quartz can be made to withstand strains more than an order of magnitude higher (Ref. 19). Using SSBW delay lines with a frequency of 165 MHz, an accelerometer with 195 ppm/G sensitivity would have a frequency sensitivity of 32 KHz/G. Assuming ± 1°C temperature control, the level of temperature sensitivity of BT-cut quartz alone (0.03 ppm/°C^2) is more than enough to realize 1 milli-G accuracy with such a device.

An accelerometer designed for 195 ppm/G sensitivity requires thinner, more fragile, quartz beams than were used in this work. Acceleration sensitivities of over 50 ppm/G can be obtained with substrates in the 0.02 to 0.03 inch range, and, based upon the temperature stability of the individual oscillators (i.e., ignoring any further temperature compensation obtained from the double oscillator

configuration), a design that produces 50 ppm/G sensitivity would provide 1 milli-G accuracy.

Combining Eqns. 5-1, 5-2, and 5-3, an expression for the acceleration sensitivity in terms of the parameters of the cantilever beam can be obtained, i.e.,

$$As(ppm/G) = 1.32*(M/T^2)*(Xt/Wt + Xb/Wb) \qquad (5\text{-}5)$$

with M in grams and T in mm. This equation, together with the following relation for the mechanical resonance frequency, provide the basis for the SSBW accelerometer design.

5.2.2 Mechanical Resonance Frequency

The lowest mechanical resonance frequency of a cantilever beam is given by (Ref. 9)

$$f(Hz) = (1/4\pi)*\sqrt{(C*W/M)*[T/(L+R)]^3}$$

$$= 2.3x10^4*\sqrt{(W/M)*[T/(L+R)]^3} \qquad (5\text{-}6)$$

with C = Cx, M in grams and W in mm. This relation assumes the beam to be of uniform width, but is applicable here with very little error if an average width is assumed.

5.2.3 Accelerometer Beam Design

One goal of the present program was to demonstrate a laboratory prototype SSBW accelerometer (LPA) with 1 milli-G accuracy. The accuracy of the SSBW sensor depends principally upon the temperature sensitivity (medium term stability), and the ageing characteristics (long term stability). While the effectiveness of the dual oscillator temperature compensation technique has yet to be demonstrated, the temperature sensitivity of SSBW's on BT-cut quartz is low enough that a 1 milli-G design can still be obtained. The original design generated for the LPA used a 0.025 inch thick beam that was 13.83 mm long and was tapered from 12.78 mm at the free end to 16.00 mm at the fixed end. Figure 5-2 illustrates this design and shows the positioning of the SSBW delay lines on the beam and the area of the beam which is bonded to the supporting structure. This design has a theoretical sensitivity of 43.4 ppm/G, so that a 1 milli-G acceleration would produce a frequency change of (43.4 ppm/G) *(165 MHz)*(0.001 G) = 7.2 Hz. The frequency stability of the SSBW oscillators is such that 7.2 Hz is easily resolved over periods of a few minutes, so that the design was capable of resolving 1 milli-G over short periods of time.

Figure 5-3 is a plot of acceleration sensitivity versus mechanical resonance frequency for a cantilever beam SSBW accelerometer with a mass of 7.8 grams and a

FIG. 5-2

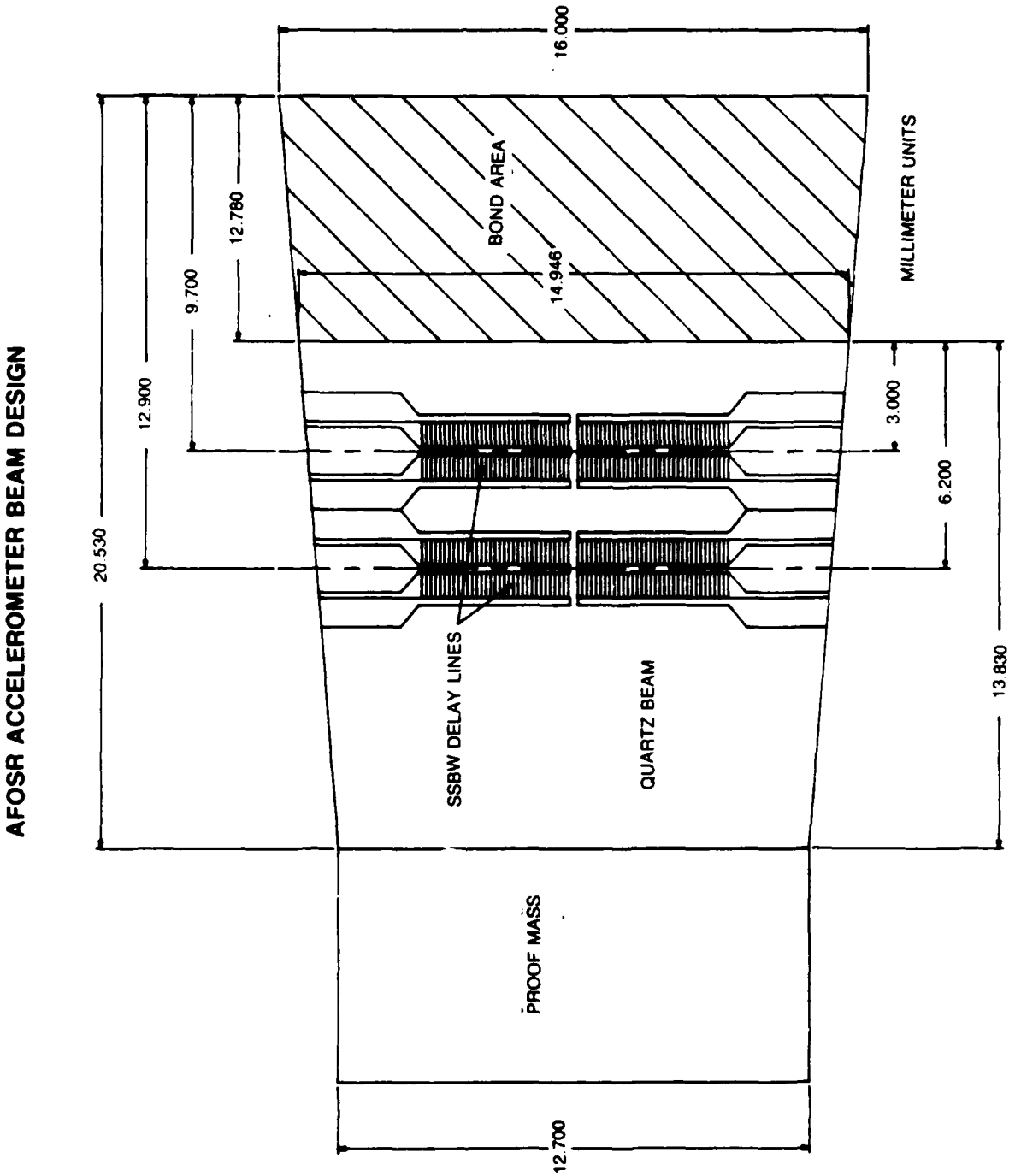

87-8-17-25

FIG. 5-3

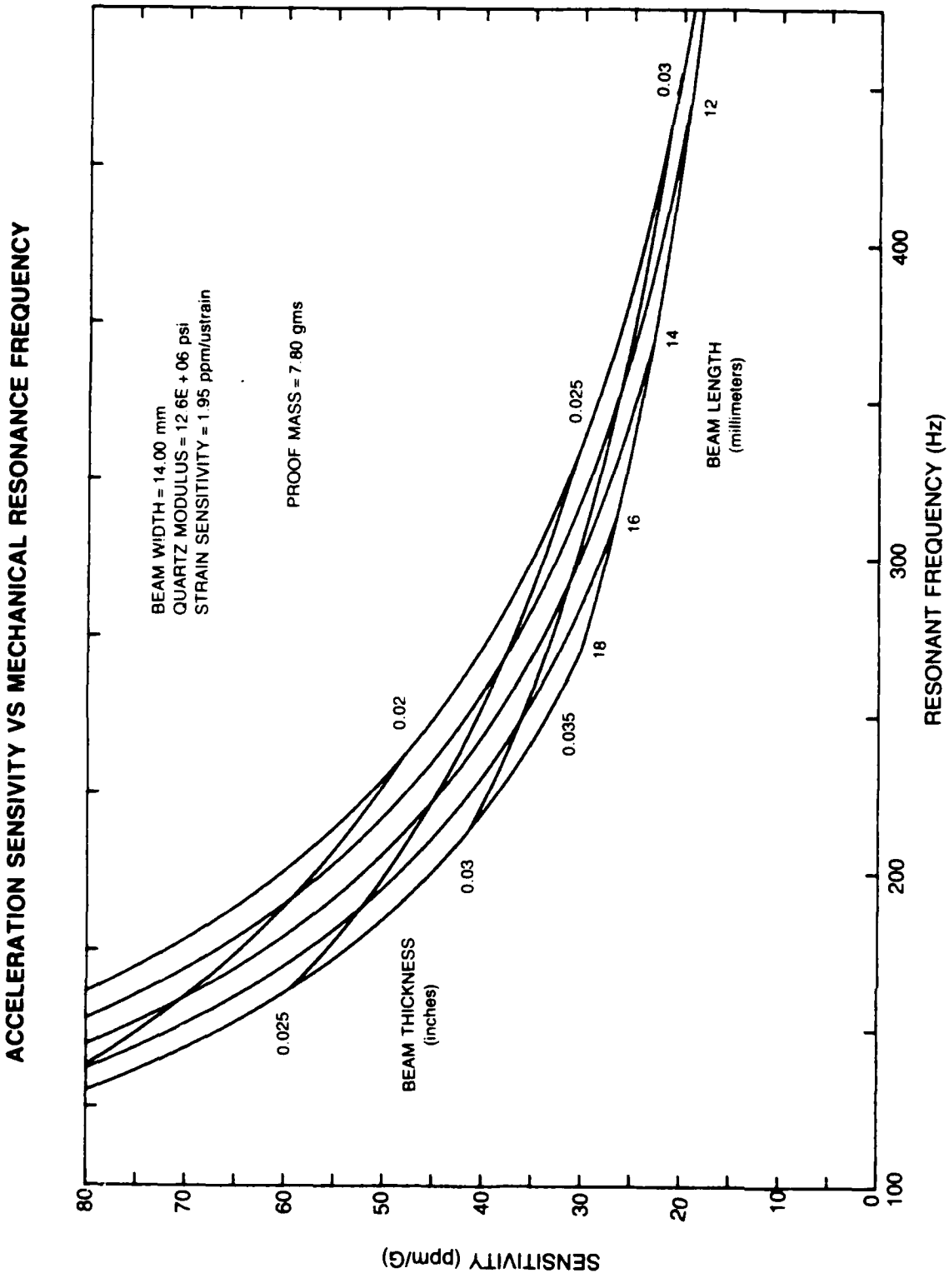

87-8-17-26

beam width of 14.0 mm. Acceleration sensitivities were calculated using the actual widths at the positions of the SSBW delay lines. The general size of the quartz beam and the overall size of the LPA's was dictated to a large extent by the 20 and 20.4 micron SSBW wavelengths and the resulting 8.4 mm length of the delay lines.

The SSBW delay lines were positioned on both sides of the beam. Because of the difficulty of fabricating low defect delay lines when there is overlap between the patterns, it was decided to use a pattern in which there was no overlap between any part of the transducer patterns. This is a conservative approach and one which would most likely be relaxed in a future design in order to achieve higher acceleration sensitivity. Acceleration sensitivity is proportional to the distance between the centerlines of the SSBW delay line and the proof mass, so that this design sacrifices approximately 11% over the optimum design. The sides of the quartz beam are tapered to prevent acoustic reflections from interfering with the desired acoustic wave. A proof mass with a length equal to the width of the beam at the narrow end and a diameter of 0.25 inches has a mass of 7.8 grams.

The LPA's that were fabricated deviated somewhat from the original design. The 0.025 inch thick BT-cut quartz substrates that were obtained for the LPA's were not used, but thicker 0.030 inch substrates were substituted because of processing difficulties. As can be seen in Fig. 5-3, this 0.005 inch increase in thickness results in a decrease in acceleration sensitivity to 30.2 ppm/G. Also, the proof mass used was made smaller to provide more clearance within the LPA chassis. The reduction from 7.8 grams to 6.5 grams further reduces the sensitivity to 25.2 ppm/G. Practical considerations dictated a very conservative approach with this first group of LPA's, and thus the sensitivity obtained was lower than planned. However, there is no fundamental reason why SSBW accelerometers with 50 to 100 ppm/G sensitivity cannot be made.

5.2.4 RF Input and Output Connections

Experience with testing numerous kinds of SAW and SSBW devices operating at RF frequencies has pointed out the importance of making good RF connections to the SSBW transducers if good IL characteristics are to be achieved. In particular, it is important to keep leads short and to make good ground connections. In the present case where the substrate is suspended above the metal chassis, leads are necessarily longer than they might otherwise be. Nonetheless, within the constraints imposed by the beam mounting, size of connectors, and the proximity of the fluid flow restrictor, the lead lengths were kept as short as possible. The ground connections from the SSBW transducers were made directly to the RF feedthroughs. This was found to be very important. Devices in which grounds were made to the aluminum chassis, relying on the metal-to-metal contact between the chassis threads and the connector threads, exhibited significantly higher levels of RF feedthru and generally poorer IL characteristics.

The electrical connections for the LPA,s were made with gold ribbon and all connections were soldered. As in the case with the double sided devices fabricated for the ageing tests, it was necessary to build up the transducer pads with copper and nickel in order to be able to solder to the pads. Figure 5-4 shows the IL characteristics for one channel of LPA #1 indicating a feedthru level 63 dB down and very clean response in the region of the IL minimum. All 8 delay lines on the 4 LPA's had similar characteristics.

5.2.5 Assembling the LPA

Figure 5-5 shows views of the assembled LPA. The aluminum accelerometer chassis is 2.0 inches in diameter and 0.63 inches thick with a 1/8" inch cover. O-ring seals around each of the RF connectors and between the cover and the chassis are necessary for retention of the silicone oil damping fluid. The quartz beam, with one end of the gold ribbon leads soldered to the transducer pads, is bonded to the support piece with epoxy cement using a special jig machined to accurately position the beam precisely 0.008 inches above the fluid flow restricting bar. This spacing should be close enough to critically damp the beam. The beam is then mounted into the chassis, the gold ribbon leads are soldered to the RF connectors, and the tungsten proof mass epoxy bonded to the beam. Table 5-1 lists the parameters for the 4 LPA's.

5.3 Evaluation Of Laboratory Accelerometers

The 4 LPA's were examined for vibration response, temperature sensitivity, and acceleration sensitivity. The results of those measurements are presented in Table 5-2 and discussed in the following.

5.3.1 Vibration Sensitivity

If a crystal oscillator is subjected to harmonic motion at frequency fv, then the frequency output of the oscillator will be modulated according to the equation (Ref. 20),

$$f(T) = fo + df \cdot \cos(2\pi fvT),$$

where fo is the "at rest" frequency, and df is the modulation amplitude given by,

$$df = Cvs \cdot Amax \cdot fo,$$

where Amax is the maximum value of the acceleration at frequency fv, and Cvs is a constant of proportionality known as the vibration sensitivity. The value of this constant depends on the mechanical configuration of the oscillator crystal,

SSBW IL CHARACTERISTICS IN LPA CHASSIS

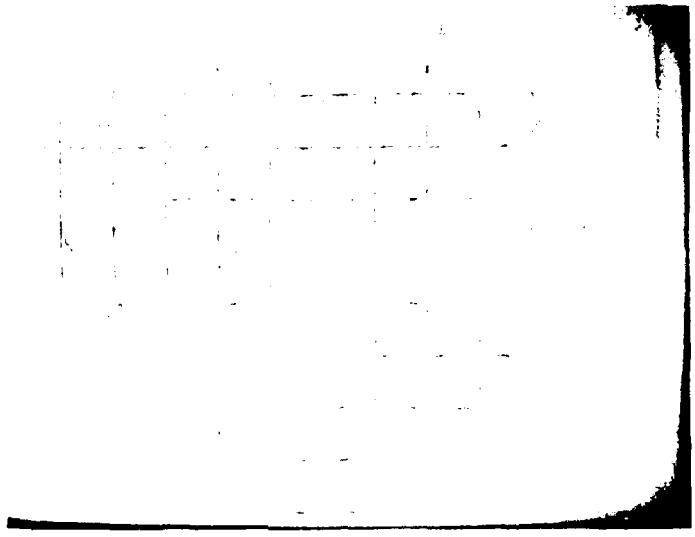

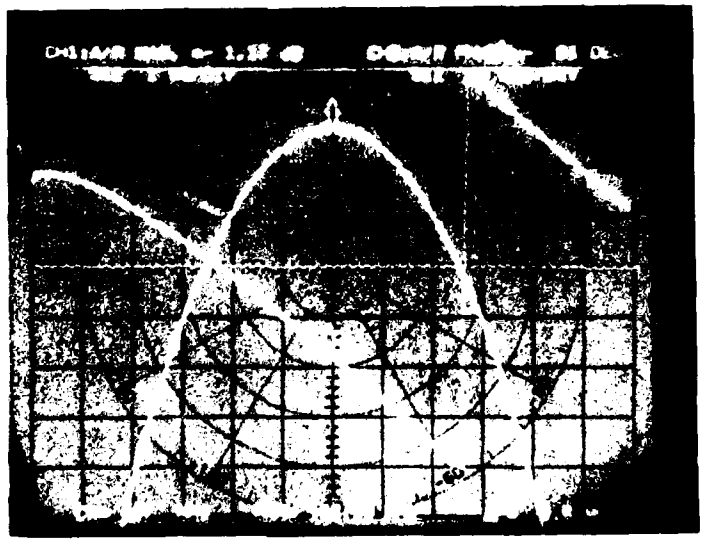

FIG. 5-5

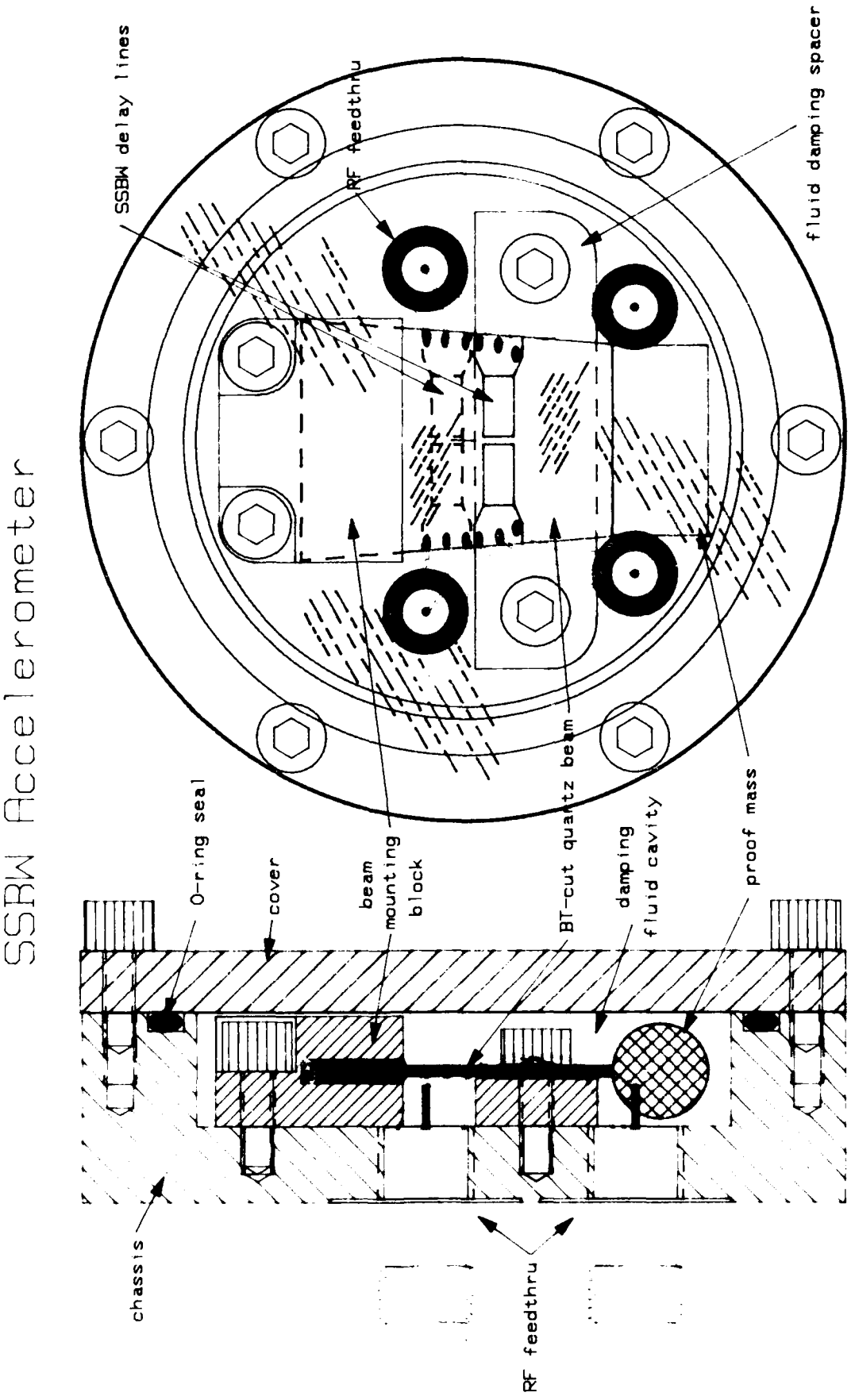
SSBW Accelerometer
SSBW delay lines
RF feedthru
fluid damping spacer
O-ring seal
cover
beam mounting block
BT-cut quartz beam
damping fluid cavity
proof mass
chassis
RF feedthru

TABLE 5-1

PARAMETERS OF LABORATORY PROTOTYPE SSBW ACCELEROMETERS

	LPA-1	LPA-2	LPA-3	LPA-4
substrate orientation	50°31'	50°26'	50°30'	50°27'
beam length (L), mm	13.8	13.8	13.8	13.8
beam width (mass end), mm	12.8	12.8	12.8	12.8
beam width (wide end), mm	16.0	16.0	16.0	16.0
SSBWt location (Xt), mm	12.47	11.10	11.68	11.28
SSBWb location (Xb), mm	15.75	14.25	14.83	14.35
beam width (@ SSBWt), mm	14.24	14.02	14.11	14.05
beam width (@ SSBWb), mm	14.75	14.52	14.61	14.53
beam thickness (T), mm	0.782	0.767	0.759	0.767
mass (M), gm	6.48	6.79	6.35	6.49

TABLE 5-2

PERFORMANCE OF LABORATORY PROTOTYPE SSBW ACCELEROMETERS

	LPA-1	LPA-2	LPA-3	LPA-4
Mechanical Resonance Frequency, Hz				
Calculated	334	323	328	330
Experimentally Measured	342	345	386	349
Temperature Sensitivity Measurements				
Delay Line @ Xt				
Turnover Temperature (°C)	68.6	62.4	60.1	48.9
2nd Order Coeff (ppm/°C^2)	-0.018	-0.015	-0.011	-0.015
Delay Line @ Xb				
Turnover Temperature (°C)	43.5	55.9	66.5	72.6
2nd Order Coeff (ppm/°C^2))	-0.024	-0.022	-0.019	-0.010
Acceleration Sensitivity, ppm/G				
Calculated				
Delay Line @ Xt	12.26	12.08	12.05	11.71
Delay Line @ Xb	14.95	14.98	14.78	14.41
Total	27.21	27.06	26.83	26.11
Experimentally Measured				
Delay Line @ Xt	8.8	9.2	5.9	8.3
Delay Line @ Xb	11.2	14.7	10.1	13.7
Total	20.0	23.9	16.0	22.0
Vibration Sensitivity, x10^8/G				
Experimentally Measured	5.0	4.7	3.8	5.1

the orientation of the crystal, and the acoustic wave mode. In the present case, the value of Cvs is taken as a measure of the effectiveness of the damping.

The oscillator frequency modulation by the mechanical vibration results in a voltage output of the form

$$V(T) = Vo\cos[2\pi foT + B\sin(2\pi fvT)],$$

where B = df/fv. Expanding V(T) so that the individual frequency components can be clearly identified, one obtains

$$\begin{aligned} V(T) = Vo\{&J0(B)\cos(2\pi foT) \\ &+ J1(B)[\cos(2\pi(fo+fv)T)-\cos(2\pi(fo-fv)T)] \\ &+ J2(B)[\cos(2\pi(fo+2fv)T)-\cos(2\pi(fo-2fv)T)] + \ldots\} \end{aligned}$$

where the J's are Bessel functions of the first kind. The output spectrum therefore contains an infinite number of Fourier components on either side of the carrier separated from the carrier by fv, 2fv, 3fv, etc. The ratio of the output at the side bands to that at fo is a function of B, hence a measurement of the sideband ratio provides a value for B, and therefore for Cvs, the vibration sensitivity.

Figure 5-6 presents 2 photos of the frequency spectrum of LPA #1 showing the accumulated effects of sweeping the mechanical vibration frequency from 100 Hz to 500 Hz. Figure 5-6a illustrates the case when the beam is damped, and Fig. 5-6b illustrates the undamped case with a prominant sideband response at the lowest mechanical resonance frequency of fv = 342 Hz. The measurements were made with the peak value of acceleration fixed at 0.5 G. With damping, the sideband at fv is down 45 dB from the output at the oscillator frequency fo, so that $20\log(J1/J0) = -45$, giving $J1/J0 = 0.0056$, and therefore $B = 0.011$. Thus, with Amax = 0.5 G and fo = 164 MHz, the vibration sensitivity Cvs is 5×10^{-8}/G. Similar values were obtained with all 4 of the LPA's as indicated in Table 5-2. Since vibration sensitivity of commercially available crystal oscillators packaged to minimize vibration effects is typically 2×10^{-9}/G (Ref. 20), the Cvs value obtained with these SSBW cantilevered beam devices is considered very good.

5.3.2 Temperature Compensation

The temperature characteristics of the 8 SSBW delay lines on the 4 LPA's were measured with the chassis filled with oil. The turnover temperatures and the second order coefficients of temperature are listed in Table 5-2. As seen by the values presented, the problem of being unable to obtain the same behavior with temperature from 2 devices on opposite sides of a substrate remained. The temperature characteristics of both devices on a substrate were measured at the same time to eliminate any errors that might be due to the method of measurement,

EFFECTS OF FLUID DAMPING ON LPA FREQUENCY SPECTRUM

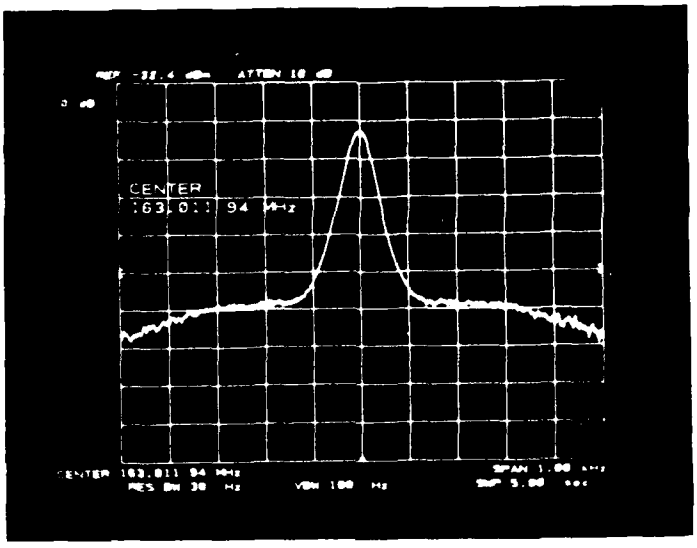

a) WITH FLUID DAMPING

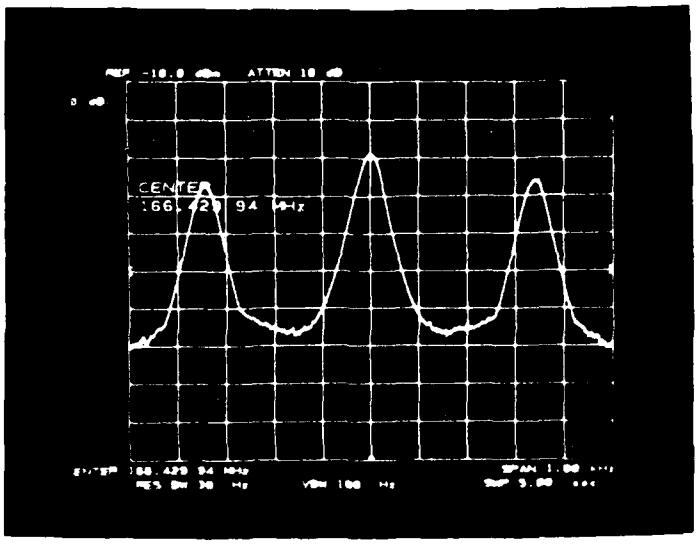

b) UNDAMPED

but again, the results were very disappointing. Further work is required in this area.

5.3.3 Acceleration Sensitivity

The theoretically predicted and measured values of acceleration sensitivity for the 4 LPA's are listed in Table 5-2 and plotted in Figure 5-7. Acceleration sensitivities were determined by measuring the change in output frequencies for a 2 G change in acceleration. The best device, i.e., the device with the highest acceleration sensitivity, is LPA-2. LPA-2 has an acceleration sensitivity of 23.9 ppm/G and is within 12% of the calculated value. LPA-2 would require temperature control of ± 1°C in order to realize 1 milli-G sensitivity (-.022 ppm/$°C^2$ is the larger of the two 2nd order temperature coefficients of LPA-2). The other 3 LPA's fell somewhat further below the predicted values for acceleration sensitivity.

The measured values of all of the LPA's were below the theoretical values. This discrepancy is due to the fact that an ideal strain field assumed in the theoretical calculations of acceleration sensitivity, and this strain field is not entirely realistic. Uniform strains in the X direction (Fig. 5-1) are realized only when the width of the beam is several times the length, and even then, only away from the edges of the beam. In the case of the LPA's, the width and length are approximately the same, and the beam is tapered, introducing further complications to the analysis. The result is that the simple analysis can only be used as a guide and cannot be expected to yield precise predictions.

While the original design for the LPA's would have easily resulted in milli-G accuracy accelerometers even without further temperature compensation above that of the BT-cut quartz substrates alone, several modifications in the design, all of which were conservative on nature, reduced the acceleration sensitivity. Most of these changes were the result of device fabrication difficulties and the desire to complete and test working SSBW accelerometers without having to solve problems associated with handling thinner and more delicate quartz beams. Smaller and higher sensitivity devices could now be fabricated with the experience gained from building these first four LPA's.

FIG. 5-7

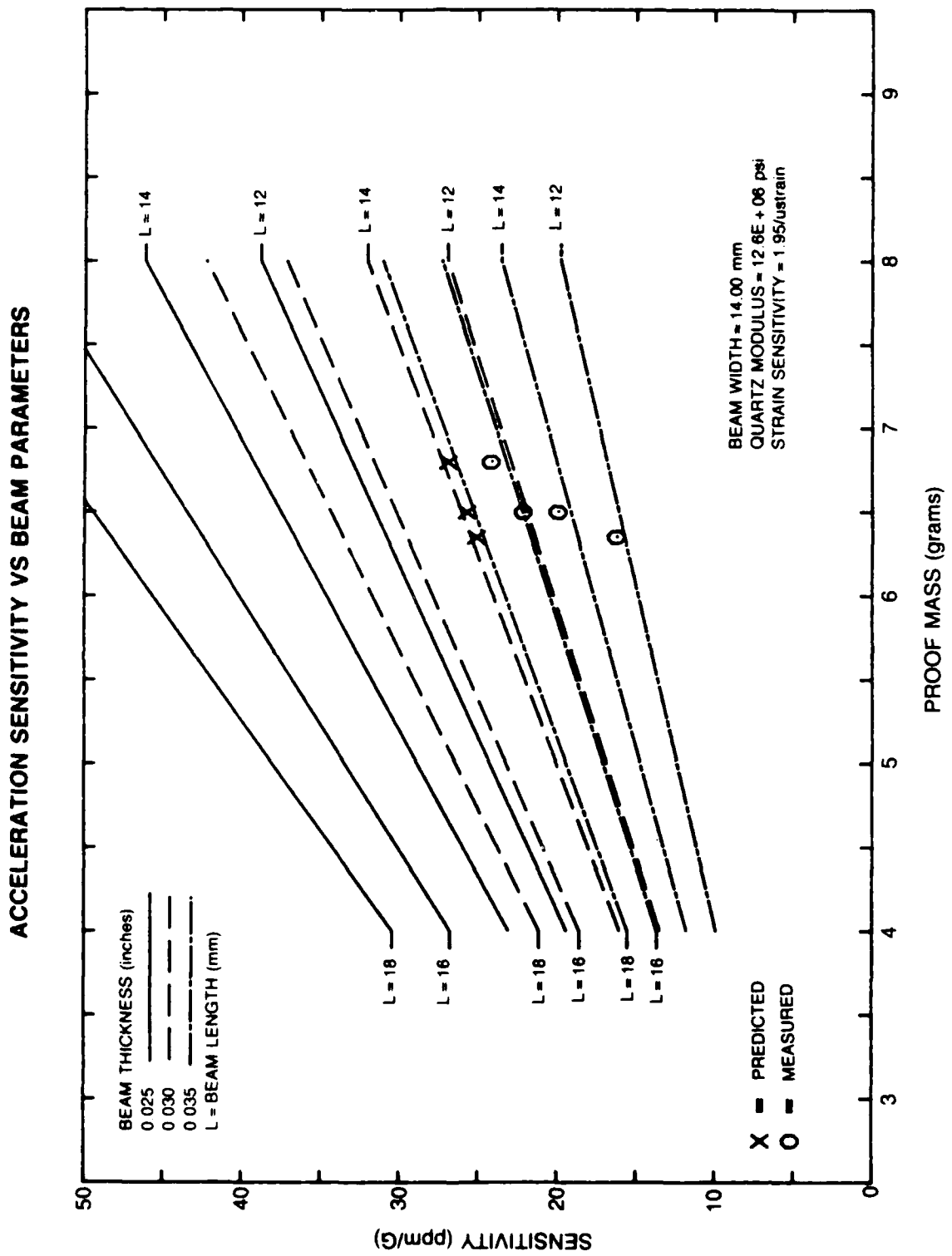

87 - 8 - 17 - 29

6.0 SUMMARY AND RECOMMENDATIONS FOR CONTINUED DEVELOPMENT

The results of this program reinforce an earlier conclusion that the SSBW mode in BT-cut quartz has outstanding potential for acoustic sensor development. Prior work established that this mode has high strain sensitivity, low temperature sensitivity, and can propagate with a fluid on the surface without excessive losses. As a result of this program, it has been shown that the ageing of SSBW delay lines in silicone oil is less than 10 ppm/year and at least as good as the ageing of similar devices that were vacuum encapsulated. It was also shown that pairs of devices on the same substrate age together, so that the difference in the ageing is less than the ageing of the individual devices. This is very important result for the development of sensors based upon the dual oscillator design.

Work on aspects of SSBW sensors specifically directed toward the development of a SSBW accelerometer showed: 1) that the dual delay line configuration, in which SSBW delay lines were fabricated on opposite sides of the same substrate, is a viable means of increasing the acceleration sensitivity, and potentially a method of achieving increased temperature compensation; and 2) that critical damping of a cantilevered quartz beam could be readily achieved using a silicone oil damping fluid and a fluid flow restriction.

Four laboratory prototype SSBW accelerometers were designed, built, and tested during the course of this program. While an overly conservative design limited the acceleration sensitivity of these first generation devices to a level that would just barely allow the resolution of 1 milli-G, the results achieved indicate that second generation devices with increased sensitivities can readily be achieved. Vibration testing of these prototype devices showed that the damping mechanism was quite satisfactory in reducing the vibration sensitivity to acceptable levels.

The one area in which the goals of the program were not met was in the area of temperature compensation. In order to achieve additional temperature compensation with the dual delay line scheme, the thermal characteristics of the two delay lines must be very closely matched. While considerable effort was made to control the fabrication processes so as to achieve repeatable temperature characteristics, the effort was unsuccessful. Large differences remained in the turnover temperatures and the second order coefficients of temperature between devices on the same substrate.

This experience is similar to that of another research group attempting to develop a sensor based upon SAW devices (Ref. 21). The relationships between the details of the delay line fabrication and the resulting temperature characteristics are simply not known with sufficient accuracy at this point in time to allow

the successful implementation of the dual delay line temperature compensation scheme. This is an area that clearly requires further work. The strain sensitivity of SSBW devices or SAW devices is not large enough to enable the development of precision sensors without additional temperature compensation. As a result, the development of such sensors awaits a refinement in the understanding of the factors influencing the temperature characteristics of these devices.

There are two approaches that can be taken in future work to solve the temperature problem. One is the development of sophisticated trimming techniques to bring the temperature characteristics of the SSBW delay lines on either side of the substrate into close agreement. Such techniques would most likely be similar to the presently used method of frequency trimming SAW devices by reactive ion etching of the quartz substrate. The other approach is an intensive investigation into the physics of the temperature characteristics of SSBW devices. Important areas requiring study are the effects of: 1) the kind and thickness of the metal layers that comprise the transducers, 2) variations in the preparation of the substrates, and 3) stresses and stress relaxation in the substrate and in the metal films.

7.0 REFERENCES

1. Cullen, D. E., G. Meltz, and T. W. Grudkowski: Investigation of the Strain Sensitivity of Subsurface Acoustic Wave Modes, 1982 IEEE Ultrasonics Symposium, San Diego, CA, October 1982.

2. Cullen, D. E., G. Meltz, and T. W. Grudkowski: Surface and Interface Waves in $SiO_2/LiNbO_3$, 1983 IEEE Ultrasonics Symposium, Atlanta, GA, October 1983.

3. Cullen, D. E., G. Meltz, and T. W. Grudkowski: Surface and Interface Waves in $SiO_2/YX\text{-}LiNbO_3$, Appl. Phys. Lett., Vol. 44, No. 2, pp. 182-184, January 1984.

4. Cullen, D. E., G. Meltz, and T. W. Grudkowski: Research and Development of Subsurface Acoustic Wave Device Configurations for Sensor Applications, Final Report on AFOSR Contract No. F49620-82-C-0074, September 1983.

5. Cullen, D. E. and T. W. Grudkowski: Strain Sensitivity of SSBW's In Quartz, Proc. 1984 IEEE Ultrasonics Symposium, pp. 290-292.

6. Cullen, D. E. and T. W. Grudkowski: Research and Development of Subsurface Acoustic Wave Devices for Sensor Applications, Final Report on AFOSR Contract No. F49620-84-C-0006, January 1985.

7. Cullen, D. E.: Experimental Development of Digital Output Pressure and Temperature Sensors Using Surface Acoustic Waves, Final Report on NASC Contract No. N00019-76-C-0566, December 1978.

8. AZ 1318-SFD photoresist, American Hoechst Corp., Sommerville, N.J.

9. DenHartog, J. P.: Mechanical Vibrations, McGraw-Hill, New York, 1956.

10. Parker, T. E.: Random and Systematic Contributions to Long Term Stability in SAW Oscillators, Proc. 1983 IEEE Ultrasonics Symposium, p. 257-262.

11. Parker, T. E.: Analysis of Ageing Data on SAW Oscillators, Proc. 34th Annual Frequency Control Symposium, May 1980.

12. Stokes, R. B. and M. J. Delaney: Advanced Ageing Studies and Experiments on Surface Acoustic Wave (SAW) Oscillators, Rome Air Development Center Report RADC-TR-84-214, October 1984.

13. Stokes, R. B., and M. J. Delaney: Ageing Mechanisms in SAW Oscillators, Proc. 1983 IEEE Ultrasonics Symposium, pp. 247-256.

14. Yen, K. H., K. G. Lau and R. S. Kagiwada: Recent Advances in Shallow Bulk Acoustic Wave Devices, Proc. 1979 IEEE Ultrasonics Symposium, pp. 776-779.

15. Lewis M.: Surface Skimming Bulk Waves, Proc. 1977 IEEE Ultrasonics Symposium, pp. 744-752.

16. Proprietary process of Valpey-Fisher Corp., Hopkinton, MA.

17. Vig, J. R. and J. W. LeBus: UV/Ozone Cleaning of Surfaces, IEEE Trans. on Parts, Hybrids, and Packaging, Vol. PHP-12, No. 4, December 1976.

18. Timoshenko, S. and S. Woinowsky-Krieger: Theory of Plates and Shells, McGraw-Hill, 1959.

19. Vig, J. R., J. W. LeBus and R. L. Filler: Chemically Polished Quartz, Proc. 31st Annual Symposium on Frequency Control, pp. 131-143, 1977.

20. Filler, R. L.: The Effect of Vibration on Quartz Crystal Oscillators, ERADCOM Report DELET-TR-80-10, May 1980.

21. Private communication with W. J. Tanski of UTRC.

8.0 PUBLICATIONS AND PRESENTATIONS

8.1 Publications

"A SSBW Accelerometer" by D. Cullen - in preparation.

8.2 Presentations

"Progress in the Development of a SSBW Accelerometer", D. E. Cullen at 1986 IEEE Ultrasonics Symposium in Williamsburg, VA, on November 17, 1986.

8.3 Patents

"Surface Skimming Bulk Acoustic Wave Accelerometer", U. S. Patent, 4,676,104, June 30, 1987, D. E. Cullen.

9.0 LIST OF PROFESSIONAL PESONNEL

Program Manager

T. W. Grudkowski - Manager, Semiconductor Research Laboratory - Ph.D in Electrical Engineering at Stanford University, 1975 - thesis title "Active Acoustic Waves and Electrons in Gallium Arsenide"

Principal Investigator

D. E. Cullen - Senior Research Scientist, Microelectronics Ph.D in Physics at the University of Illinois, 1970 thesis titled "Tunneling Spectroscopy in P-Type Silicon"

APPENDIX 1

SSBW AGEING EXPERIMENT DATA FOR 52 WEEK STUDY

FIG. A-1

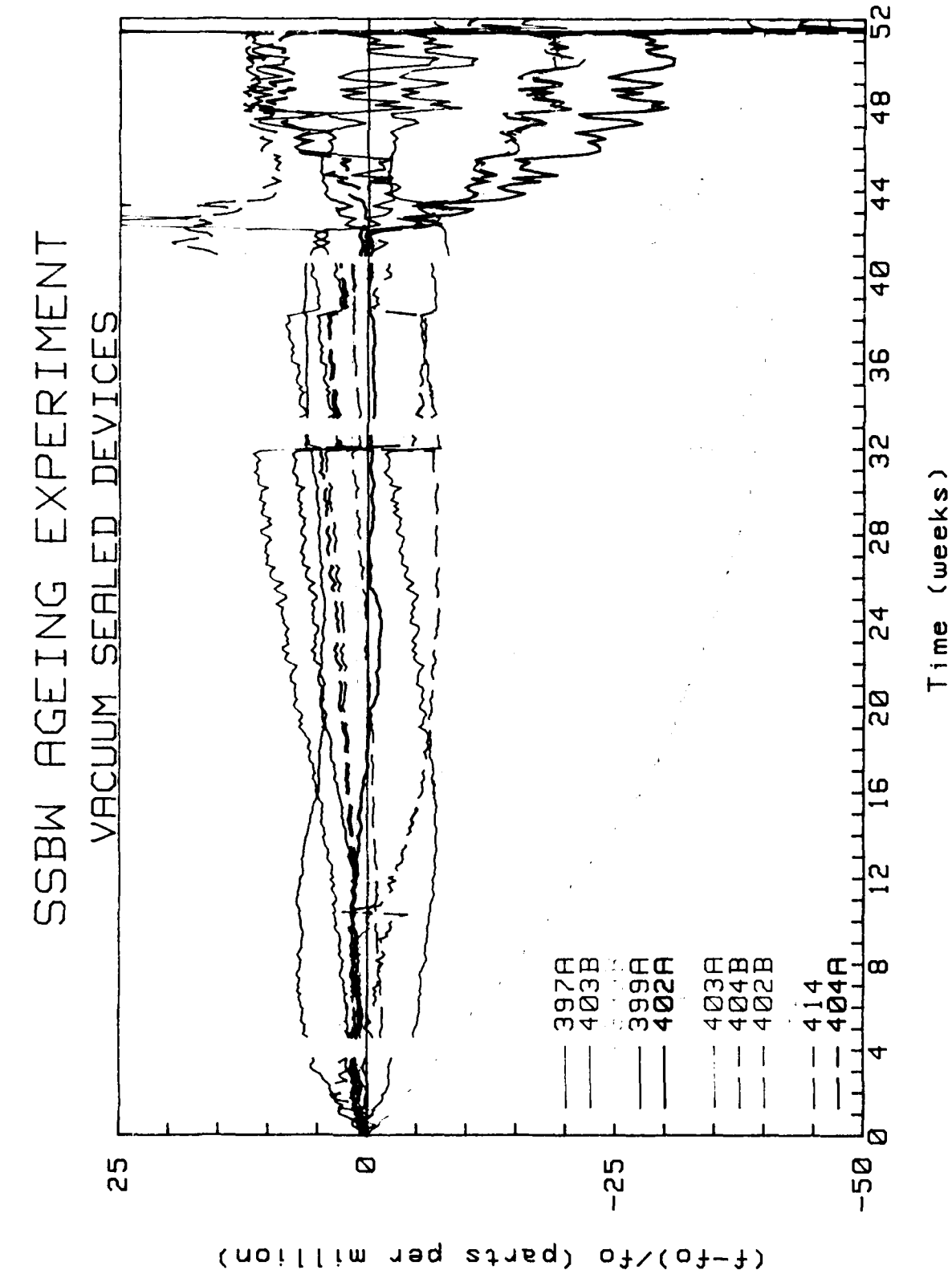
SSBW AGEING EXPERIMENT
VACUUM SEALED DEVICES
(f-fo)/fo (parts per million)
25
0
-25
-50
0
4
8
12
16
20
24
28
32
36
40
44
48
52
Time (weeks)
397A
403B
399A
402A
403A
404B
402B
414
404A

FIG. A-2

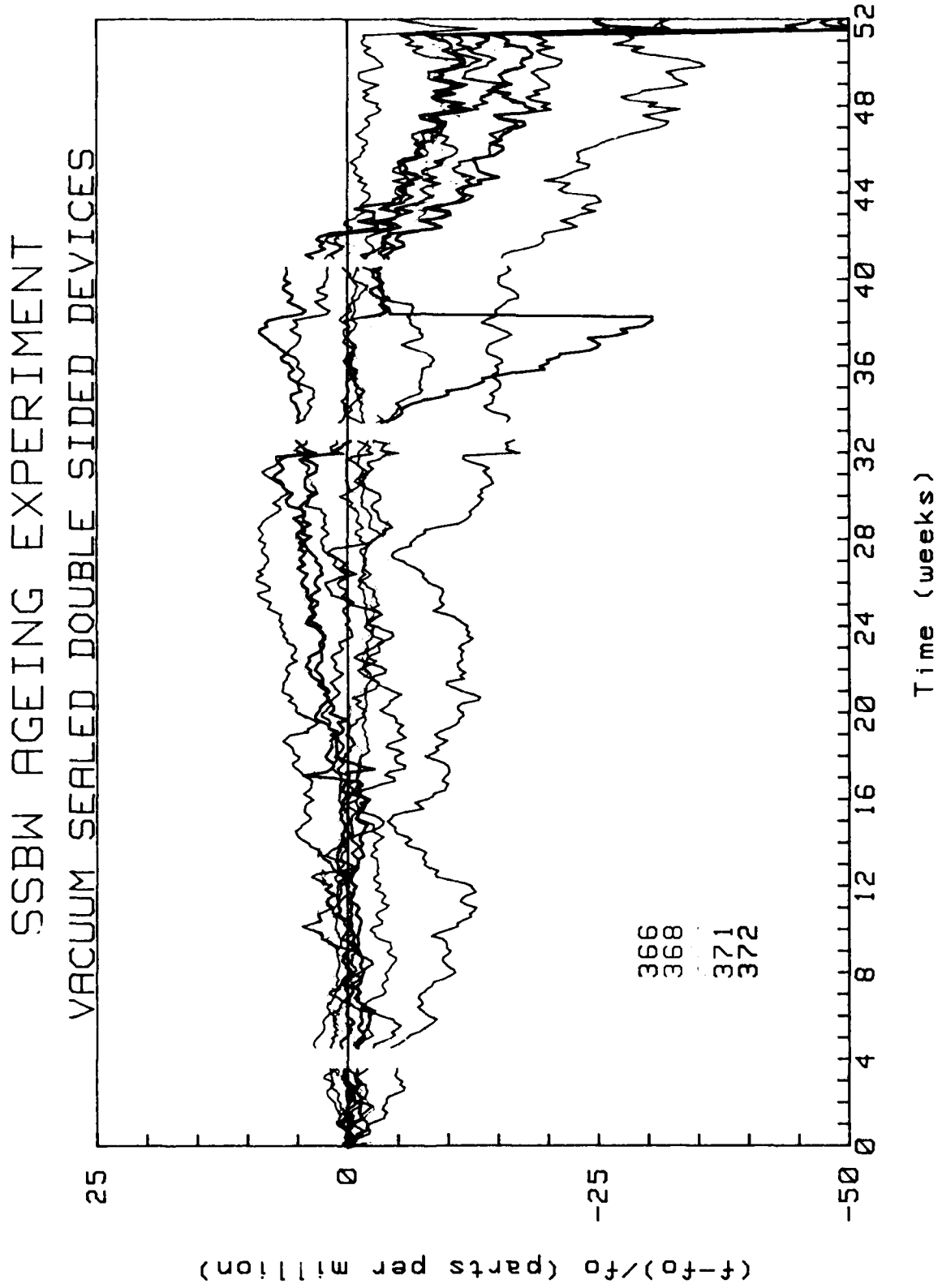
SSBW AGEING EXPERIMENT
VACUUM SEALED DOUBLE SIDED DEVICES
366
368
371
372
25
0
-25
-50
0
4
8
12
16
20
24
28
32
36
40
44
48
52
Time (weeks)
(f-fo)/fo (parts per million)

FIG. A-3

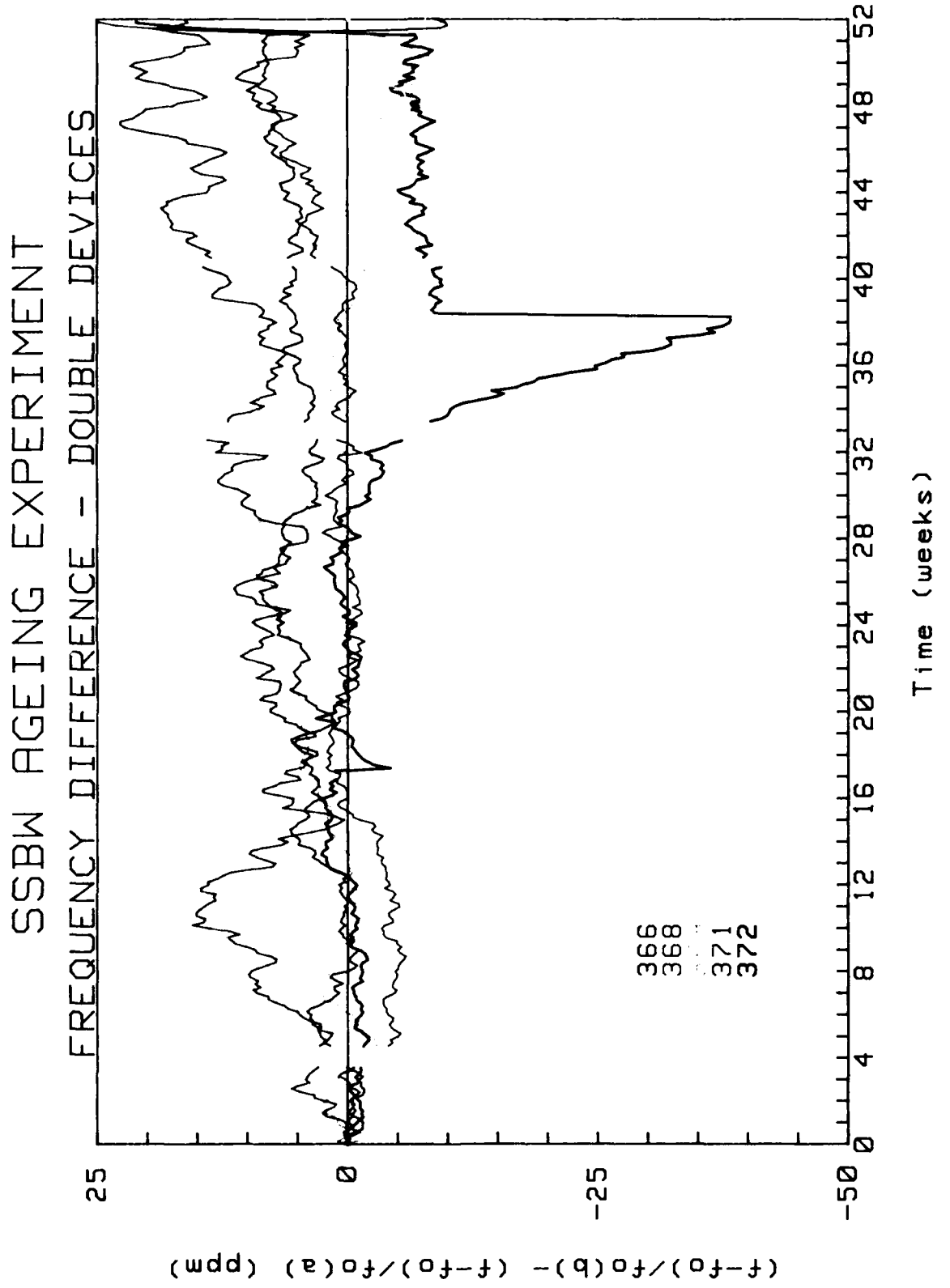
SSBW AGEING EXPERIMENT
FREQUENCY DIFFERENCE - DOUBLE DEVICES
366
368
371
372
25
0
-25
-50
0
4
8
12
16
20
24
28
32
36
40
44
48
52
Time (weeks)
(f-fo)/fo(b)- (f-fo)/fo(a) (ppm)

FIG. A-4

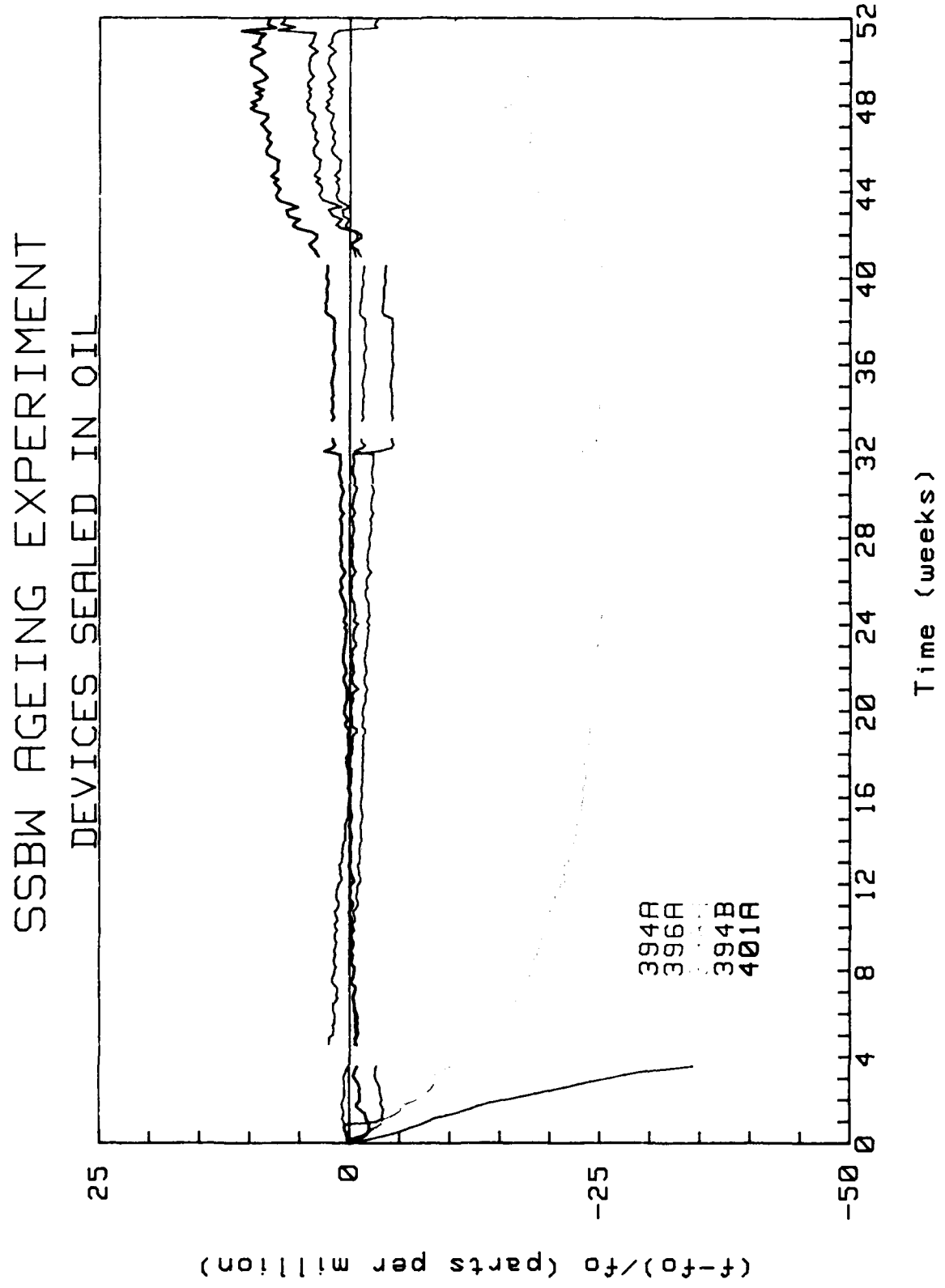
SSBW AGEING EXPERIMENT
DEVICES SEALED IN OIL
394A
396A
394B
401A
25
0
-25
-50
0
4
8
12
16
20
24
28
32
36
40
44
48
52
Time (weeks)
(f-fo)/fo (parts per million)

END

Feb.

1988

DTIC